

The background is a dark blue field filled with intricate, glowing patterns. On the left side, there are several concentric circles of varying radii, some with small square markers. On the right side, there are curved lines that resemble a grid or a series of parallel paths curving towards the center. The overall effect is a sense of depth and technological complexity.

# Detector Technologies

Daniela Bortoletto

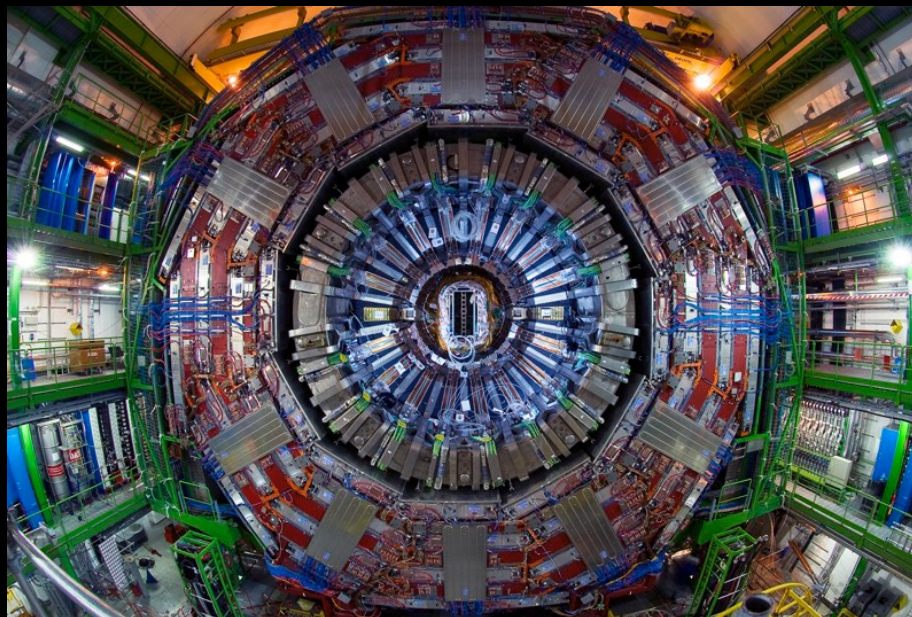
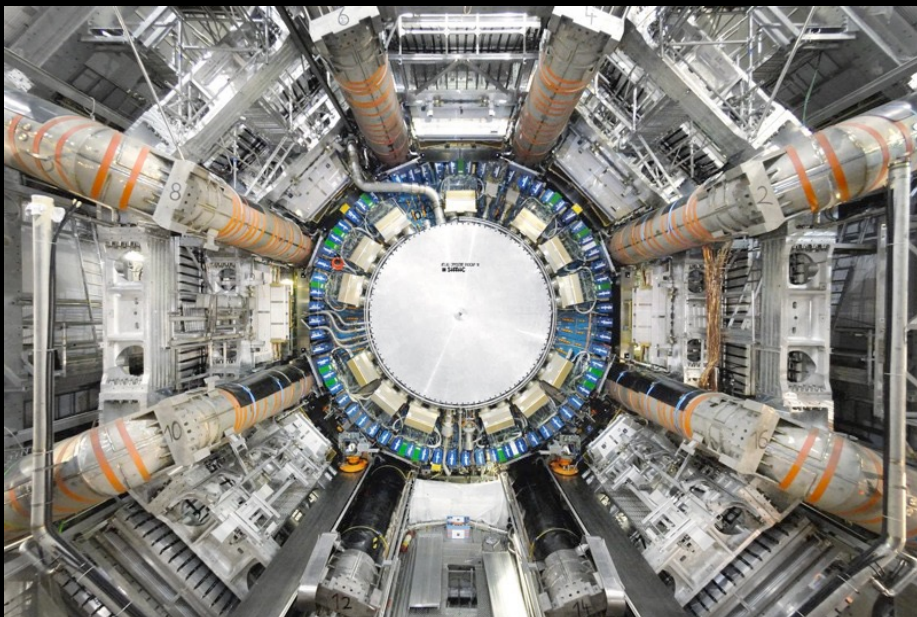
# Road path to the instrumentation lectures

- Why instrumentation is important ?
- Introduction on how we detect particles
- Note that experiments can be very different according to their physics focus



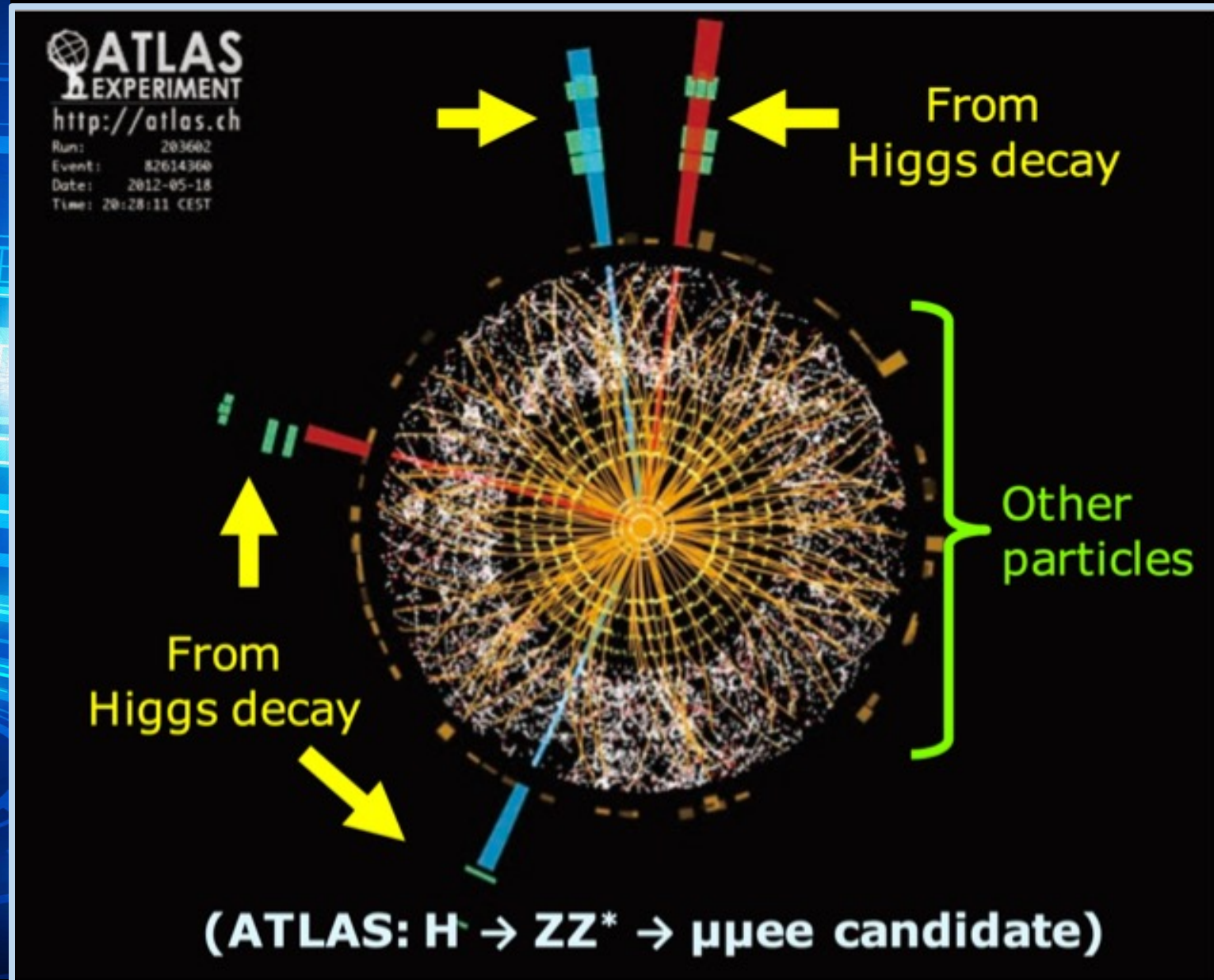
# Road path to the instrumentation lectures

- Why instrumentation is important ?
- Introduction on how we detect particles
- Motivations for the general purpose LHC detectors (ATLAS and CMS)



- Tomorrow: silicon detectors and innovative technologies needed for the LHC upgrades and FCC

# Very complex events



- Demonstrating that a luminosity of  $10^{34} \text{ s}^{-1} \text{ cm}^{-2}$  could be usable was not easy and required a large RD effort that took decades
- We will have to do the same for future colliders like the FCC

# Large Hadron Collider (LHC)



A 27km discovery machine colliding pp at 13 TeV

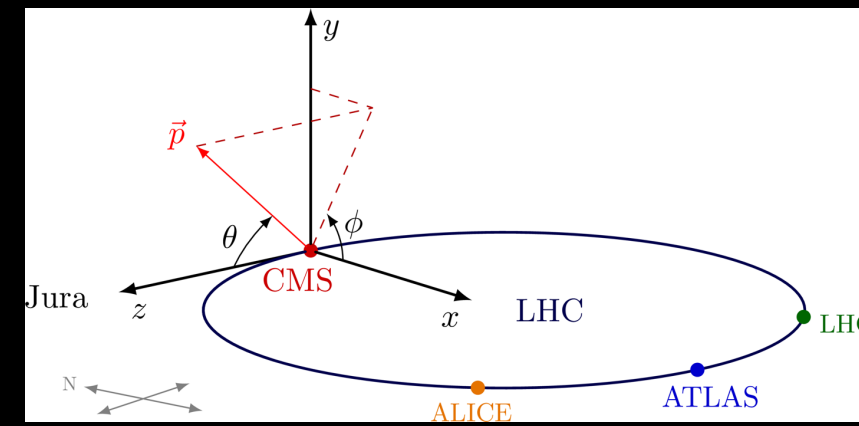
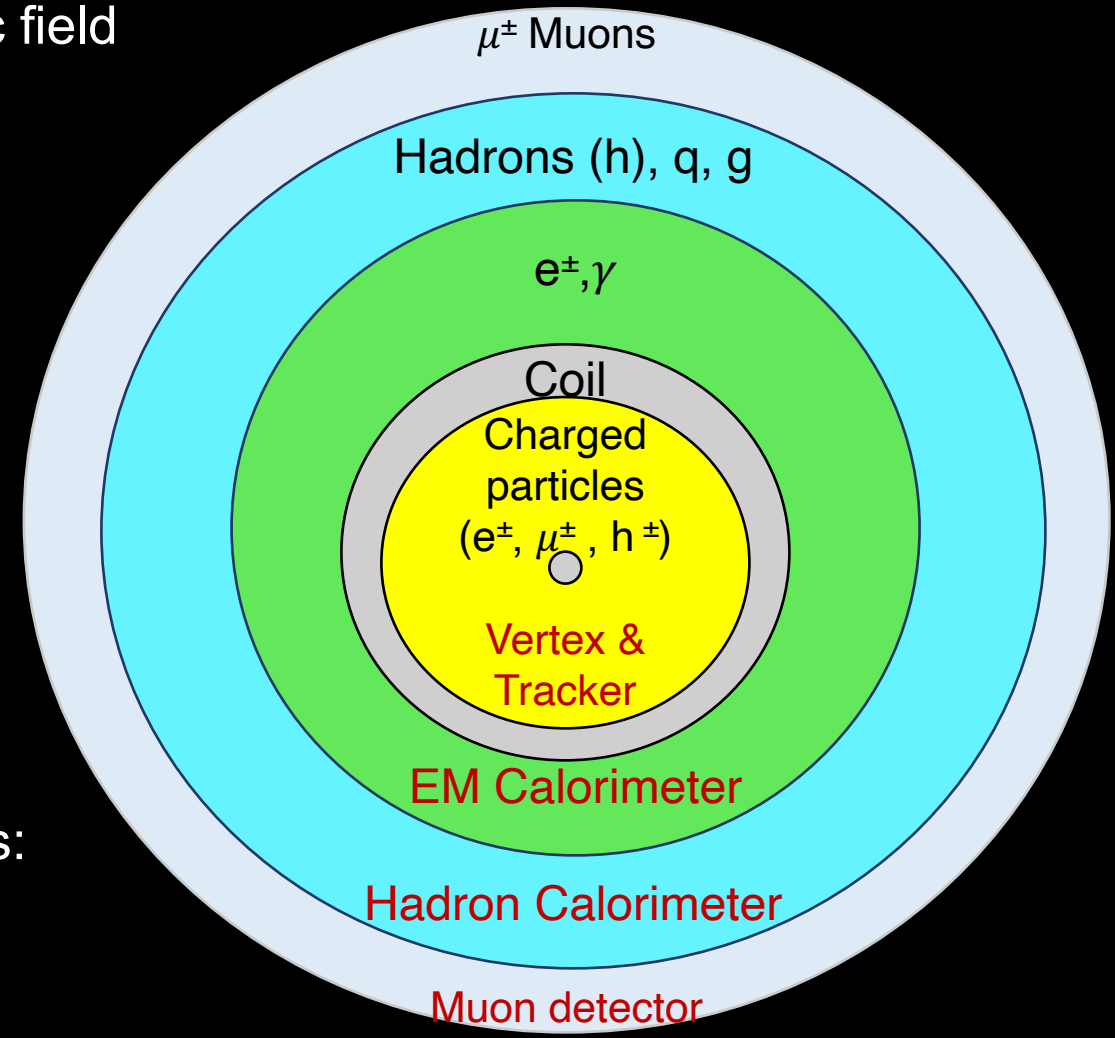
# Collider detectors

## Coordinate system

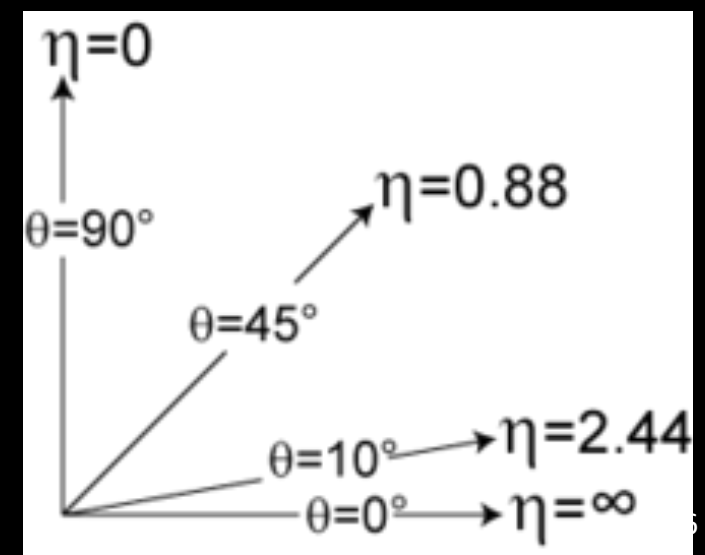
- Tracker detector: Measure position and determine charge and momentum by bending the charged particles in magnetic field

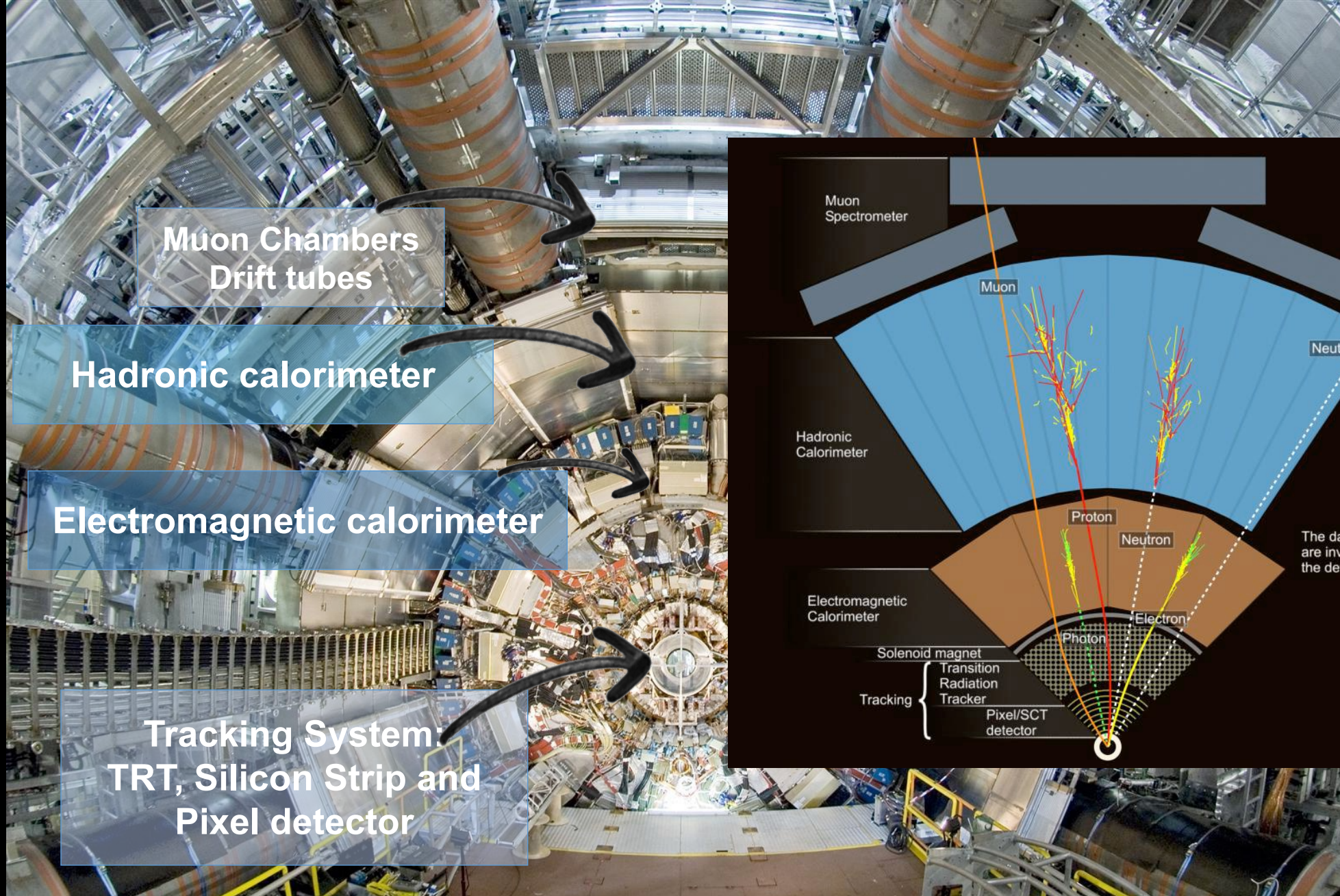
- Calorimeters: measure energy through total absorption (destructive for almost all particles except muons and neutrinos)

- Muon detectors: tracking detectors



$$\eta = -\ln \left( \tan \left( \frac{\theta}{2} \right) \right)$$



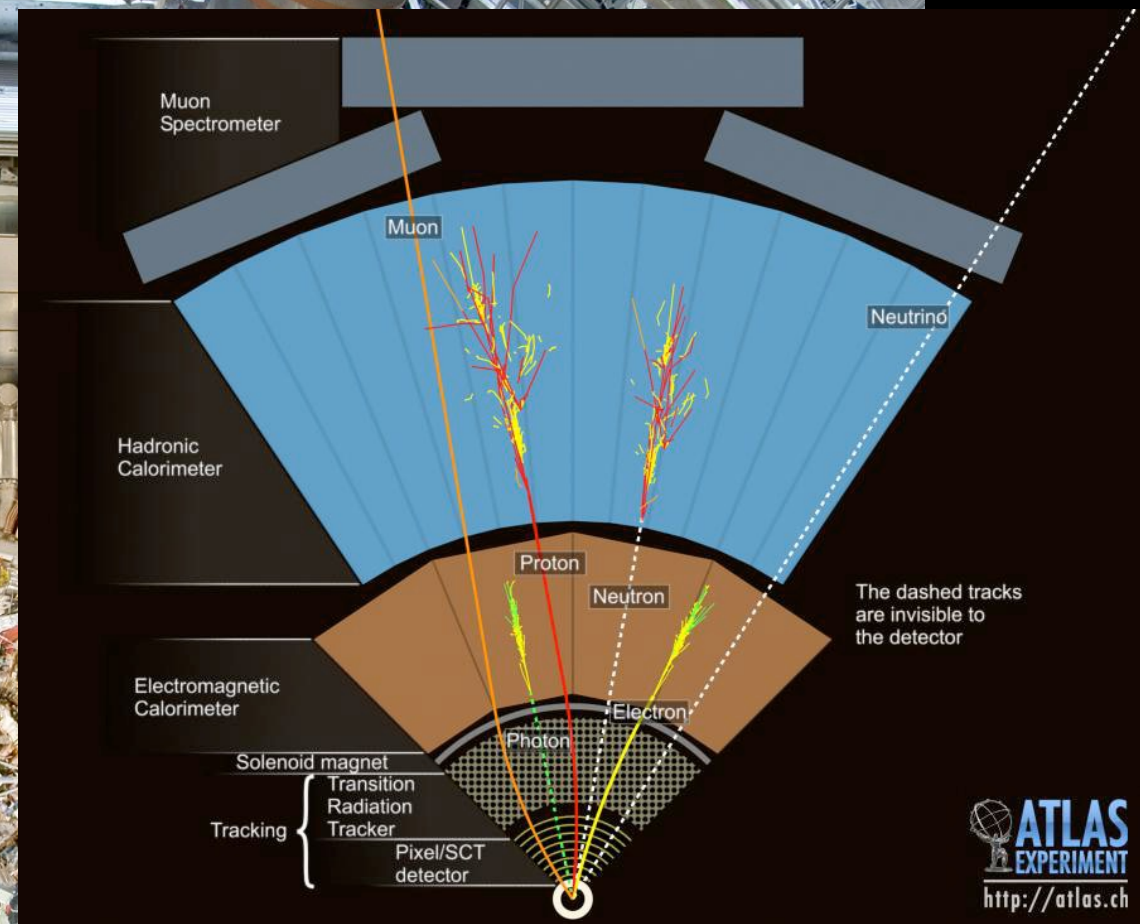


Muon Chambers  
Drift tubes

Hadronic calorimeter

Electromagnetic calorimeter

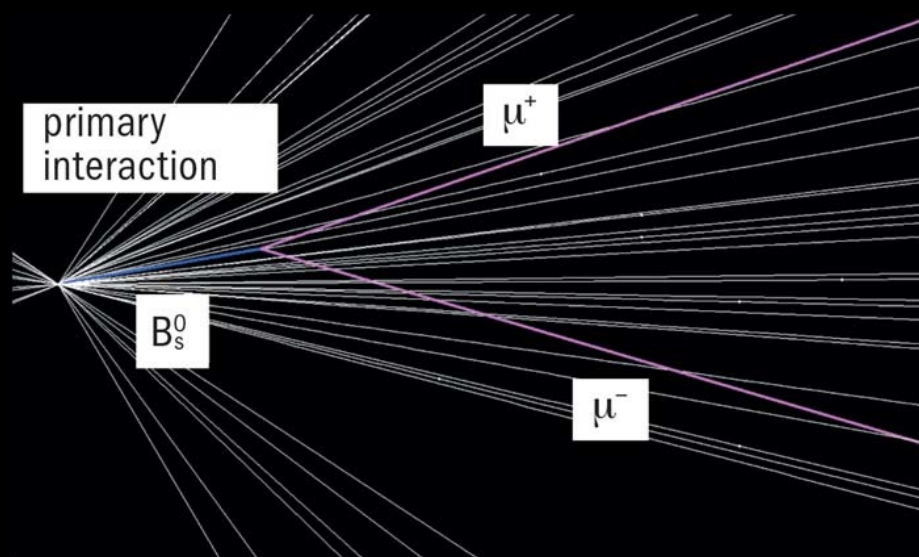
Tracking System:  
TRT, Silicon Strip and  
Pixel detector



# Detecting Elementary Particles

- The goal of LHC detectors was to measure well:  $e$ ,  $\mu$ ,  $\tau$ ,  $\gamma$ ,  $W$ ,  $Z$ , jets, missing  $E_T$ ,  $b$  tagging
- For  $W$  and  $Z$ , the information would be reconstructed through their decay to:  $Z \rightarrow e^+e^-, \mu^+\mu^-, qq\dots$  and  $W \rightarrow e\nu, \mu\nu, qq'\dots$
- $b$ -tagging: reconstructing vertices of charged particles ( $e, \mu, p, \pi^\pm, K^\pm$ ) with a precision of  $\approx 10 \mu m$

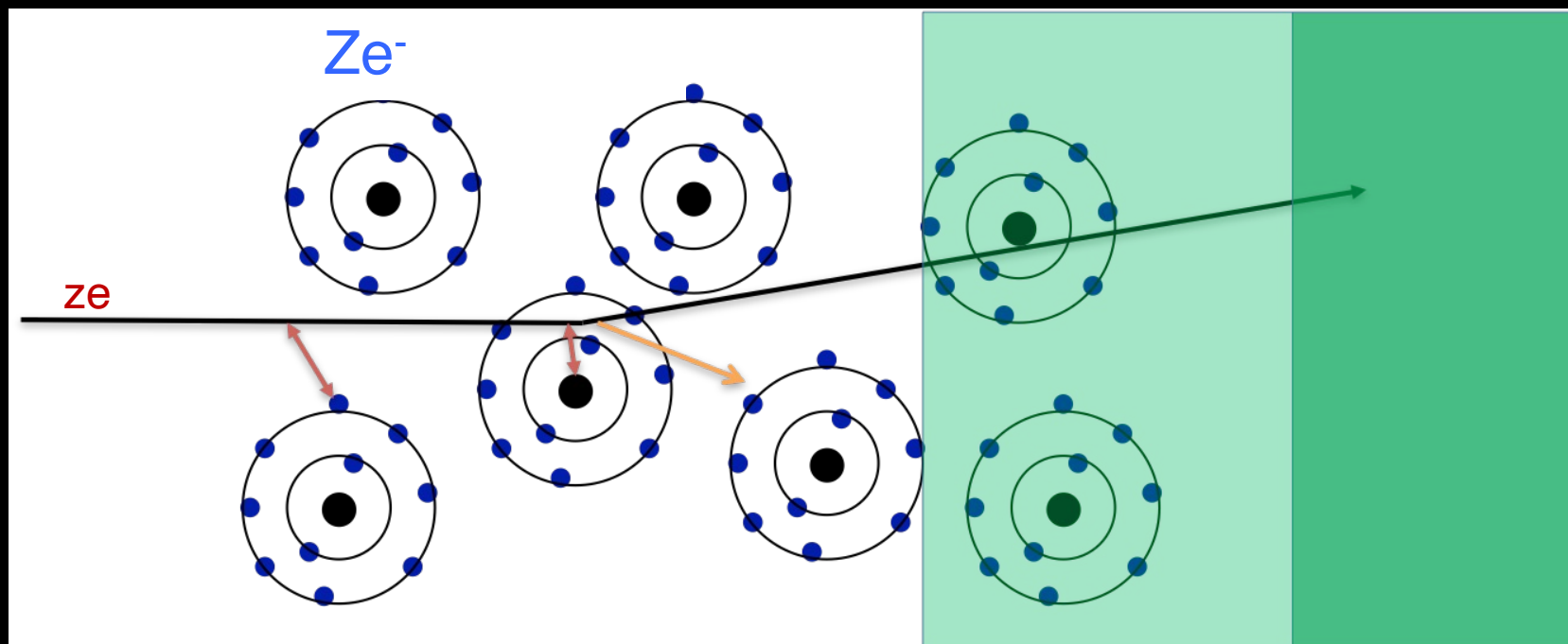
Claus Grupen



- Every effect of particles or radiation can be used as a working principle for a particle detector.



# EM interaction of charged particles with matter



Interaction with the atomic electrons

Incoming particles lose energy and atoms are excited or ionized.

Interaction with the atomic nucleus.

Particles are deflected and a Bremsstrahlung photon can be emitted.

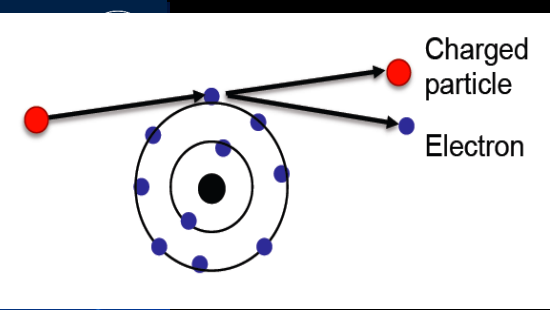
If the particle's velocity is  $>$  the velocity of light in the medium  $\rightarrow$  Cherenkov Radiation.

When a particle crosses the boundary between two media, there is a probability  $\approx 1\%$  to produce an X ray photon Transition radiation.



# Energy loss by ionization

- The Bethe-Bloch equation for energy loss



Valid for heavy charged particles ( $m_{\text{incident}} \gg m_e$ ), e.g. proton,  $k$ ,  $\pi$ ,  $\mu$

$$-\left\langle \frac{dE}{dx} \right\rangle = 2\pi N_a r_e^2 m_e c^2 \rho \frac{Z}{A} \frac{z^2}{\beta^2} \left[ \ln\left(\frac{2m_e c^2 \beta^2 \gamma^2}{I^2} W_{\text{max}}\right) - 2\beta^2 - \delta(\beta\gamma) - \frac{C}{Z} \right]$$

$$= 0.1535 \text{ MeV cm}^2/\text{g}$$

$$\frac{dE}{dx} \propto \frac{Z^2}{\beta^2} \ln(a\beta^2\gamma^2)$$

## Fundamental constants

$r_e$  = classical radius of electron  
 $m_e$  = mass of electron  
 $N_a$  = Avogadro's number  
 $c$  = speed of light

## Absorber medium

$I$  = mean ionization potential  
 $Z$  = atomic number of absorber  
 $A$  = atomic weight of absorber  
 $\rho$  = density of absorber  
 $\delta$  = density correction  
 $C$  = shell correction

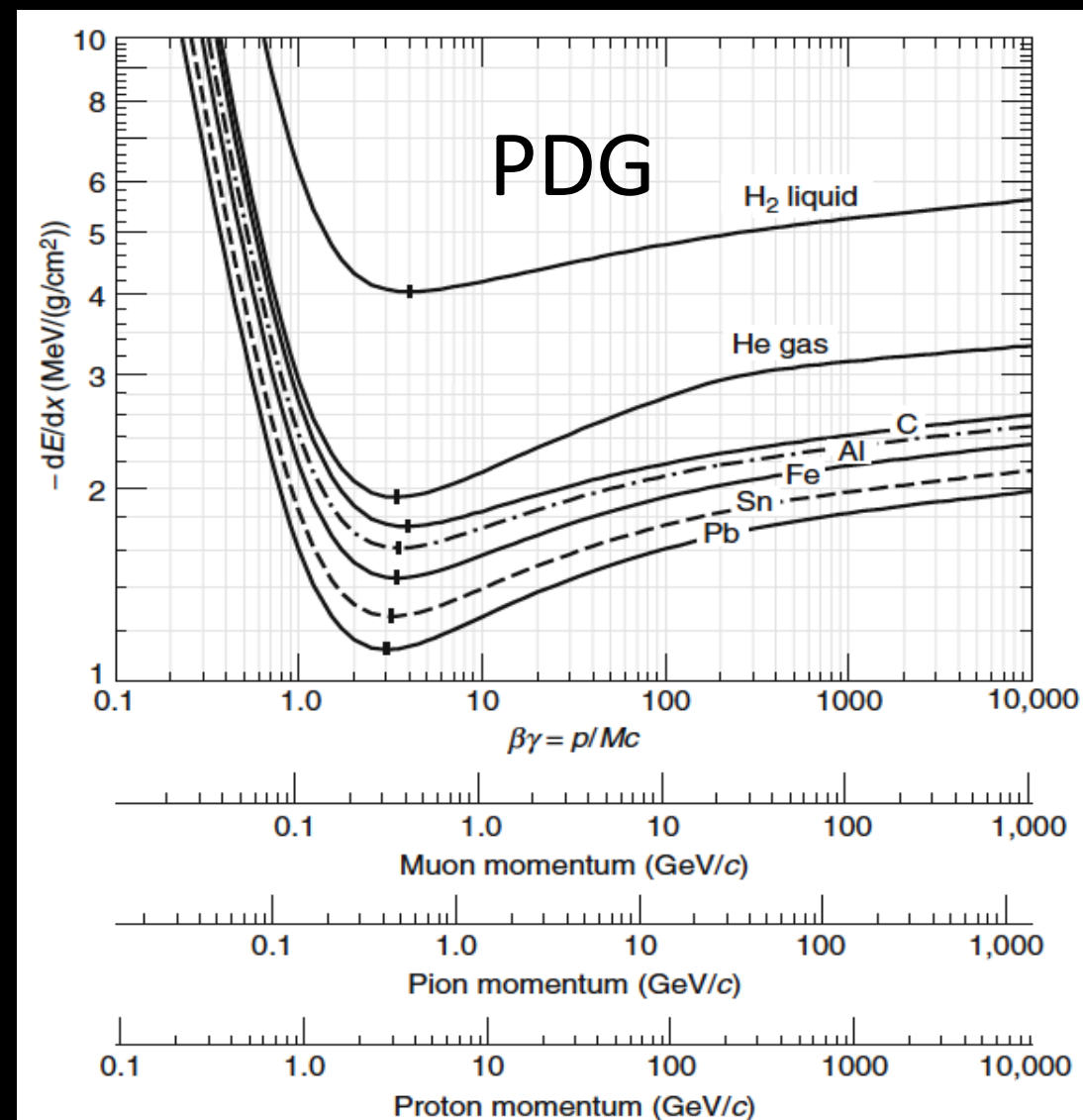
## Incident particle

$z$  = charge of incident particle  
 $\beta$  =  $v/c$  of incident particle  
 $\gamma$  =  $(1-\beta^2)^{-1/2}$   
 $W_{\text{max}}$  = max. energy transfer in one collision

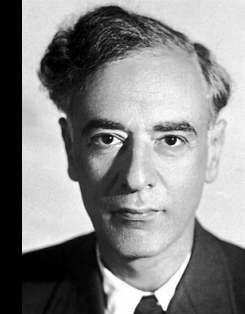
$$r_e = \frac{1}{4\pi\epsilon_0} \frac{e^2}{m_e c^2}$$

# The Bethe-Bloch Formula

- Common features:
  - fast growth, as  $1/\beta^2$ , at low energy
  - wide minimum in the range  $3 \leq \beta\gamma \leq 4$ ,
  - slow increase at high  $\beta\gamma$ .
- A particle with  $dE/dx$  near the minimum is a **minimum-ionizing particle or mip**.
- The mip's ionization losses for all materials except hydrogen are in the range 1-2 MeV/(g/cm<sup>2</sup>)
  - increasing from large to low Z of the absorber.

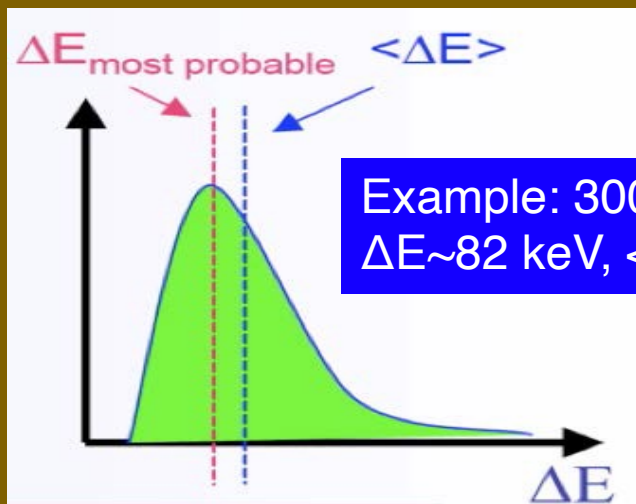


# dE/dx Fluctuations

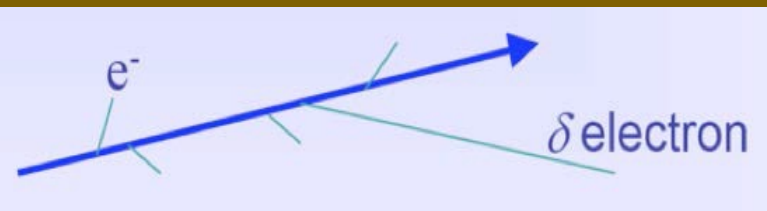


- A real detector cannot measure  $\langle dE/dx \rangle$ 
  - It measures the energy  $\Delta E$  deposited in layers of finite thickness  $\Delta x$
  - Repeated measurements are needed

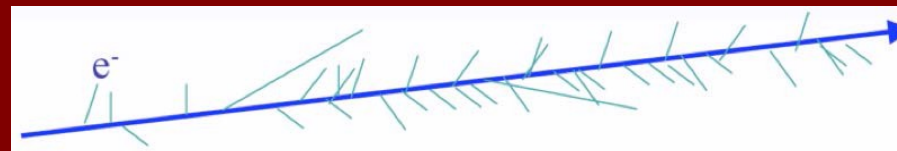
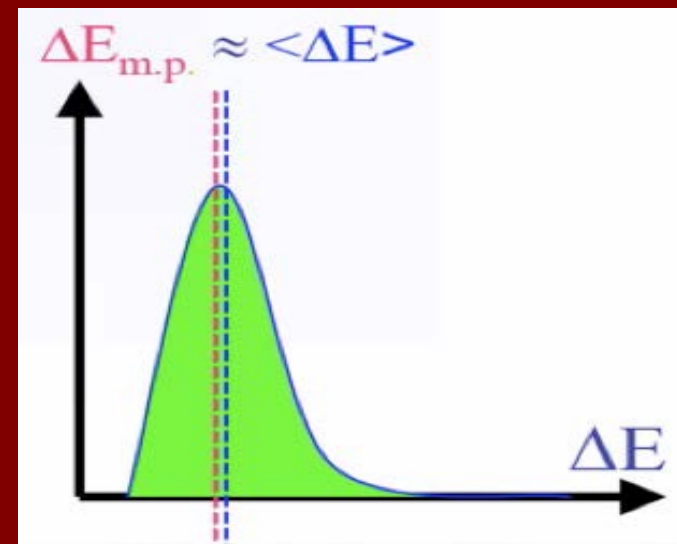
- Thin layers or low density materials:  
dE/dx has large fluctuations towards high losses (Landau-Vavilov, Bichsel )



Example: 300  $\mu\text{m}$  thick Silicon  
 $\Delta E \sim 82$  keV,  $\langle \Delta E \rangle \sim 115$  keV



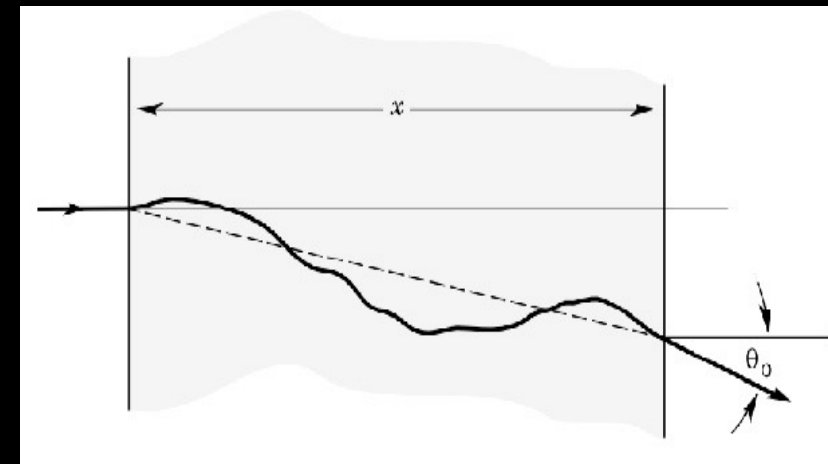
- Thick layers and high density materials: the dE/dx is a more Gaussian-like (many collisions



# Multiple scattering

- A particle passing through material undergoes also multiple deflections due to Coulomb scattering with the nuclei
- The scattering angle as a function of the thickness  $x$  is

$$\theta_{\text{rms}}^{\text{proj}} = \sqrt{\langle \theta^2 \rangle} = \frac{13.6 \text{ MeV}}{\beta c p} z \sqrt{\frac{x}{X_0}} [1 + 0.038 \ln(x/X_0)]$$



- Where:

- $p$  (in MeV/c) is the momentum,  $\beta c$  the velocity
- $z$  the charge of the scattered particle
- $x/X_0$  is the thickness of the medium in units of radiation radiation length ( $X_0$ ).

$$X_0 \cong \frac{716.4 \text{ g} \cdot \text{cm}^{-2} A}{Z(Z+1) \ln(287/\sqrt{Z})}$$

In g/cm must multiply by density to get a length!

- Small deflections:

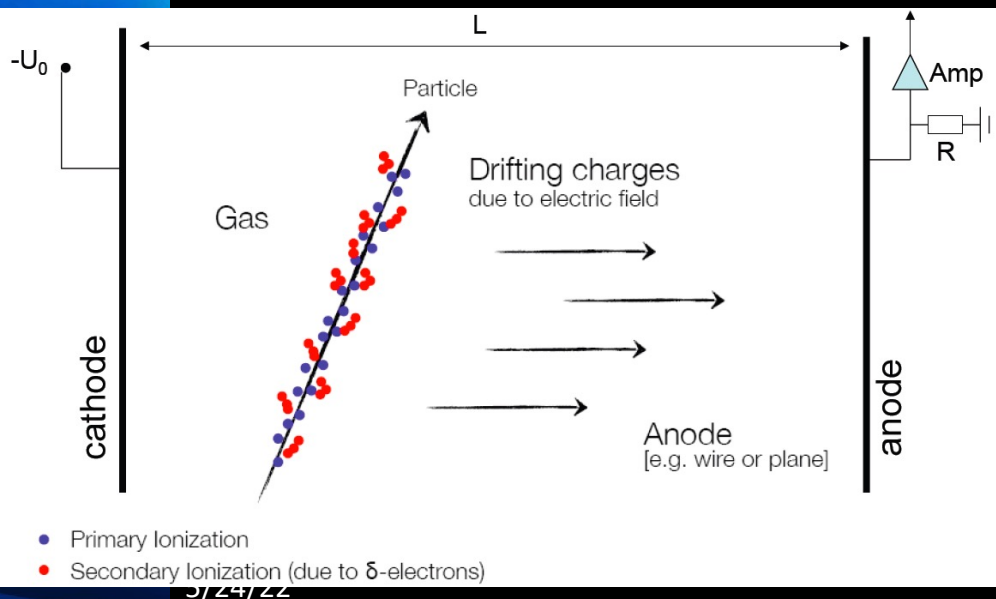
- Large Radiation length  $X_0$  – i.e. low  $Z$  and low density material (Be, C ...)
- Small  $x$  i.e. very thin detector elements

- Multiple scattering limiting tracking performance at low  $p$

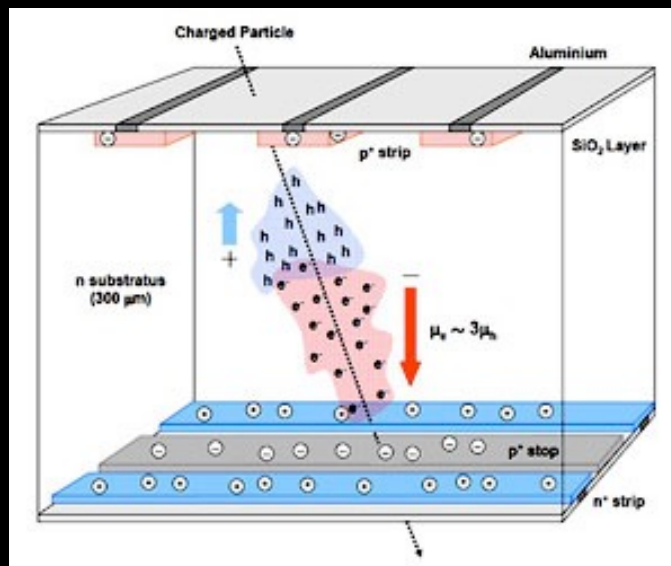
# Tracking detectors

- High granularity detectors close to the interaction region measuring the trajectory using “hits” due to charged particles ionizing a material (gas, silicon)
  - charged particles’ momenta determined from their curvature in a B field ( $R[m]=p[GeV/c]/(0.3B[T])$ )
  - Extrapolation to origin allows the reconstruction of Primary Vertex of the “hard scattering”, while secondary vertices identify tau-leptons, b and c-hadrons by lifetime tagging ( $d = \beta\gamma c\tau$ )

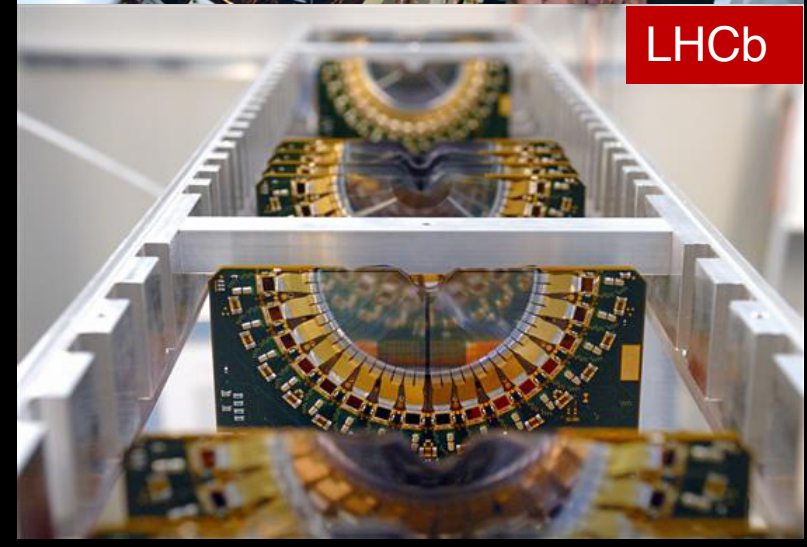
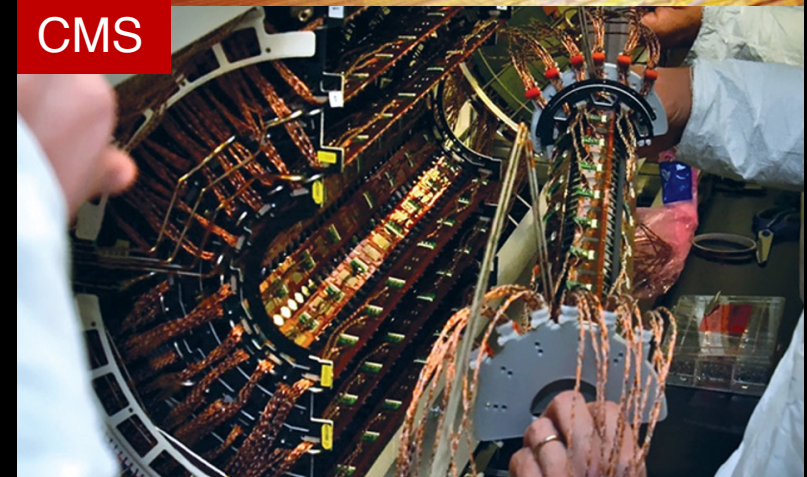
## Gas Detectors



## Silicon Detectors



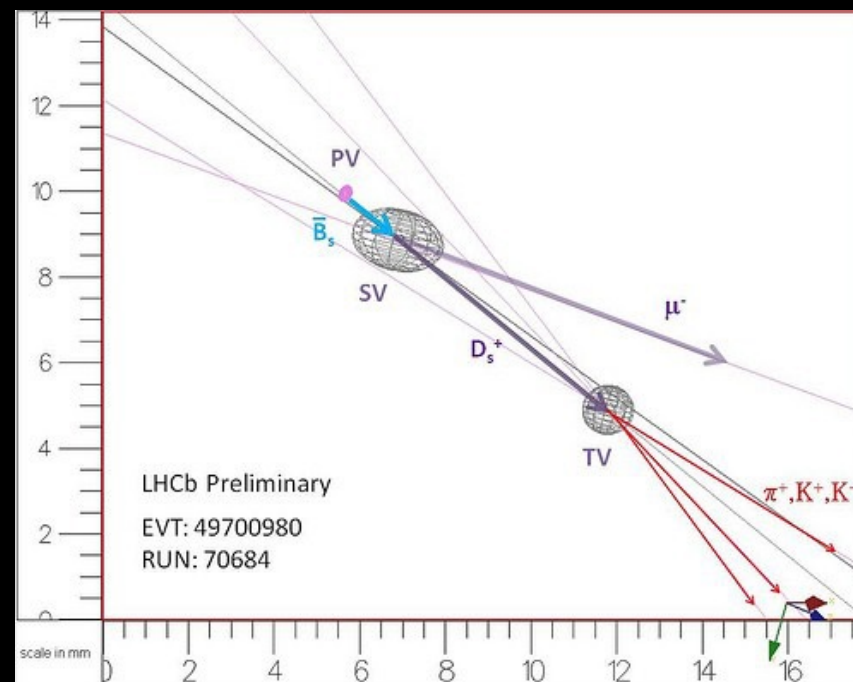
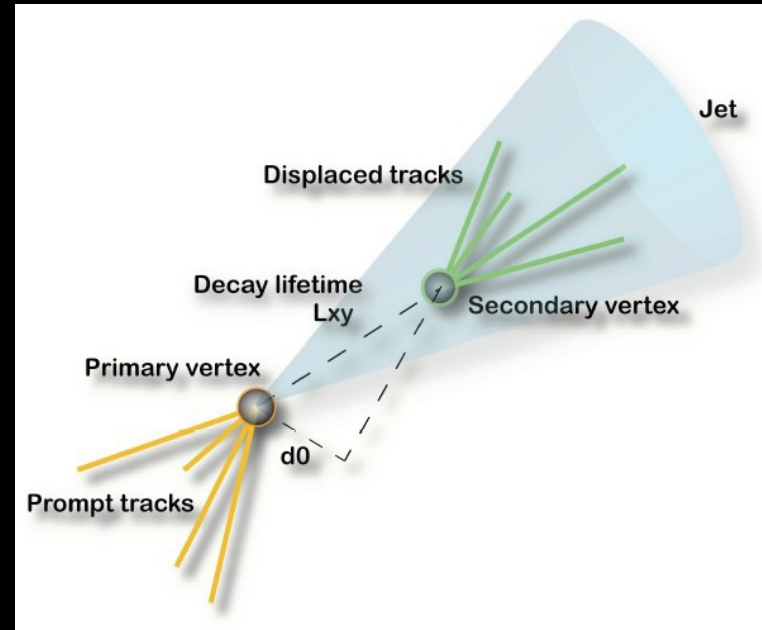
D. Bortoletto, Lecture 1



LHCb

# Impact Parameter

- Distance between primary vertex and prolongation is called impact parameter ( $d$ ).
- If  $d$  is large the probability is high that the track comes from a secondary vertex
- Distance can be used for tagging b-jets and c-jets ( $\beta\gamma c\tau$ )

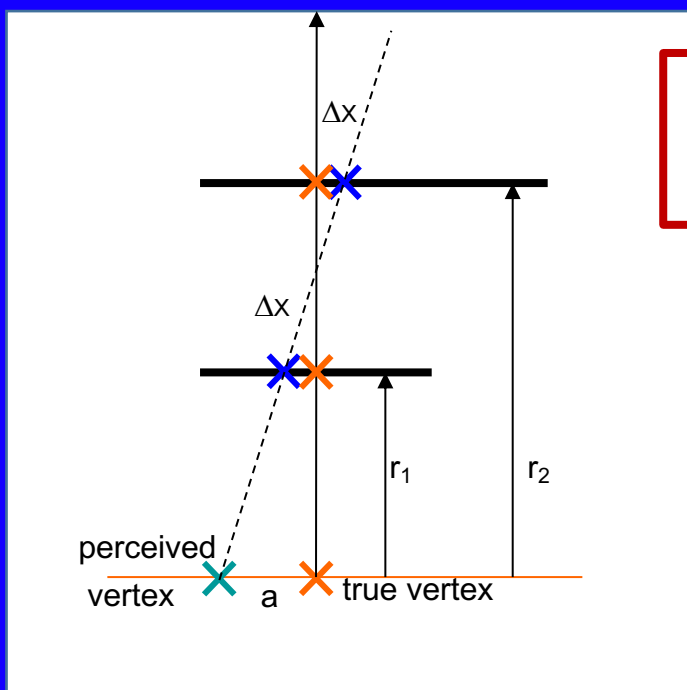


# Impact Parameter resolution

- Vertex projection from two points: simplified telescope equation

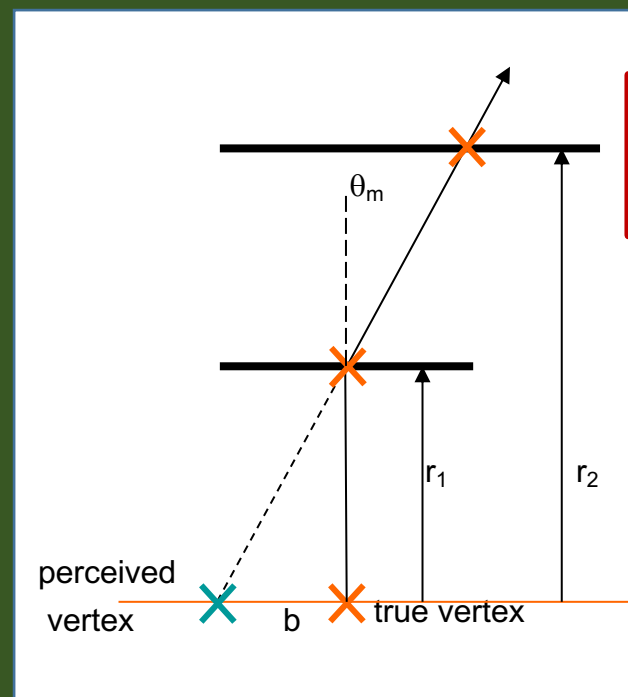
$$\text{Pointing resolution} = ( a \oplus b ) \mu\text{m}$$

a= depends on detector position resolution



$$a = \Delta x \cdot \sqrt{\frac{r_2^2 + r_1^2}{(r_2 - r_1)^2}}$$

b= depends on multiple scattering



$$\theta_m = \frac{13.6 \text{ MeV}}{\beta \cdot c \cdot p} \cdot \sqrt{x / X_0}$$

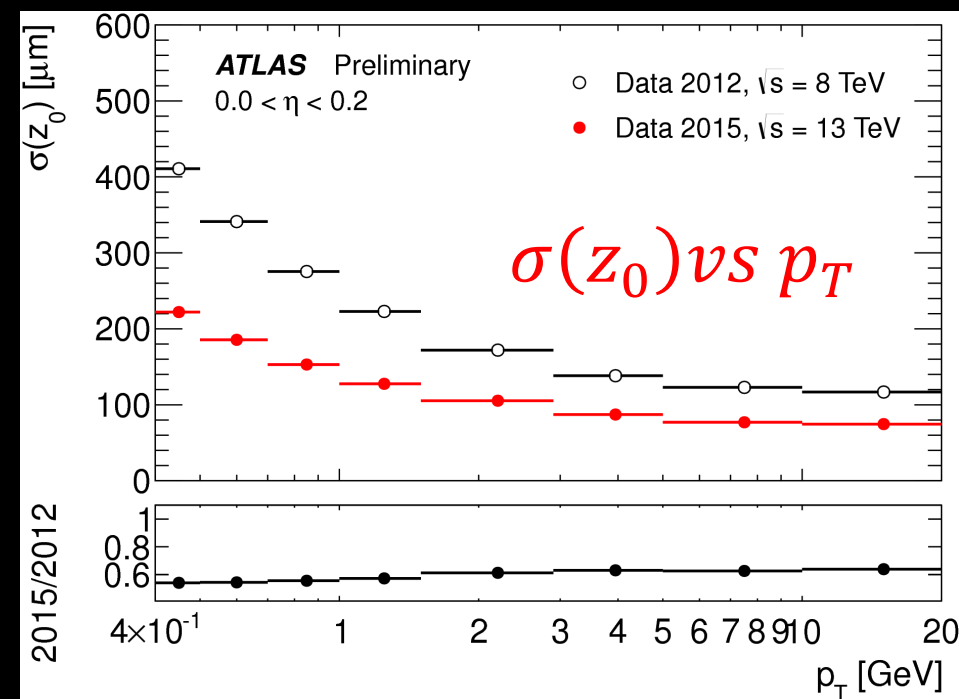
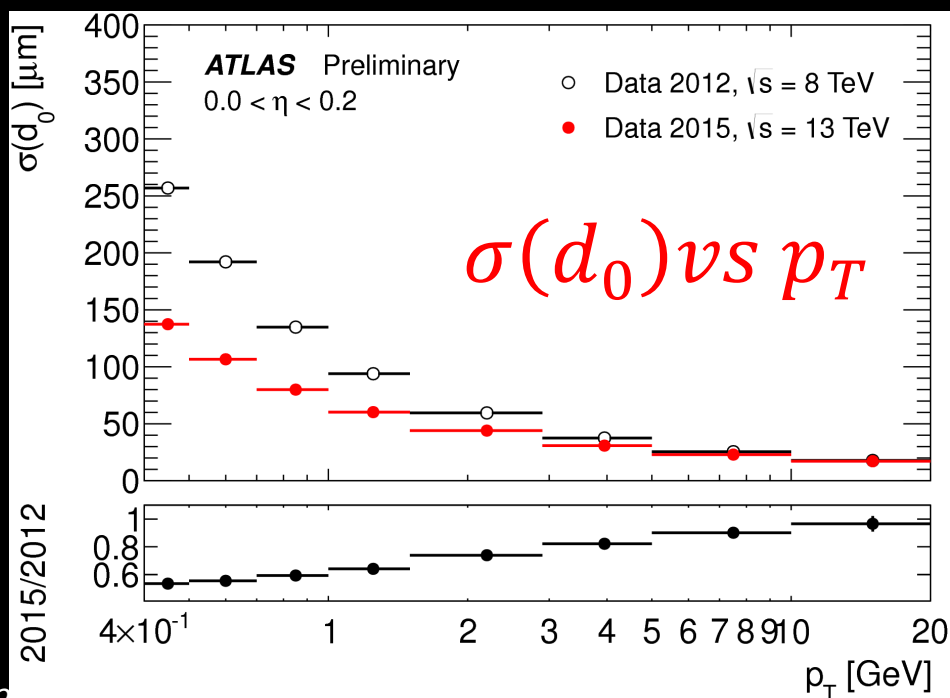
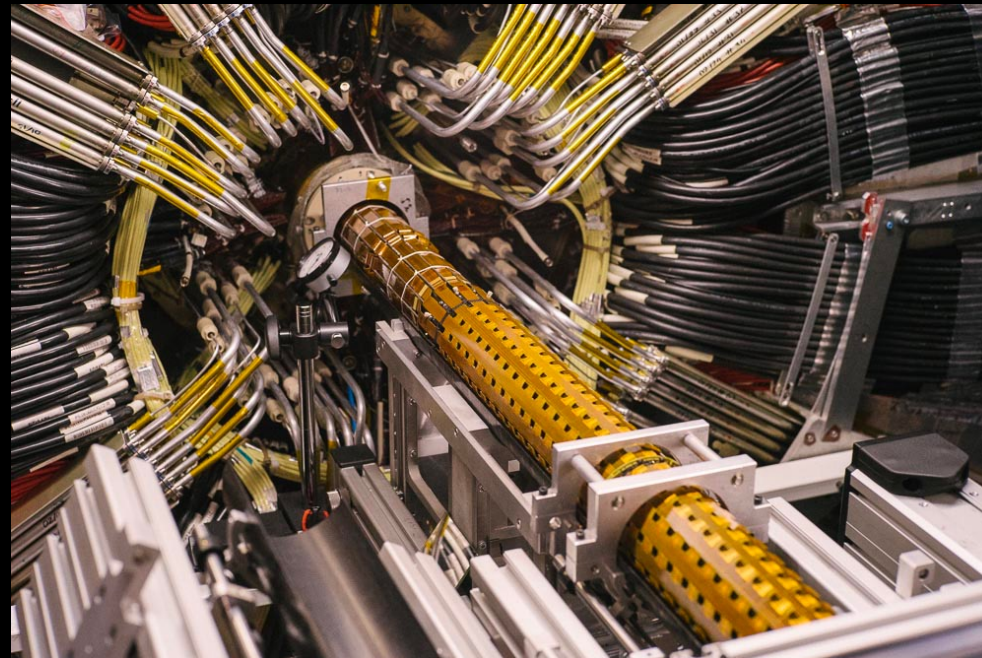
Minimize  $\Delta x$ : e.g.  $50 \mu\text{m}$  pixel and  $r_2$  very large compared to  $r_1$  (first layer as close as possible to IP)  $\rightarrow a = \Delta x = 50 / \sqrt{12} = 15 \mu\text{m}$

First layer with minimal amount of material: e.g.  $x/X_0 = 0.0114$ ,  $r_1 = 39\text{mm} \rightarrow b = 57 \mu\text{m}$  for  $p = 1\text{GeV}/c$



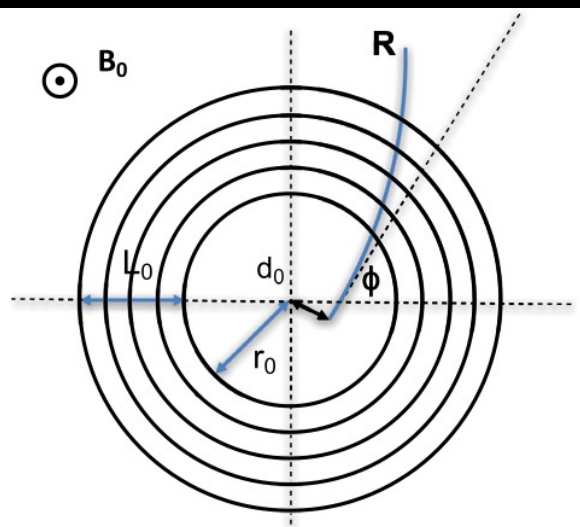
# Impact Parameter resolution

- Improvement by inserting IBL in the ATLAS Pixel system just before the start of Run 2 in 2015
- IBL: radius of 3.3 cm, smaller pixels  $50 \mu\text{m} \times 250 \mu\text{m}$  (instead of  $50 \mu\text{m} \times 400 \mu\text{m}$ ) and lower mass

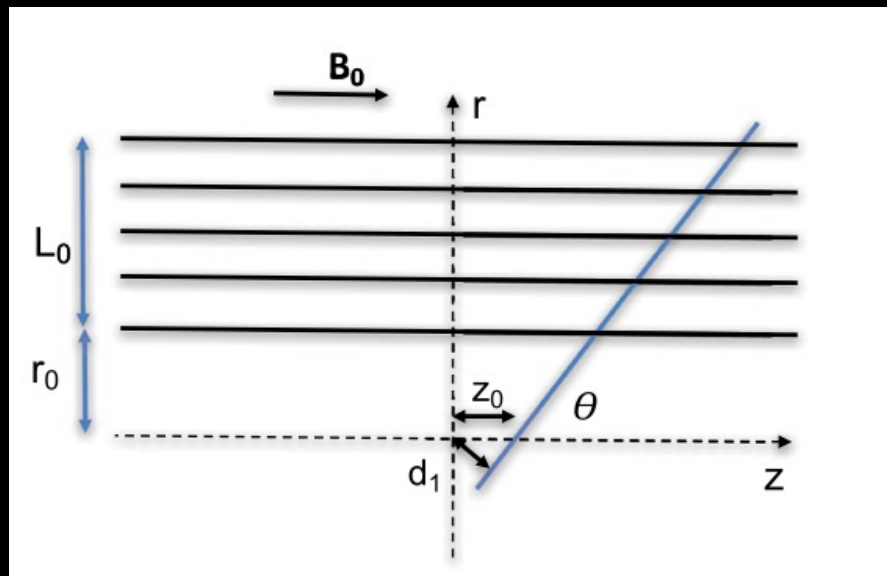


# Momentum resolution

- Analytic expressions for momentum, track angle and impact parameter resolution have been calculated for equidistant layers



$$R[\text{m}] = p[\text{GeV}/c] / (0.3B[\text{T}])$$



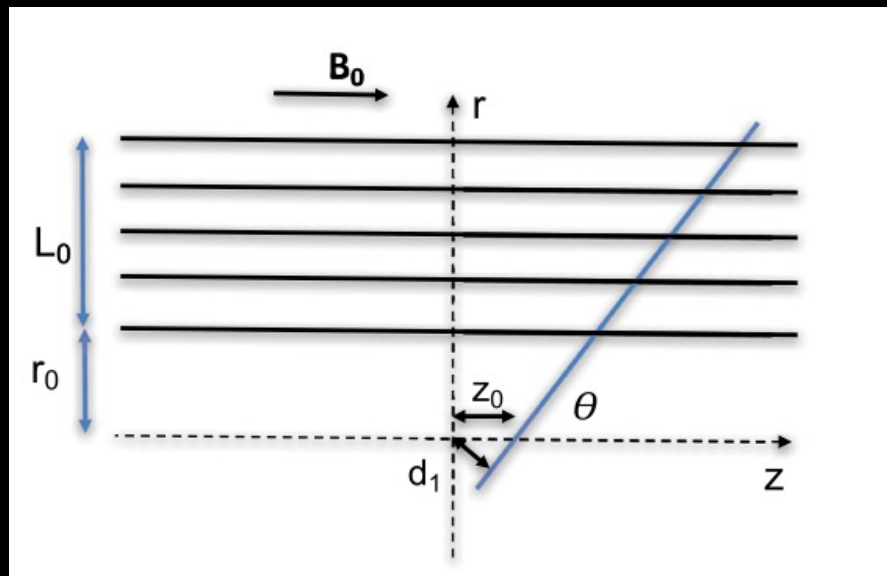
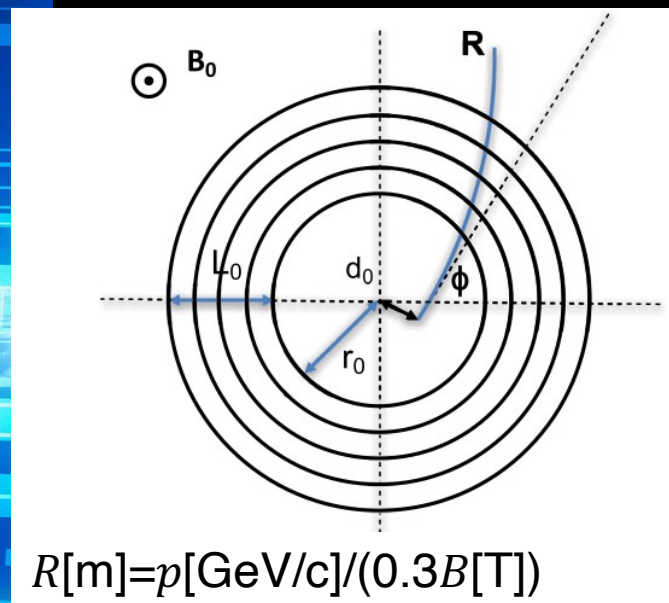
- solenoid spectrometer with a constant B-field  $B_0$
- $N + 1$  equal and equidistant detector planes.
- $d_i$  the thickness of a single detector plane in  $X_0$  units
- $d_{tot} = (N + 1) d_i$

$$\begin{aligned} \frac{\Delta p_T}{p_T} \Big|_{res.} &= \frac{\sigma_{r\phi} p_T}{0.3 B_0 L_0^2} \sqrt{\frac{720 N^3}{(N-1)(N+1)(N+2)(N+3)}} \\ &\approx \frac{12 \sigma_{r\phi} p_T}{0.3 B_0 L_0^2} \sqrt{\frac{5}{N+5}} \end{aligned}$$

$$\begin{aligned} \frac{\Delta p_T}{p_T} \Big|_{m.s.} &= \frac{N}{\sqrt{(N+1)(N-1)}} \frac{0.0136 \text{ GeV}/c}{0.3\beta B_0 L_0} \\ &\times \sqrt{\frac{d_{tot}}{X_0 \sin \theta}} \left( 1 + 0.038 \ln \frac{d}{X_0 \sin \theta} \right) \\ &\approx \frac{0.0136 \text{ GeV}/c}{0.3\beta B_0 L_0} \sqrt{\frac{d_{tot}}{X_0 \sin \theta}} \end{aligned}$$

# Momentum resolution

- Analytic expressions for momentum, track angle and impact parameter resolution have been calculated for equidistant layers



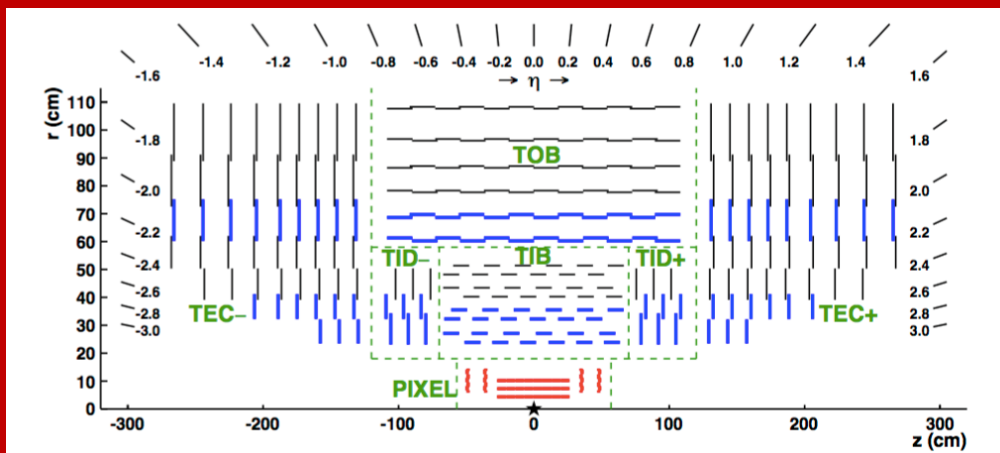
- solenoid spectrometer with a constant B-field  $B_0$
- $N + 1$  equal and equidistant detector planes.
- $d_i$  the thickness of a single detector plane in  $X_0$  units
- $d_{tot} = (N + 1) d_i$

- Good transverse momentum resolution requires: small  $\sigma_{r\phi}$ , strong  $B_0$  field, large  $L_0$  (as  $L_0^2$ ), many measurement layers  $N$  (as  $\sqrt{N}$ ), thin measurement layers ( $d_i$ ), long  $X_0$ , low  $Z$  materials
- Momentum resolution gets worse at large  $p_T$

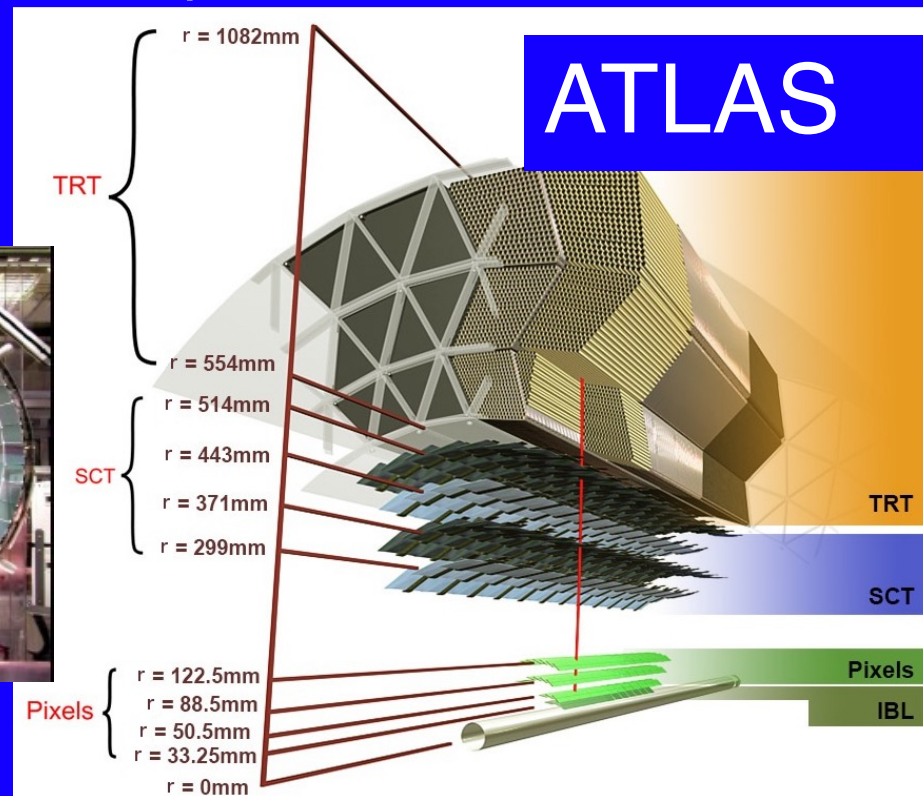
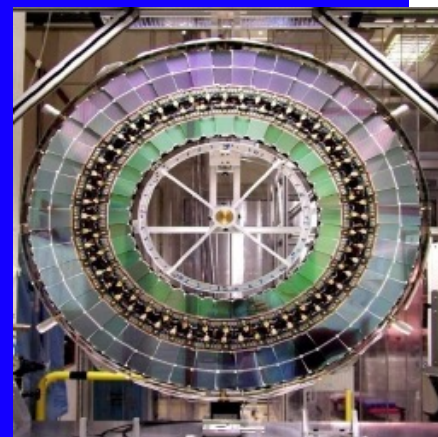
# Atlas and CMS tracking

All silicon system in 3.8 T solenoid field

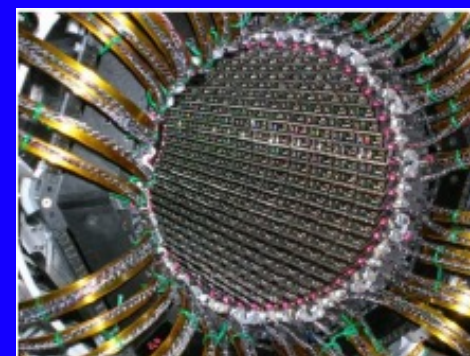
C  
M  
S



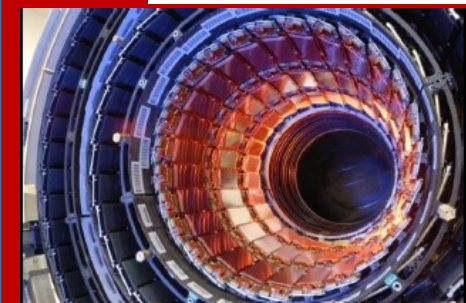
Silicon pixel and strip + transition radiation tracker (TRT) in 2 T field



Strips: 61 m<sup>2</sup> with 6.2 M channels  
4 barrel layers + 9 disks per endcap  
30 cm <R< 52 cm



Pixels: 80M pixels each 50 x 400 μm<sup>2</sup>  
3 Barrel layers  
3 endcap disks/side  
IBL: 50 x 250 μm<sup>2</sup>

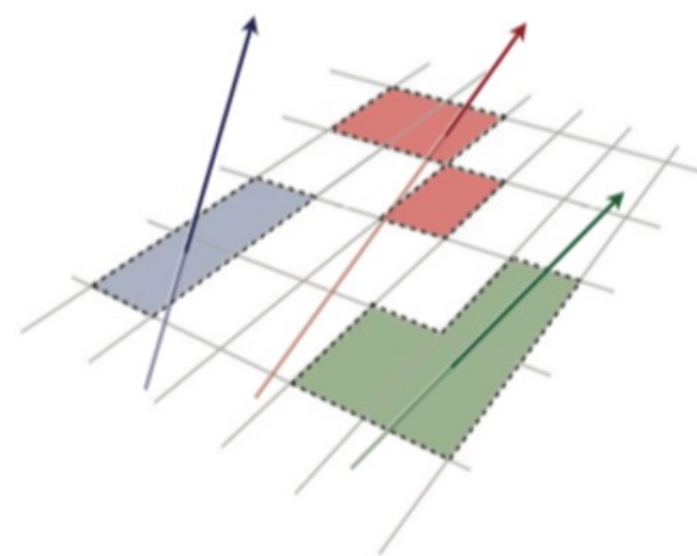


Strips: 198 m<sup>2</sup> with 9.3 M channels  
Inner: 4 barrel layers, 3 end-cap disks  
Outer: 6 barrel layers, 9 wheels

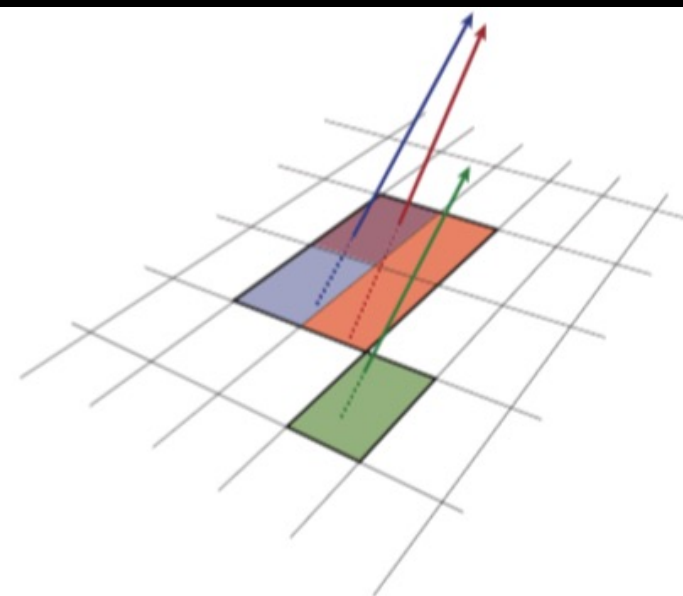
Pixels: 66 M pixels each 150 x 100 μm<sup>2</sup> pixels  
3 barrel layers, 2 endcap disks/side (Upgraded in phase 1 to 4 barrel layers + 3 endcaps/side)

# From particle to hits

- Charged particle will create  $O(24000)$  electron-hole pairs
- Charge  $>$  threshold is considered a hit
- If charge is collected in multiple adjacent pixel/strips, the hits are grouped together into a cluster
  - Challenge: this can lead to merged clusters in dense environments
- Detector granularity critical to maintain low occupancy
  - Need higher granularity (more smaller pixels) as the luminosity increases
- Hit reconstruction efficiency (in working modules) is  $> 99\%$  typically
- As a rule of thumb the position resolution is  $\text{pitch}/\sqrt{12}$



(a) Single-particle pixel clusters

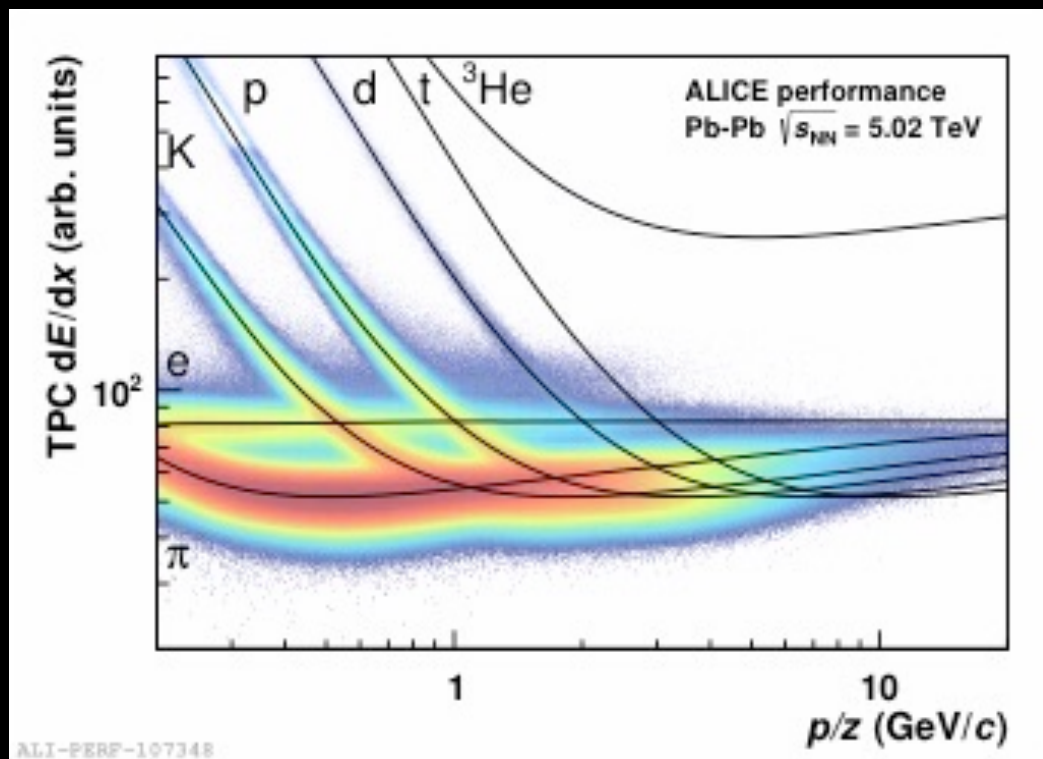


(b) Merged pixel cluster

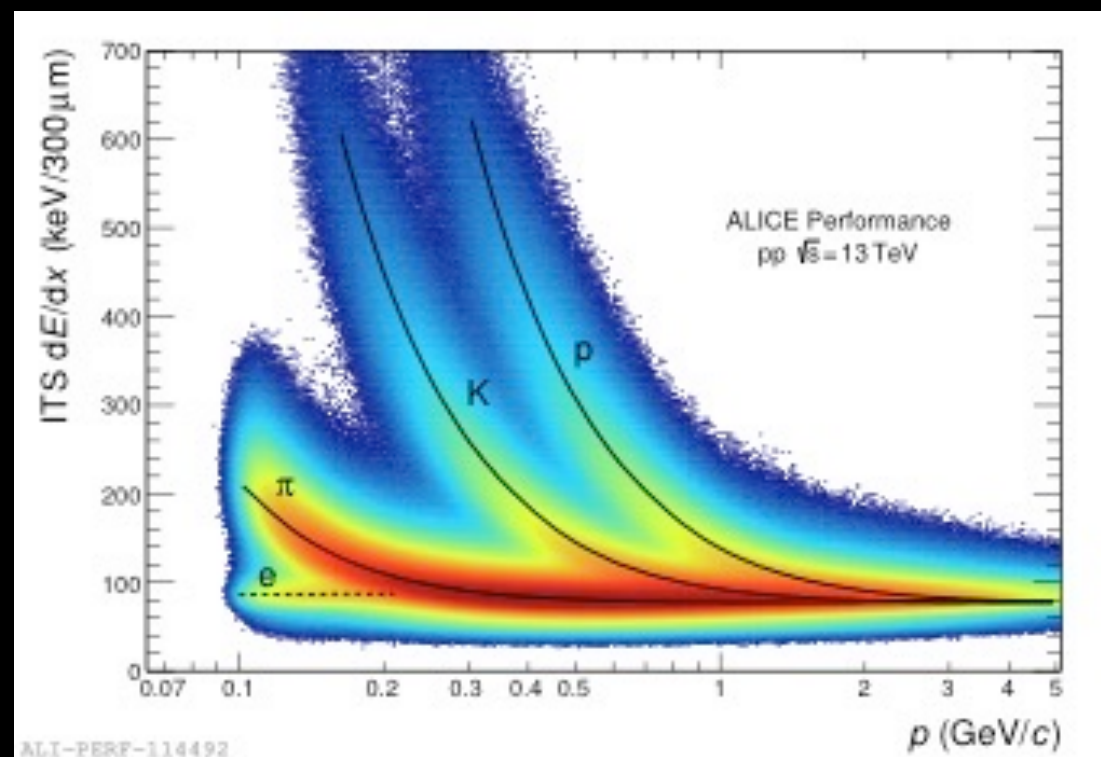
# dE/dx and particle ID

- dE/dx is a function of  $\beta\gamma = P/Mc$  and can be used to separate different particles once p is known
- $\mu/\pi$  separation impossible, but  $\pi/K/p$  generally achievable

ALICE TPC – Gas detectors



ALICE TPC – silicon ITS

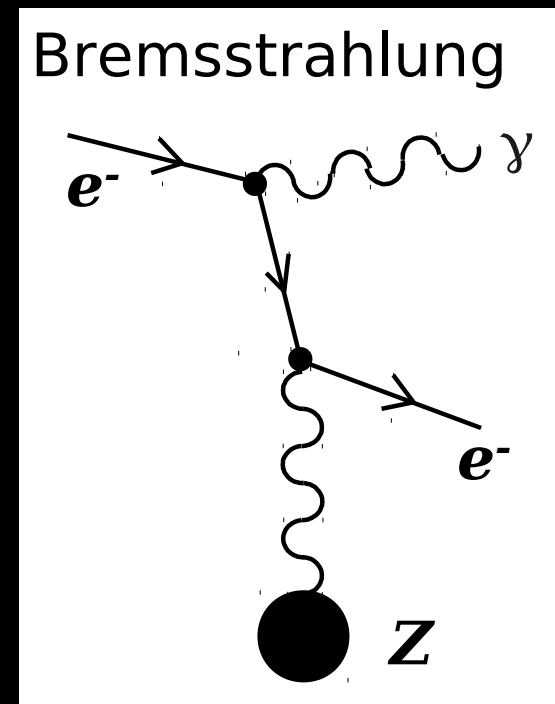


# Electron energy loss

- Electrons lose energy in their interaction with matter mainly through:
  - **Ionization** – modified Bethe-Bloch formula for identical particles
  - **Bremsstrahlung** - energy loss proportional to  $1/m^2$ 
    - Dominant for electrons with  $E_e > 10$  MeV (and for h.e. muons) leading to exponential attenuation of the electron energy

$$\left(\frac{dE}{dx}\right)_{Brem} = -\frac{E(0)}{X_0} \quad E(x) = E(0)\exp\left(-\frac{x}{X_0}\right)$$

- $\langle dE/dx \rangle_{brem}$  increases linearly with the initial energy  $E$
- After a layer of material  $x = X_0$  the electron has  $1/e$  of its initial energy.



$$X_0 \cong \frac{716.4 \text{ g} \cdot \text{cm}^{-2} A}{Z(Z+1)\ln(287/\sqrt{Z})}$$

$X_0 = \text{radiation length g/cm}^2$

Must multiply by density to get a length!

- To contain an electron need small  $X_0$  high  $Z$  materials
- The Moliere radius is the transverse size of the electron shower:

$$R_M \cong \frac{21.2 \text{ MeV}}{E_c} X_0$$

# Total Energy loss and Critical energy

## Critical energy

$$\left. \frac{dE}{dx}(E_c) \right|_{\text{brems}} = \left. \frac{dE}{dx}(E_c) \right|_{\text{ion}}$$

For solid and liquids

$$E_c = \frac{610 \text{ MeV}}{Z + 1.24}$$

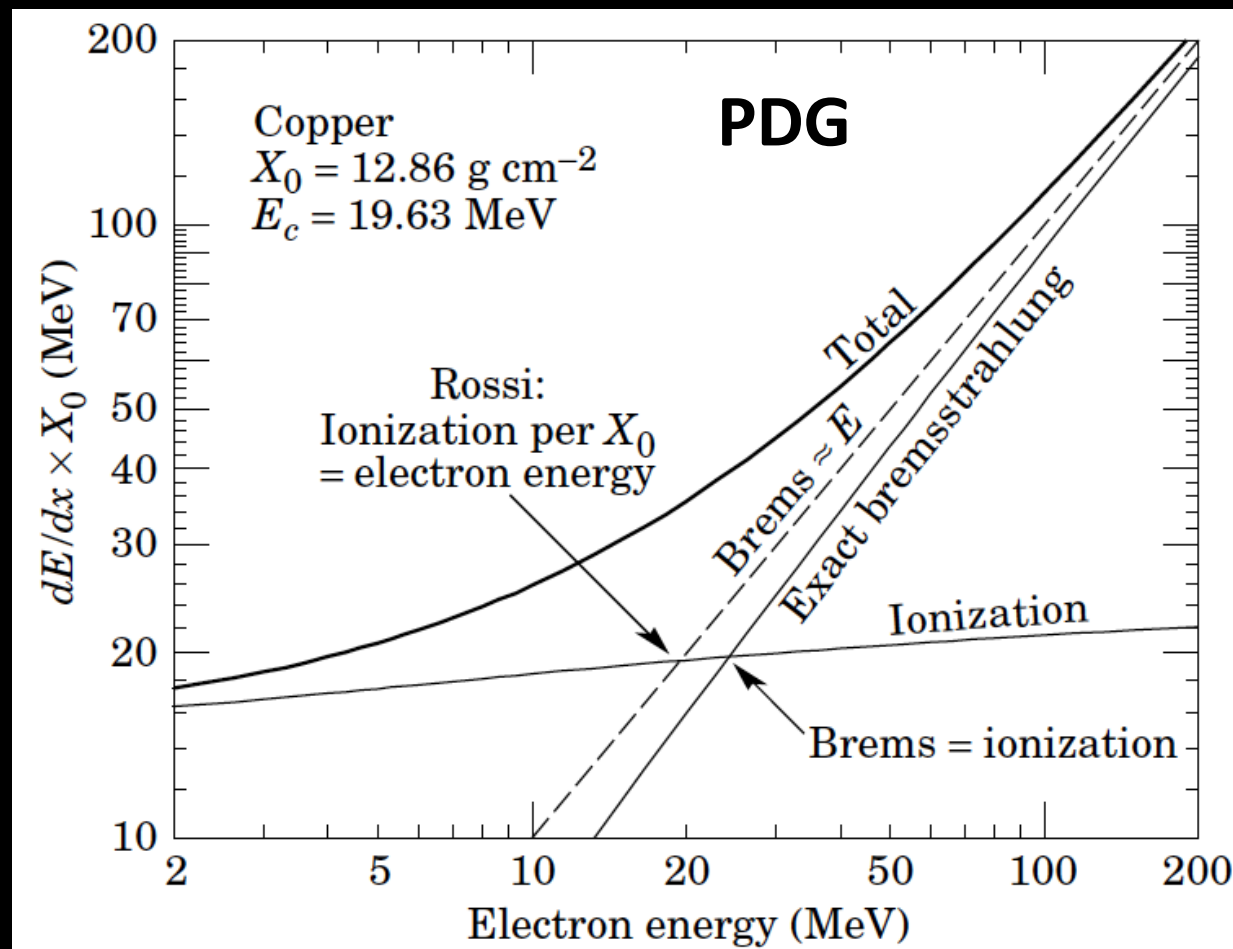
For gasses

$$E_c = \frac{710 \text{ MeV}}{Z + 0.92}$$

Example Copper:

$$E_c \approx 610/30 \text{ MeV} \approx 20 \text{ MeV}$$

$$\left( \frac{dE}{dx} \right)_{\text{Tot}} = \left( \frac{dE}{dx} \right)_{\text{Ion}} + \left( \frac{dE}{dx} \right)_{\text{Brems}}$$



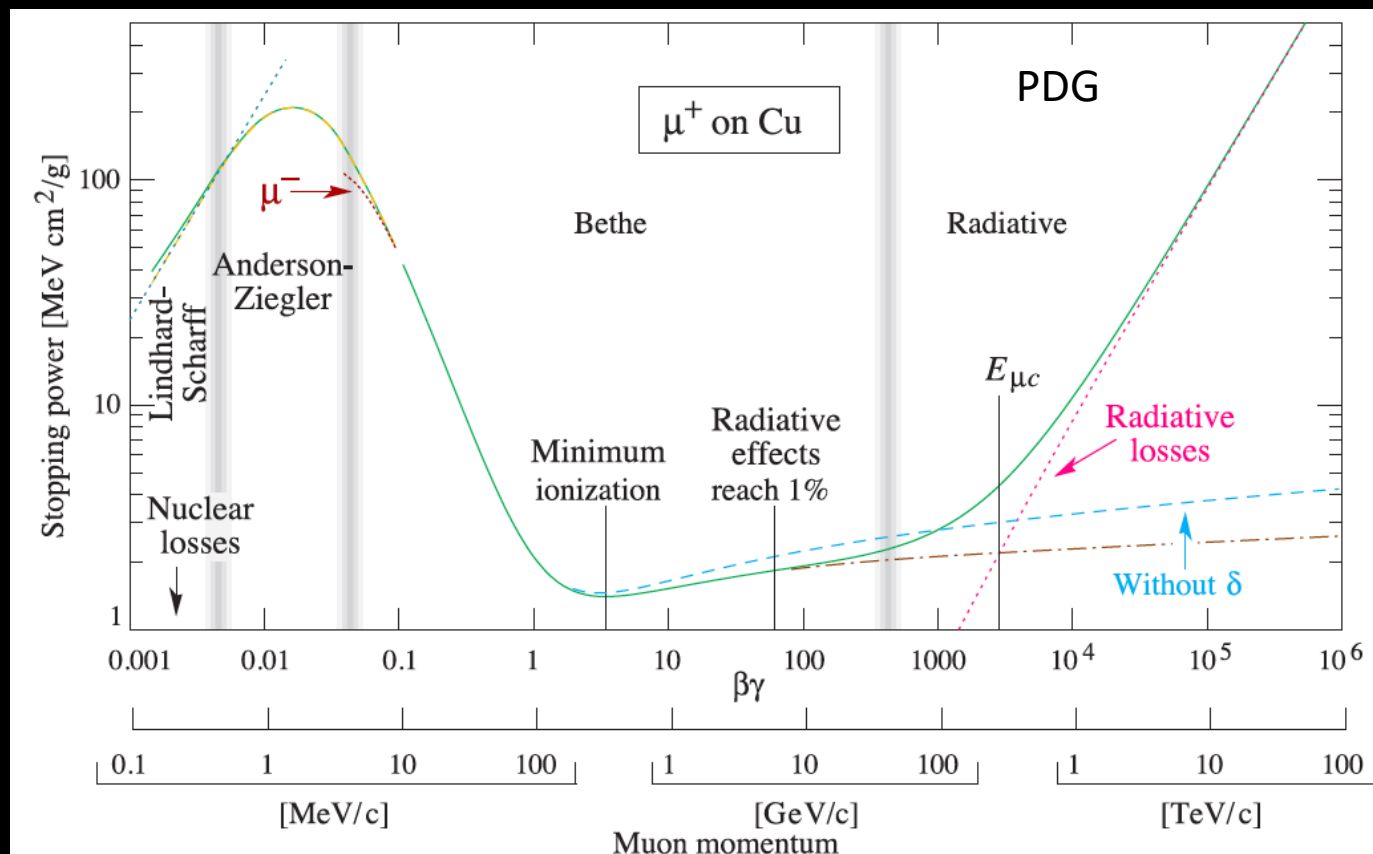


# Muon Energy loss

The bremsstrahlung cross section is proportional to  $1/m^2$

$$-\left\langle \frac{dE}{dx} \right\rangle_{brem} \propto \frac{E}{m^2}$$

Since  $(m_\mu/m_e)^2 \approx 44100$   $E_c$  for muons  $> 100s$  GeV.



- Critical energy for muons is 450 GeV in copper
- At high energies ( $E \gg 1$  TeV) bremsstrahlung contributes about 40% to average muon energy loss.
- Muons with energies  $> \sim 10$  GeV can penetrate thick layers of matter
- This is the key signature for muon identification

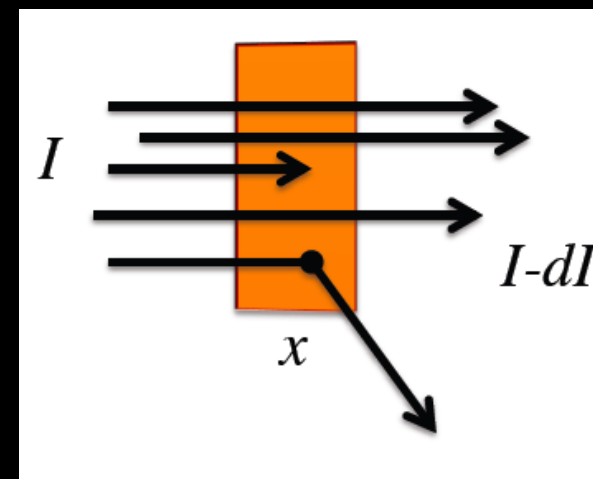
# Interaction of photons with matter

- A photon can disappear or its energy can change dramatically at every interaction

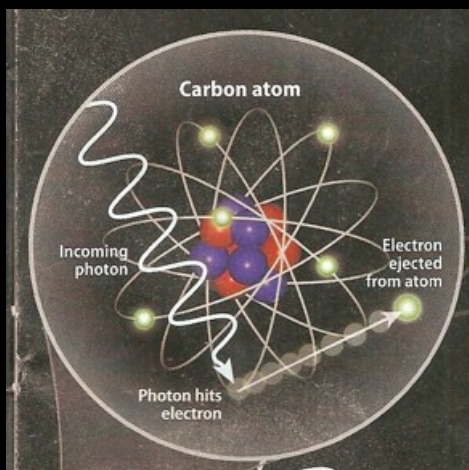
$$I(x) = I_0 e^{-\mu x} \quad \mu = \frac{N_A}{A} \sum_{i=1}^3 \sigma_i$$

$$\lambda = \frac{1}{\mu}$$

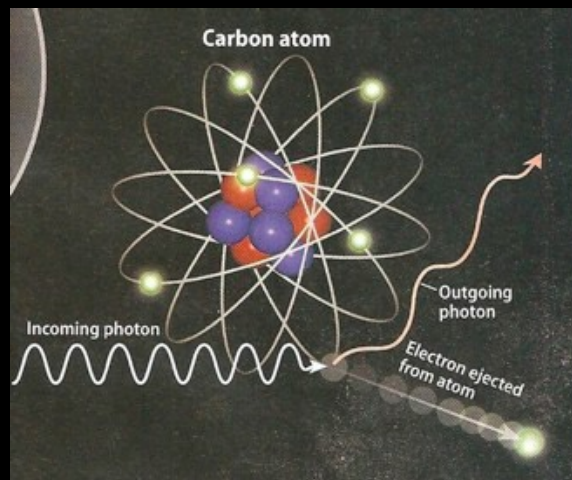
$\mu$ =total attenuation coefficient  
 $\sigma_i$ =cross section for each process



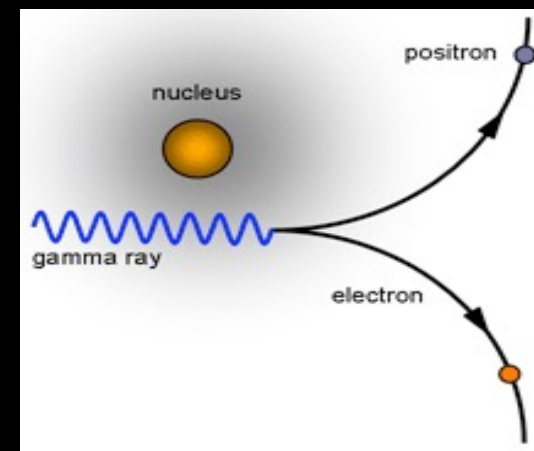
Photoelectric Effect



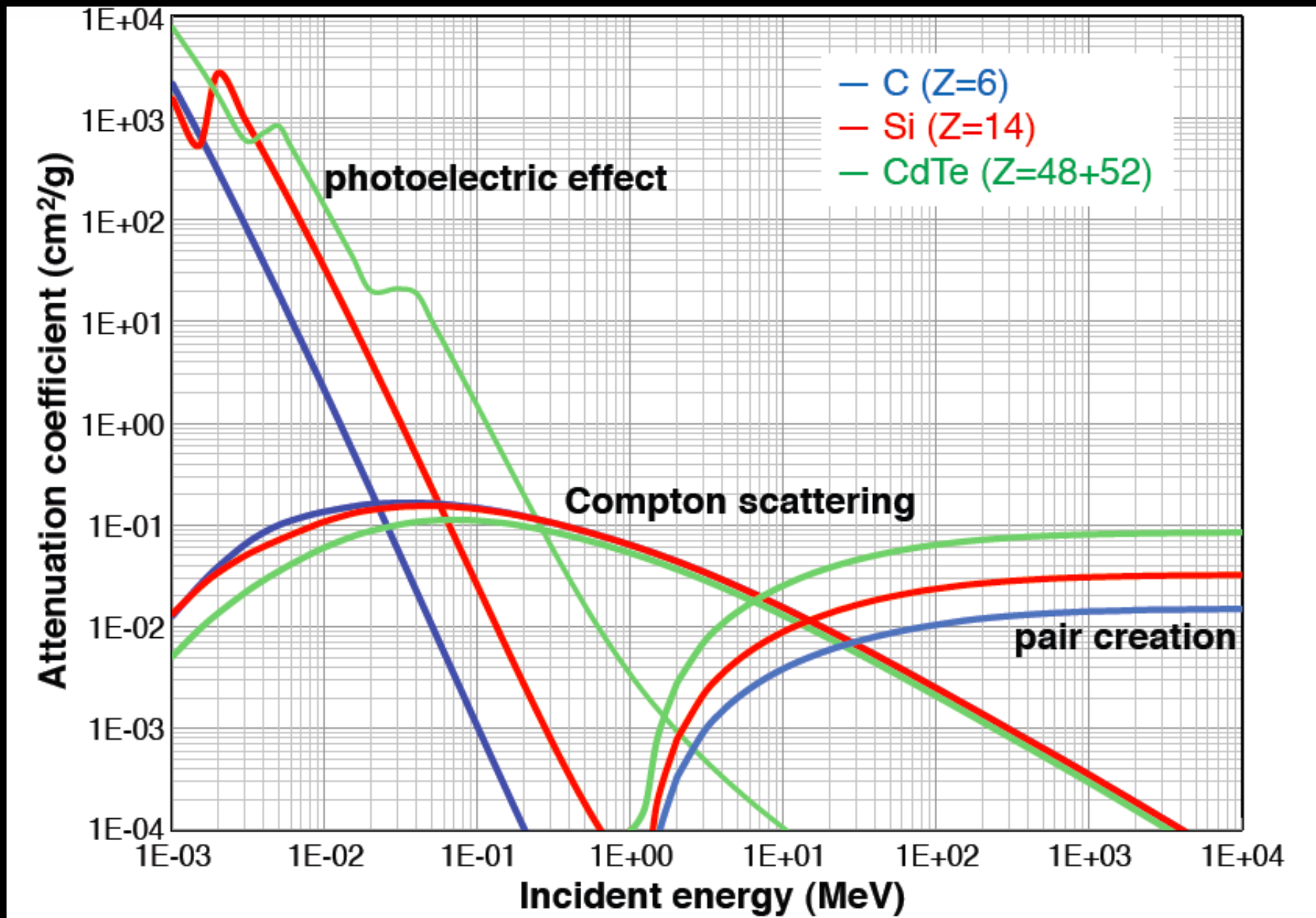
Compton Scattering



Pair production



# Interaction of photons with matter



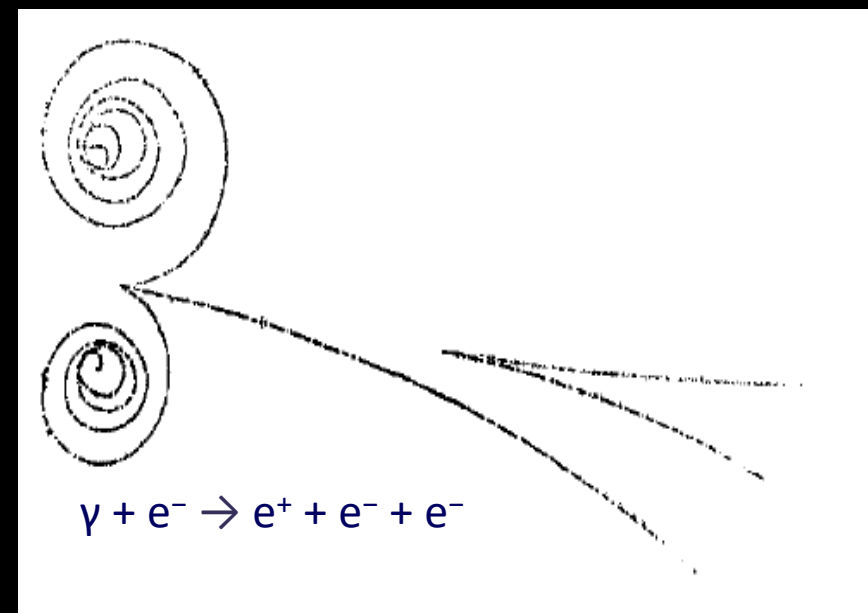
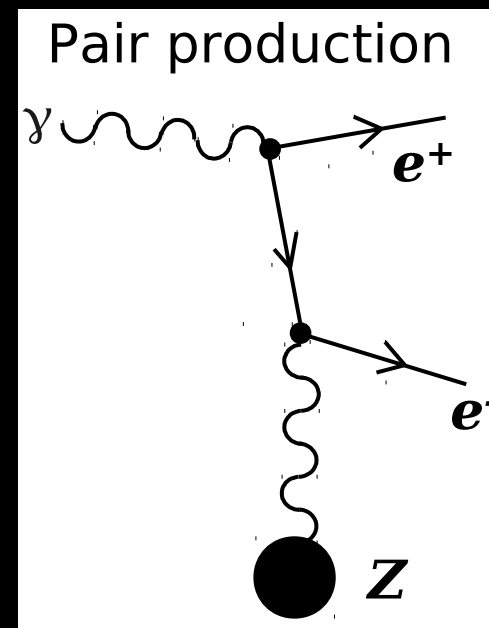
# Pair production

- Photons with  $E > 100$  MeV lose most of their energy in  $e^+e^-$  pair production
  - The threshold in the field of nuclei is  $T = 2m_e c^2 = 1.022$  MeV
- The pair production cross section is:

$$\sigma_{pair} \sim \frac{7}{9} \frac{A}{N_A} \frac{1}{X_0}$$

Where  $A$  is the mass number of the target and  $N_A$  Avogadro Number

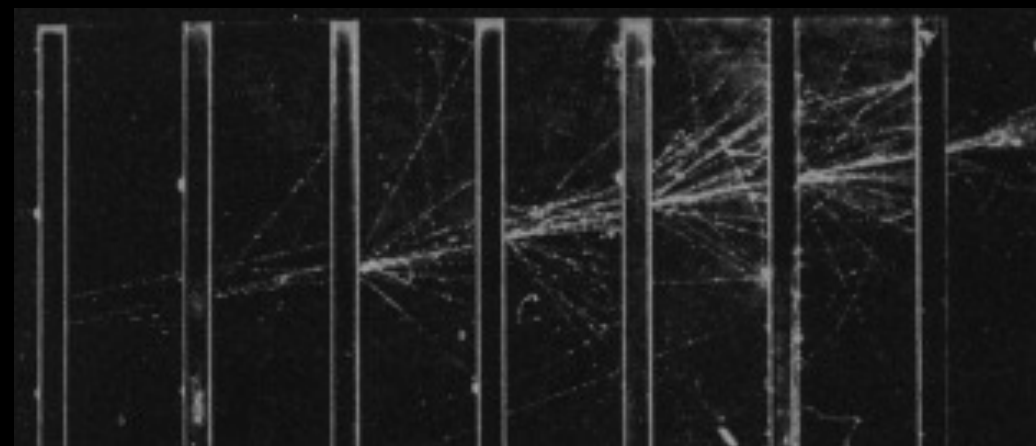
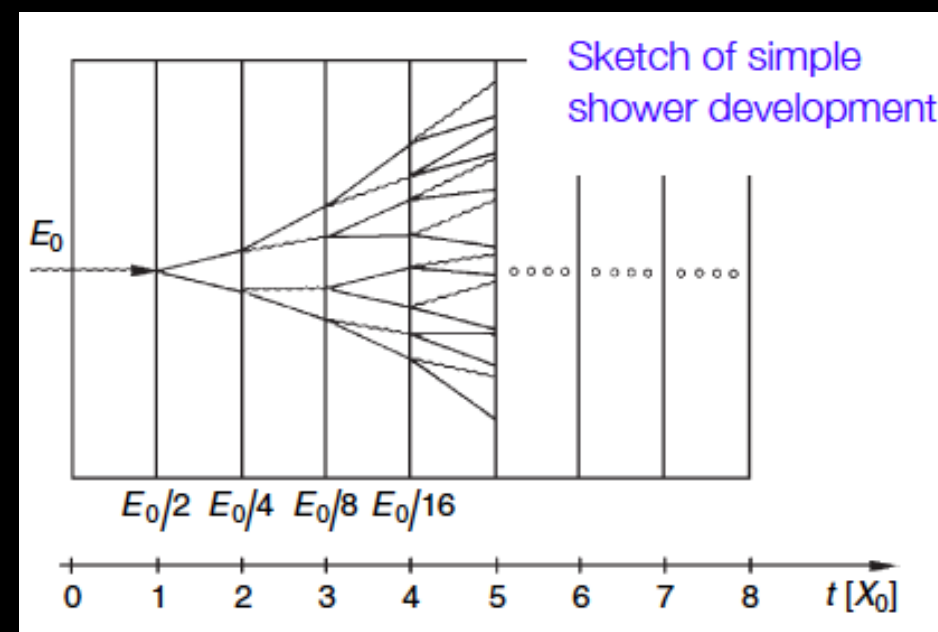
- The radiation length  $X_0$  is also  $7/9$  of the mean free path for pair production by a high-energy photon



# EM showers and $X_0$

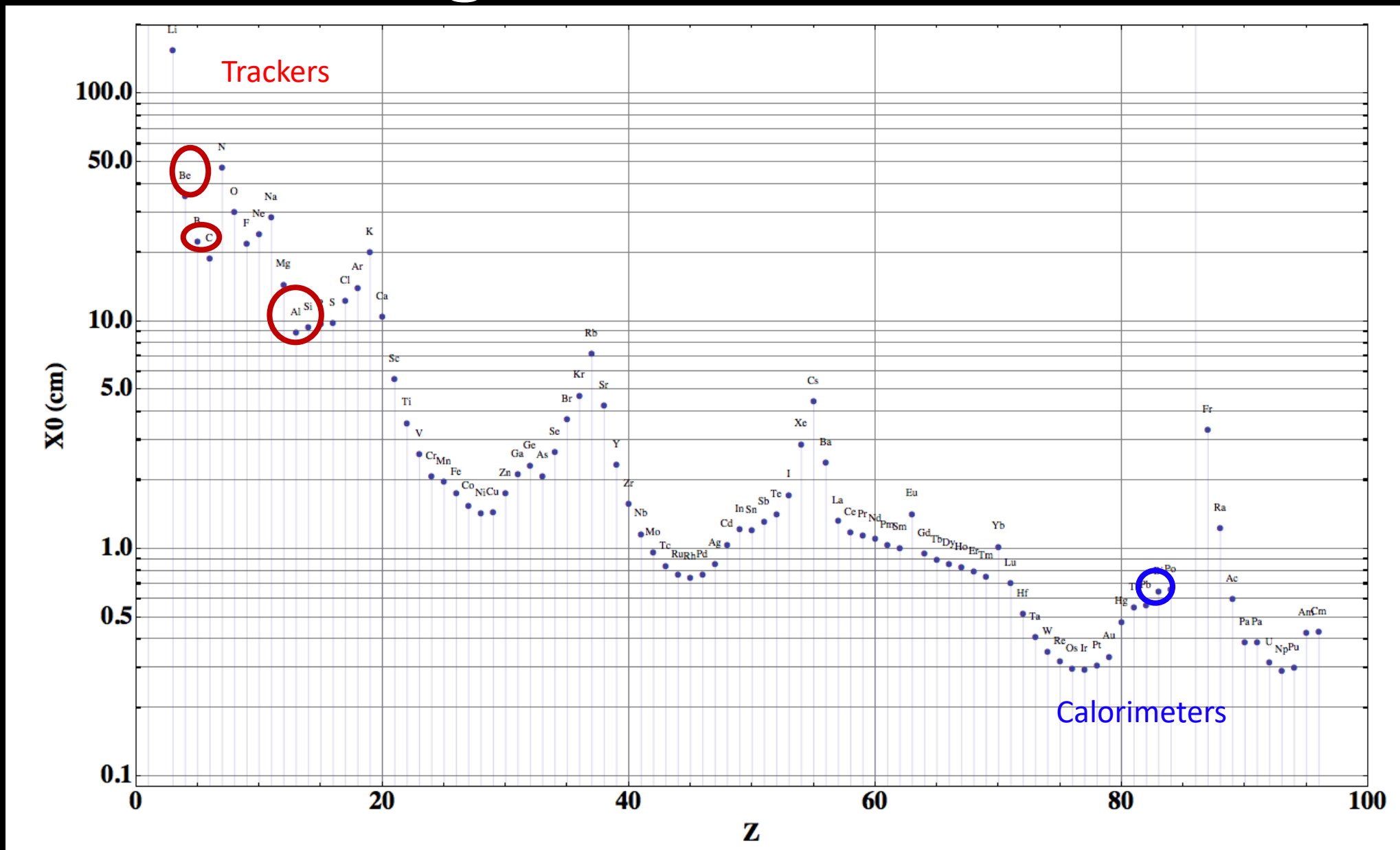
- Simplified model [Heitler]: shower development governed by  $X_0$ 
  - $e^-$  loses  $[1 - 1/e] = 63\%$  of energy in 1  $X_0$  (Brems.)
  - A  $\gamma$  will convert into a  $e^+e^-$  (pair prod.) with a probability  $P = 1 - \exp(-7/9) = 0.54$
- Assume  $e \approx 2$  and that for  $E > E_c$  no energy loss by ionization/excitation
- Simple shower model:
  - $N(t) = 2^t$  particles after  $t = x/X_0$  each with energy  $E(t) = E_0/2^t$
  - Stops if  $E(t) < E_c = E_0 2^{t_{\max}}$
  - Location of shower maximum at

$$t_{\max} = \frac{\ln(E_0/E_c)}{\ln 2} \propto \ln \left( \frac{E_0}{E_c} \right)$$



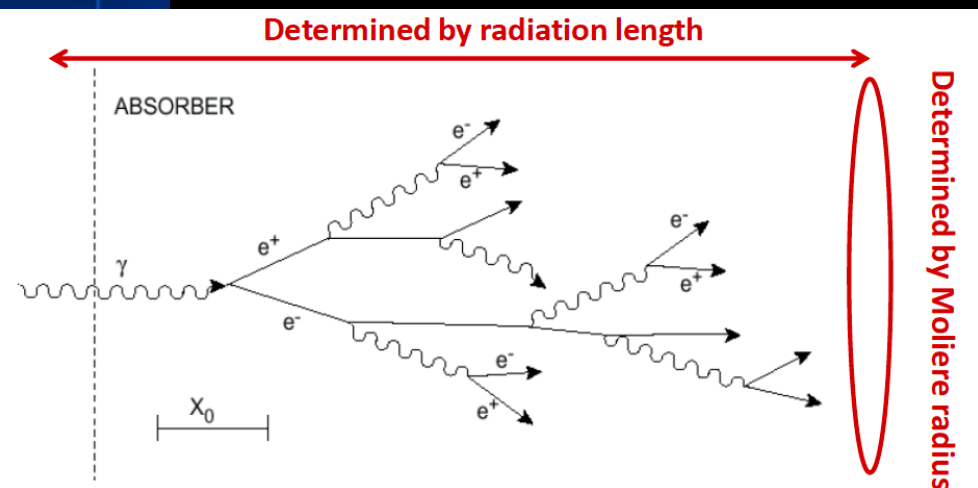
$$N_{\max} = 2^{t_{\max}} = \frac{E_0}{E_c}$$

# Radiation length of different elements

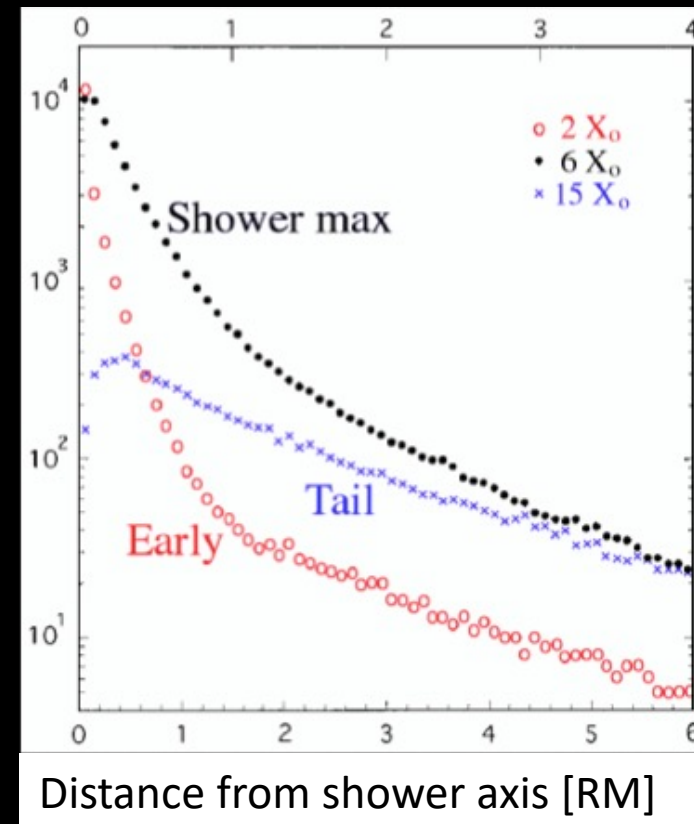
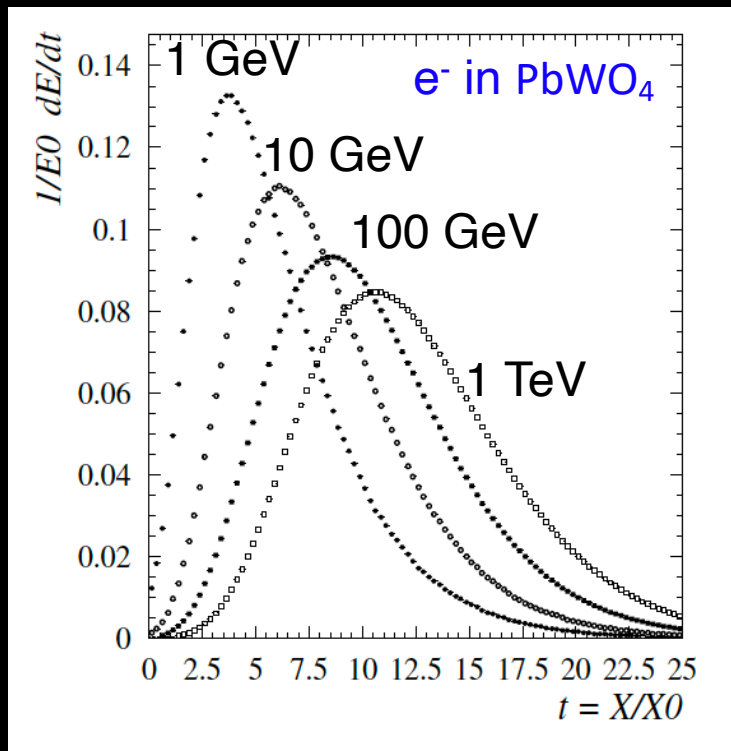


# EM Shower development

Transverse development for 10 GeV electron showers in Cu



## Longitudinal development



- Size of calorimeter driven by  $X_0$
- Cell size related to  $R_M$  and chosen such that 70-80% of energy of a particle is deposited in the cell
- Granularity: size of detector elements in transverse and longitudinal direction. Determines the ability to resolve two showers induced by nearby particles

95% of energy within:  
 $L(95\%) = t_{max} + 0.08 Z + 9.6 X_0$

$$X_0 = \frac{180A}{Z^2} \text{ (g cm}^{-2}\text{)} \text{ and } t_{max} = \ln \frac{E}{E_c} - 1$$

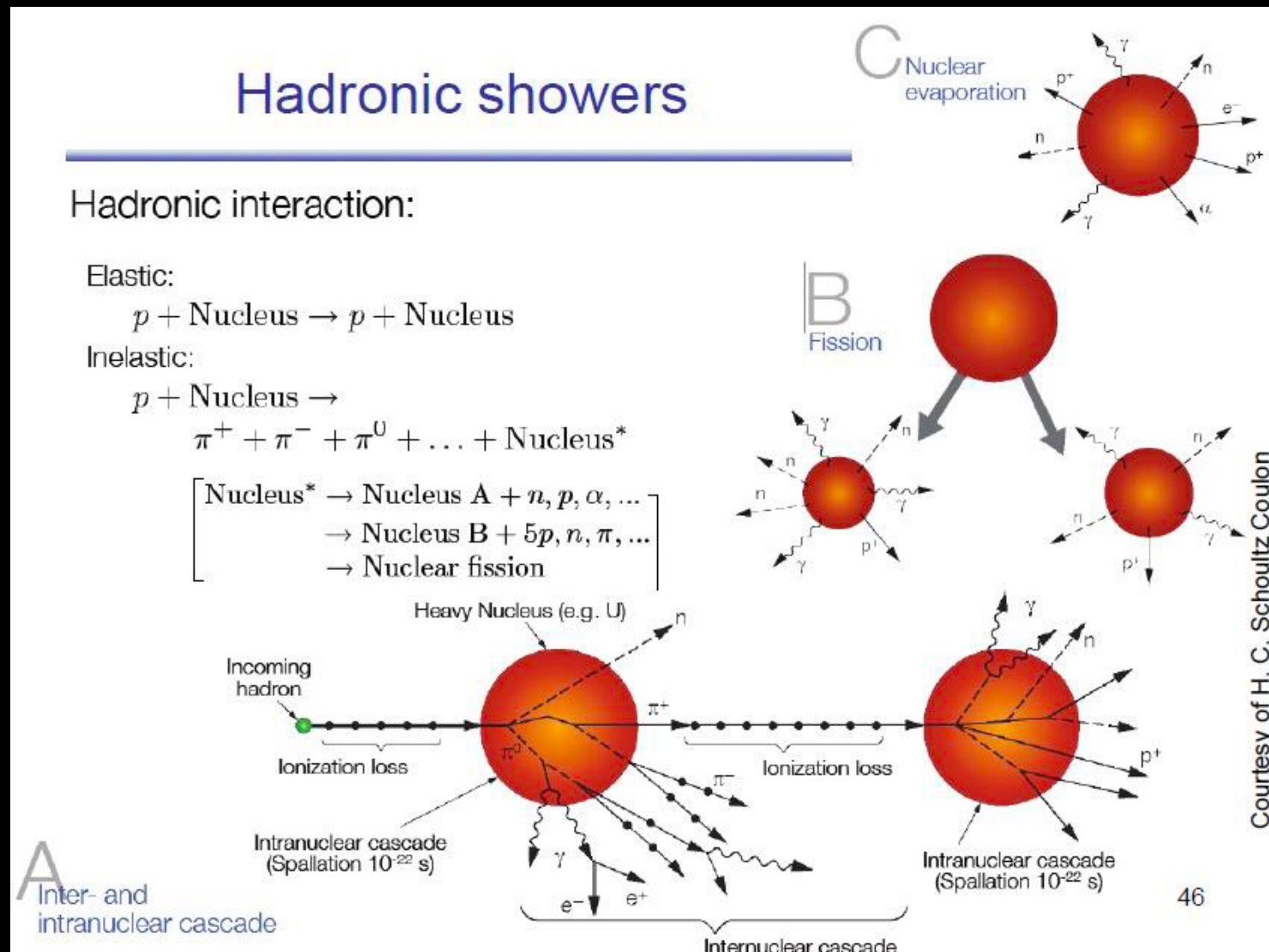
(for e induced showers)

90% of energy:  $R_M$   
 Beyond shower max  
 broadening due to low energy  $\gamma$

$$R_M = \frac{21 \text{ MeV}}{E_c} X_0$$

# Hadron interactions with matter

- Many processes involved:
  - Ionization,
  - hadron production (fragmentation, ...)
  - Charge exchange  $\pi^{+/-}n \rightarrow \pi^0 p/pbar$
  - nuclear de-excitation,
  - nuclear breakup,
  - spallation neutrons,
  - muon and pion decay+
  - .....





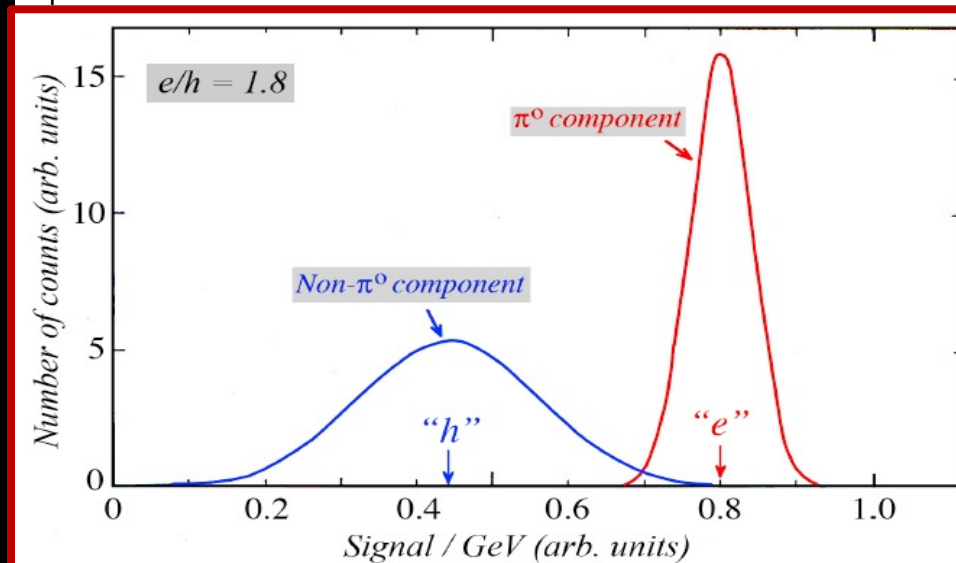
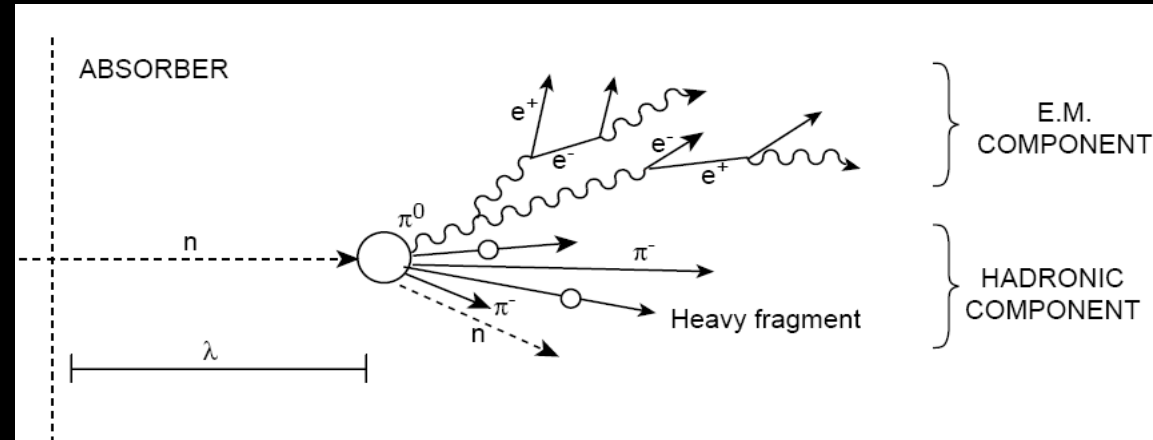
# Hadronic Showers

- **Electromagnetic component:**

- Electrons, photons (from excitation, radiation, decay of hadrons, photo-effect, ...)
- Neutral pions (eg,  $\pi^0 \rightarrow \gamma\gamma, \eta \rightarrow \gamma\gamma$ )

- **Hadronic component:**

- Charged hadrons  $\pi^\pm, K^\pm, \dots$ : ionization, excitation, nuclei interaction (spallation p/n production, evaporation n, spallation products)
- Neutrons: Elastic collisions, thermalization + capture ( $\Rightarrow \gamma$ 's)
- Break-up of nuclei



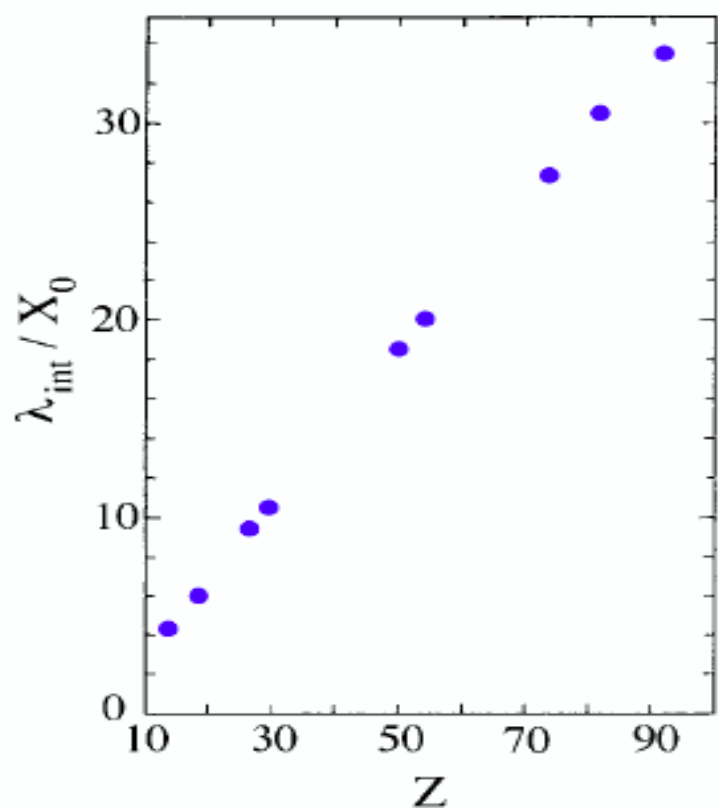
Part of the energy is lost in breaking nuclei (nuclear binding energy)

- Large **non-Gaussian** fluctuations of each component (EM vs non-EM)
- Large, **non-Gaussian** fluctuations in “invisible” energy losses

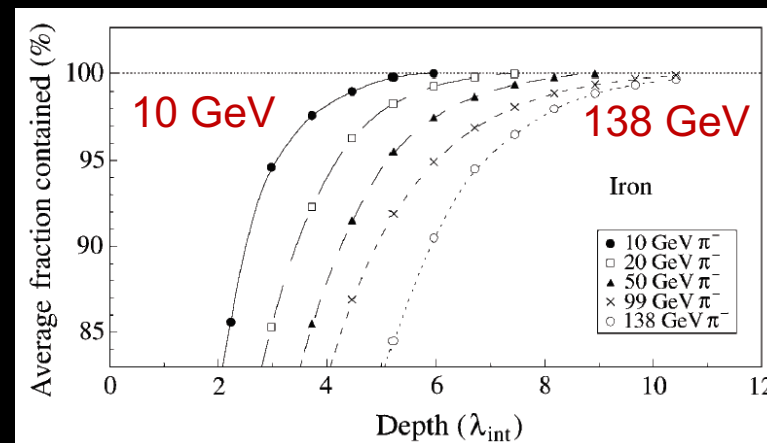
# Nuclear Interaction Length

- Hadronic showers are governed by the interaction length  $\lambda_{int}$ : the mean free path between inelastic interaction

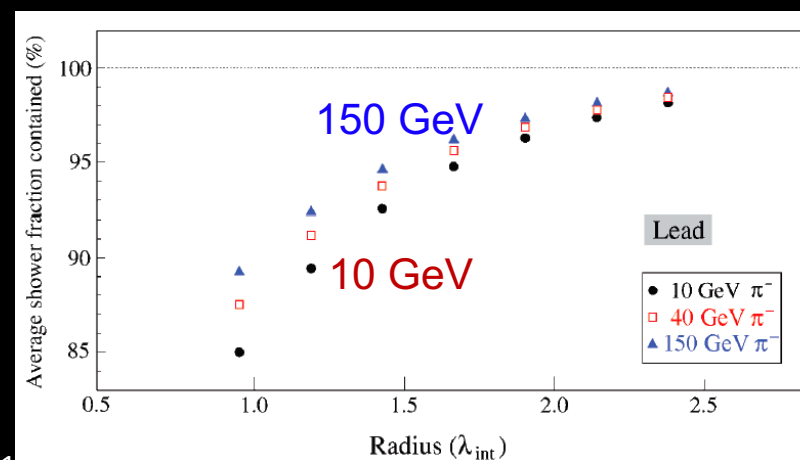
$$\lambda_{int} \approx \frac{35 \text{ cm}}{\rho} A^{1/3}$$



- **Longitudinal:** Need about  $\sim 10 \lambda_{int}$  to contain most of the hadronic showers



- **Transverse:** Need about  $\sim 1.5 \lambda_{int}$  to contain most of the hadronic showers



# Nuclear Interaction length

- To contain an hadronic, you need small  $\lambda_{int}$
- $\lambda_{int}$  (Fe)=17 cm

	Lead	Iron
<b>Ionization by pions</b>	19%	21%
<b>Ionization by protons</b>	37%	53%
<b>Total ionization</b>	56%	74%
<b>Nuclear binding energy loss</b>	32%	16%
Target recoil	2%	5%
<b>Total invisible energy</b>	34%	21%
<b>Kinetic energy evaporation neutrons</b>	10%	5%
Number of charged pions	0.77	1.4
Number of protons	3.5	8
Number of cascade neutrons	5.4	5
Number of evaporation neutrons	31.5	5
<b>Total number of neutrons</b>	36.9	10
<b>Neutrons/protons</b>	10.5/1	1.3/1

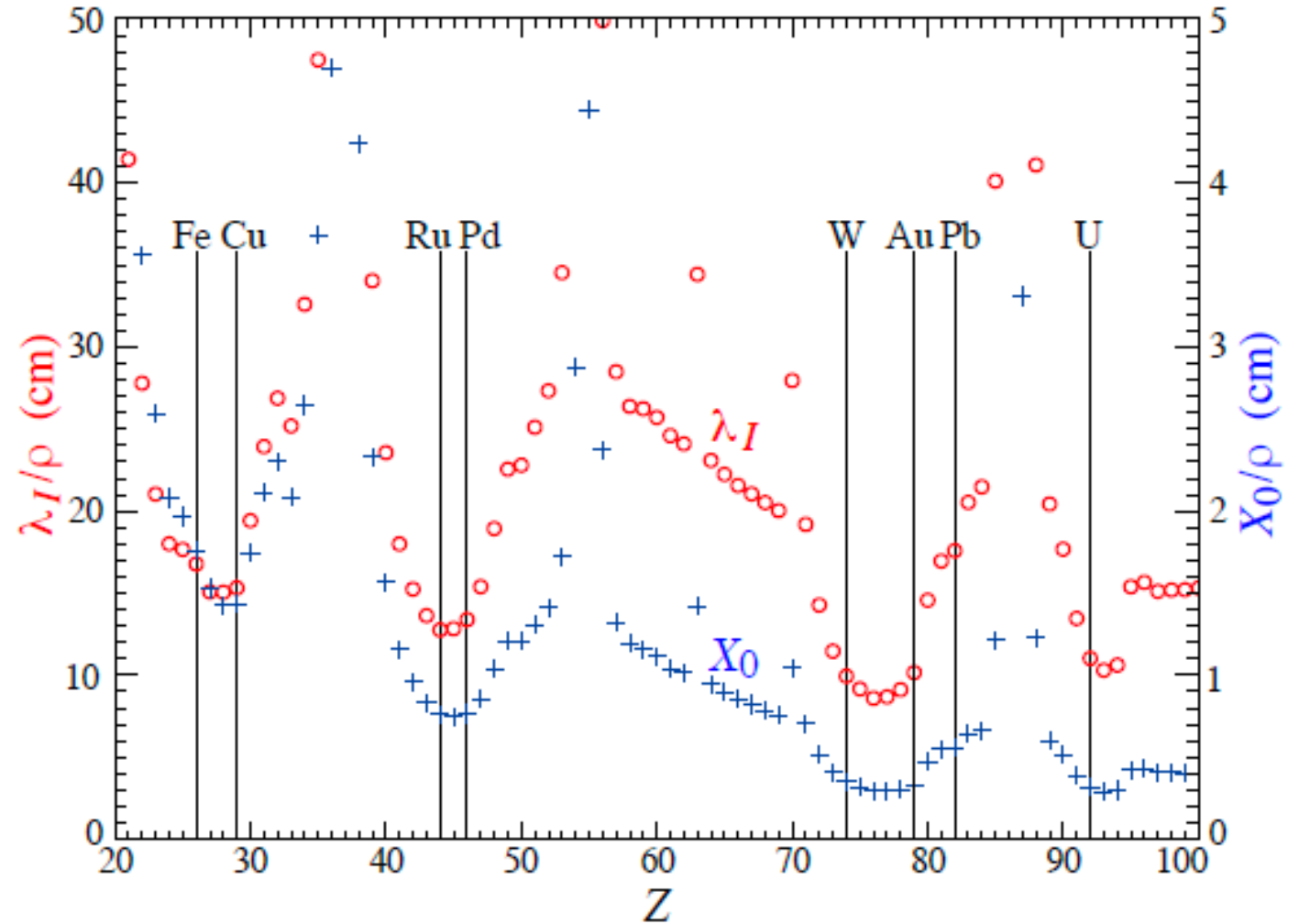
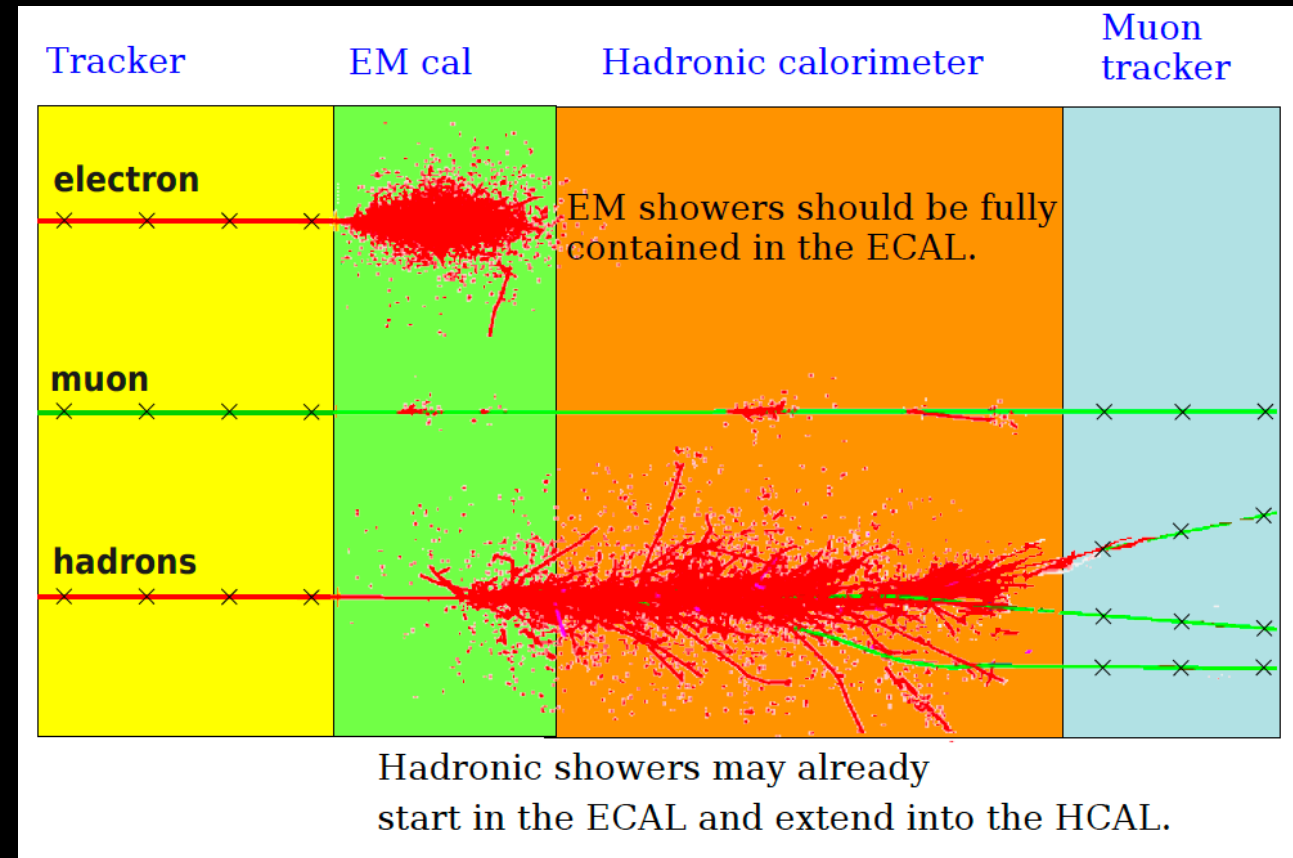


Figure 34.21: Nuclear interaction length  $\lambda_I/\rho$  (circles) and radiation length  $X_0/\rho$  (+'s) in cm for the chemical elements with  $Z > 20$  and  $\lambda_I < 50$  cm.

# Calorimetry

- Calorimetry refers to the detection of particles through total absorption in a block of matter
  - The measurement process is destructive for almost all particle
  - The exception are muons (and neutrinos) → identify muons easily since they penetrate a substantial amount of matter
- Calorimeters are essential to measure neutral particles

- **Homogenous calorimeters:** whole volume filled by high-density material (BGO, Lead glass, noble gases ...)
  - Exclusively used for EM part
  - Best resolution
  - Expensive



- **Sampling calorimeters:** alternating layers of “absorbers” and active materials
  - Absorbers: Iron, Copper, Lead....
  - Active: Plastic scintillators, silicon detectors, gas detectors...

# Energy resolution

- Calorimeters are the ideal instrument to measure the full energy of particles, particularly at high momentum

$$E \propto N \quad \sigma_E \approx \sqrt{N} \approx \sqrt{E}$$

$$\sigma_E = a\sqrt{E} \oplus bE \oplus c$$

$$\frac{\sigma_E}{E} = \frac{a}{\sqrt{E}} \oplus b \oplus \frac{c}{E}$$

■ a: stochastic term

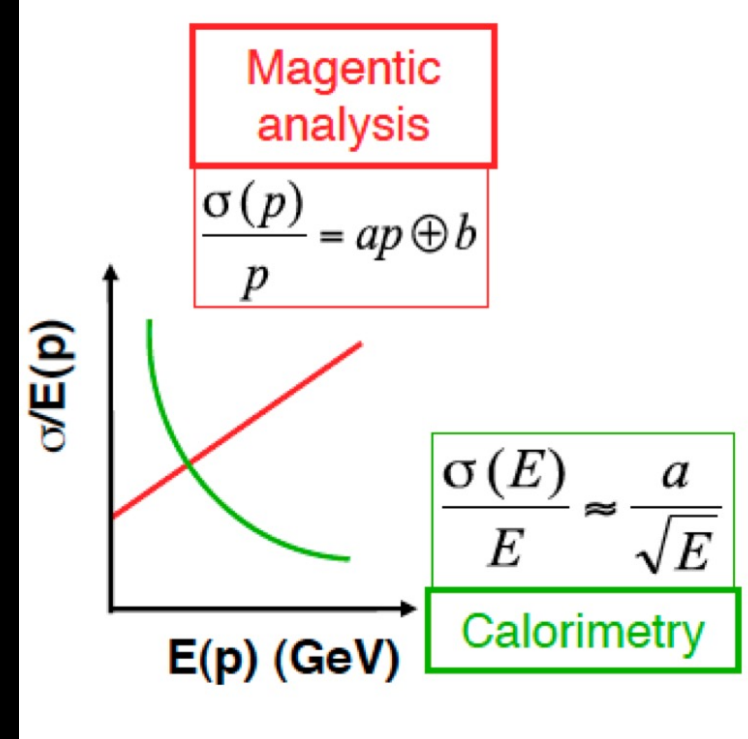
- intrinsic statistical shower fluctuations
- sampling fluctuations
- signal quantum fluctuations (e.g. photo-electron statistics)

■ c: noise term

- readout electronic noise
- Radio-activity, pile-up fluctuations

■ b: constant term

- inhomogeneities (hardware or calibration)
- imperfections in calorimeter construction (dimensional variations, etc.)
- non-linearity of readout electronics
- fluctuations in longitudinal energy containment (leakage can also be  $\sim E^{-1/4}$ )
- fluctuations in energy lost in dead material before or within the calorimeter





# The CMS detector

## Inner tracker

75M silicon pixels and strips

## Electromagnetic calorimeter (ECAL)

76,000  $\text{PbWO}_4$  crystals

## Hadronic calorimeter (HCAL)

brass / plastic scintillator

## Superconducting solenoid

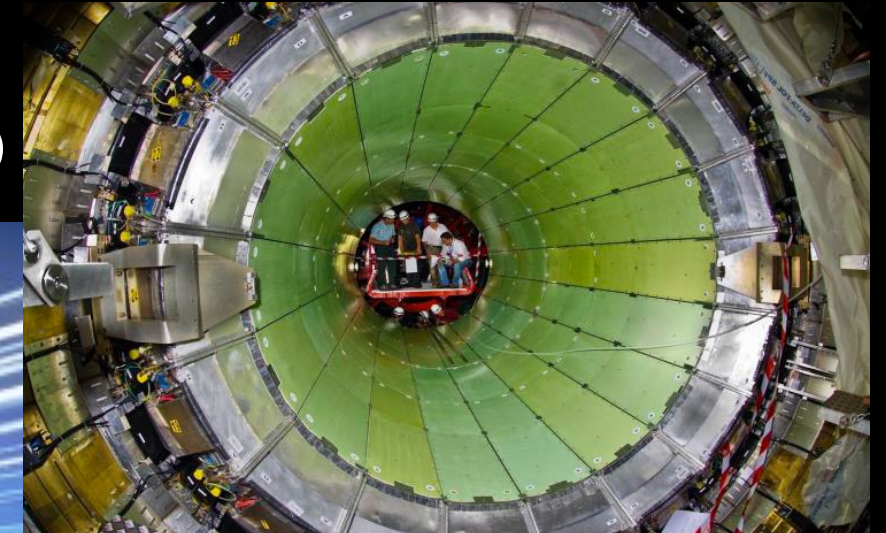
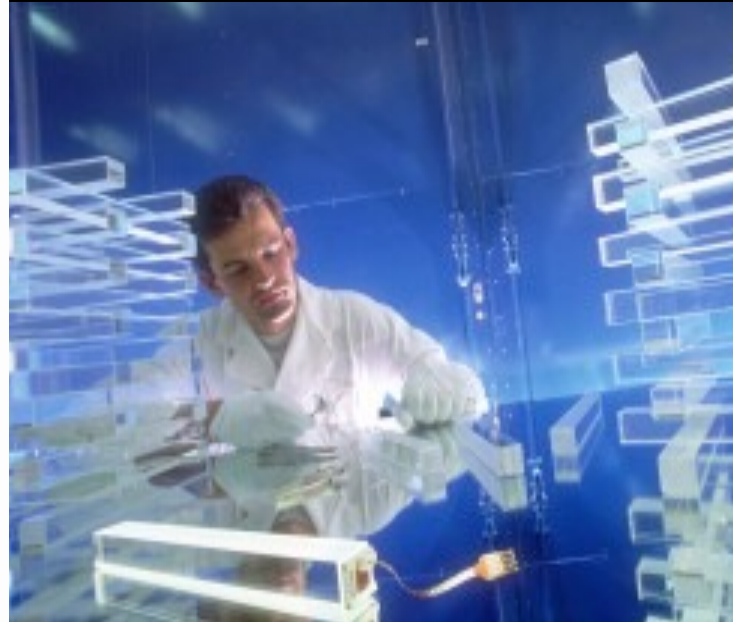
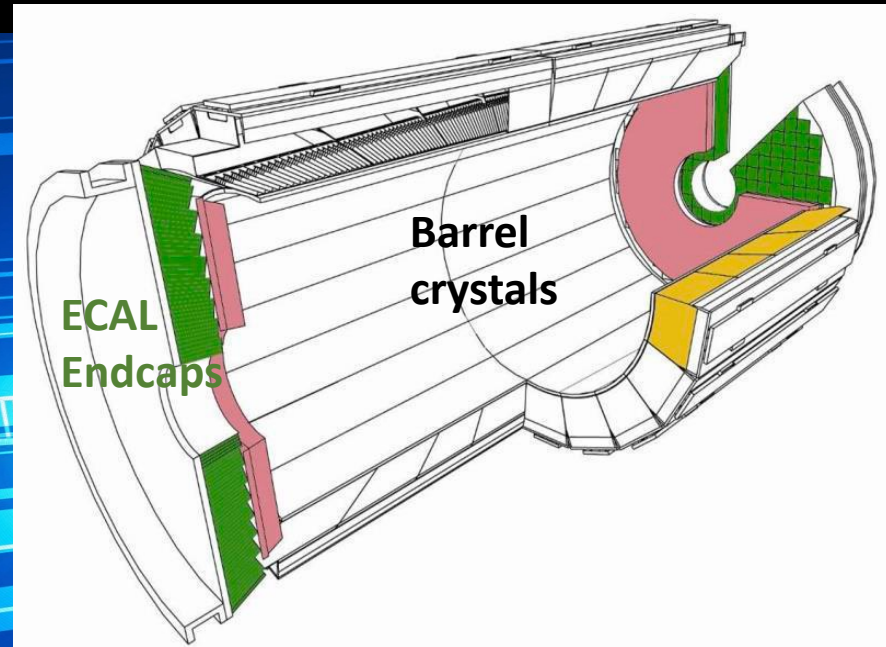
providing 3.8 T magnetic field

## Muon chambers

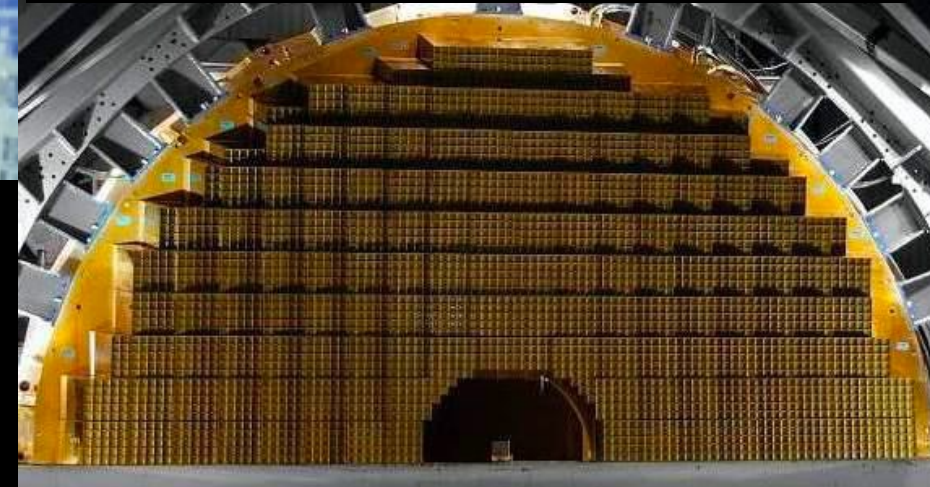
embedded in the steel return yoke

# CMS ECAL

Homogeneous Ecal,  $\text{PbWO}_4$  crystals 23 (22) cm long in Barrel (endcap)



- Barrel ( $|\eta| < 1.48$ ),  $\sim 67$  t
- 61200 crystals in 36 super-modules

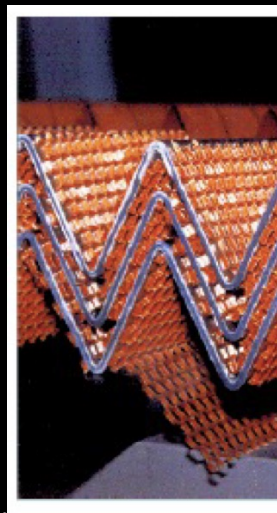
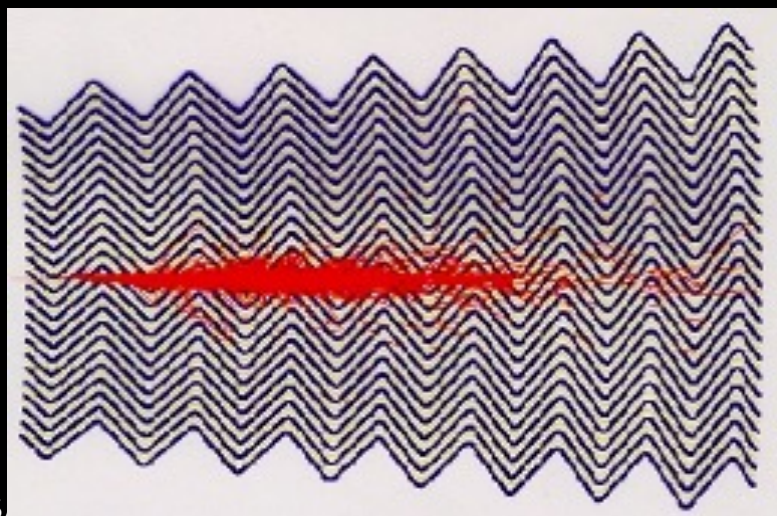


- Endcap I ( $1.48 < |\eta| < 3$ ),  $\sim 23$  t
- 14648 crystals over 4 Dees (2 per endcap)

- Excellent energy resolution
  - $X_0 = 0.89$  cm  $\Rightarrow$  compact calorimeter
  - $R_M = 22$  cm  $\Rightarrow$  compact shower development
- Fast light emission
- Radiation hard ( $10^5$  Gy)
- But low light yield ( $150 \gamma/\text{MeV}$ ) and response depends on Temperature and dose

# ATLAS ECAL

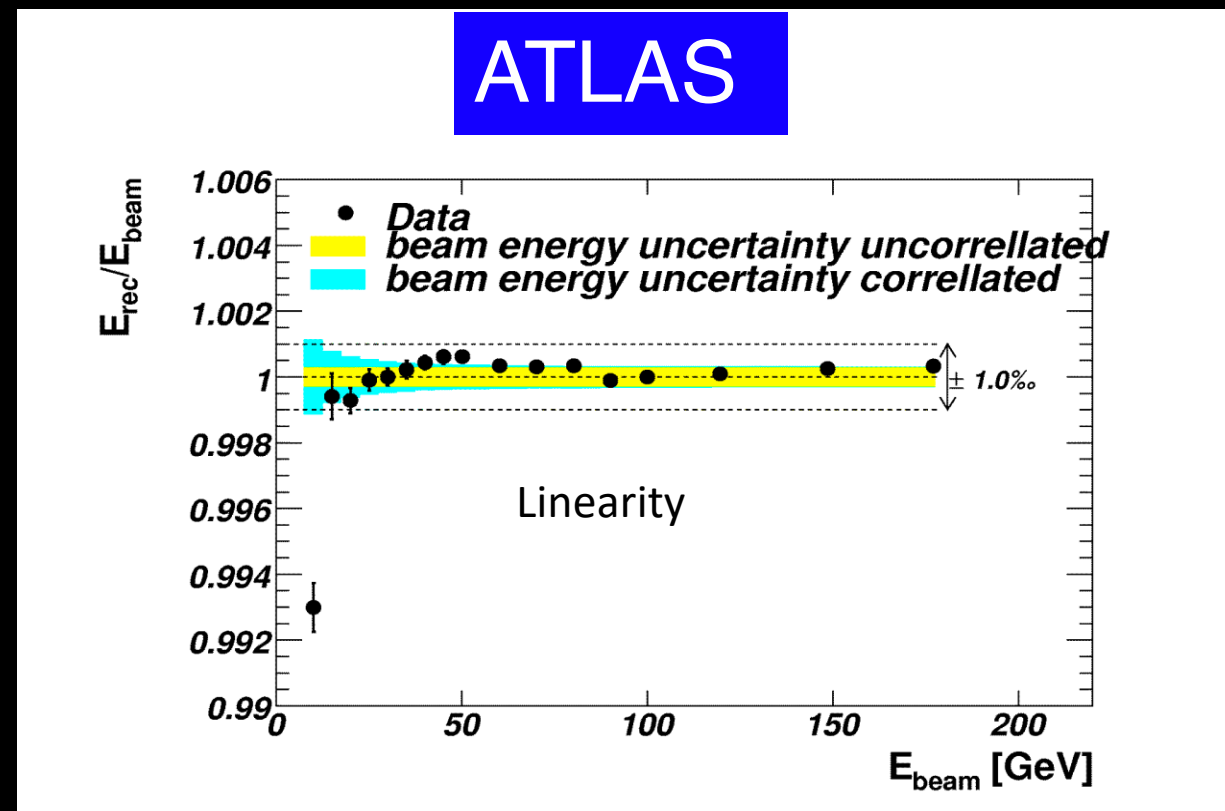
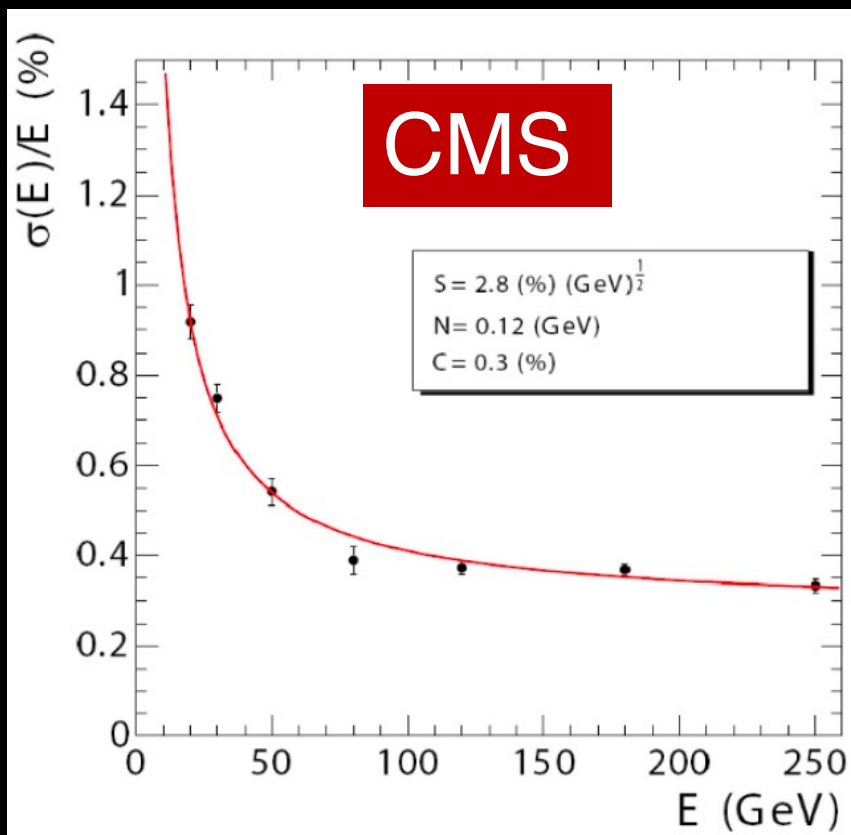
- Sampling Pb/LAr calorimeter with “accordion” geometry
- Longitudinal depth  $\sim 25 X_0$ , (47 cm vs 22 cm for CMS)
- 3 layers up to  $|\eta|=2.5$
- 2 layers  $2.5 < |\eta| < 3.2$
- Usage of Liquid Argon
  - Radiation Hard
  - High number of electron-ion pair produced by ionization (1 GeV deposit  $\rightarrow 5 \times 10^6 e^-$ )
  - Stable vs time but needs cryostat (90K)





# CMS and ATLAS calorimeter performance

- Standalone performance in test beams

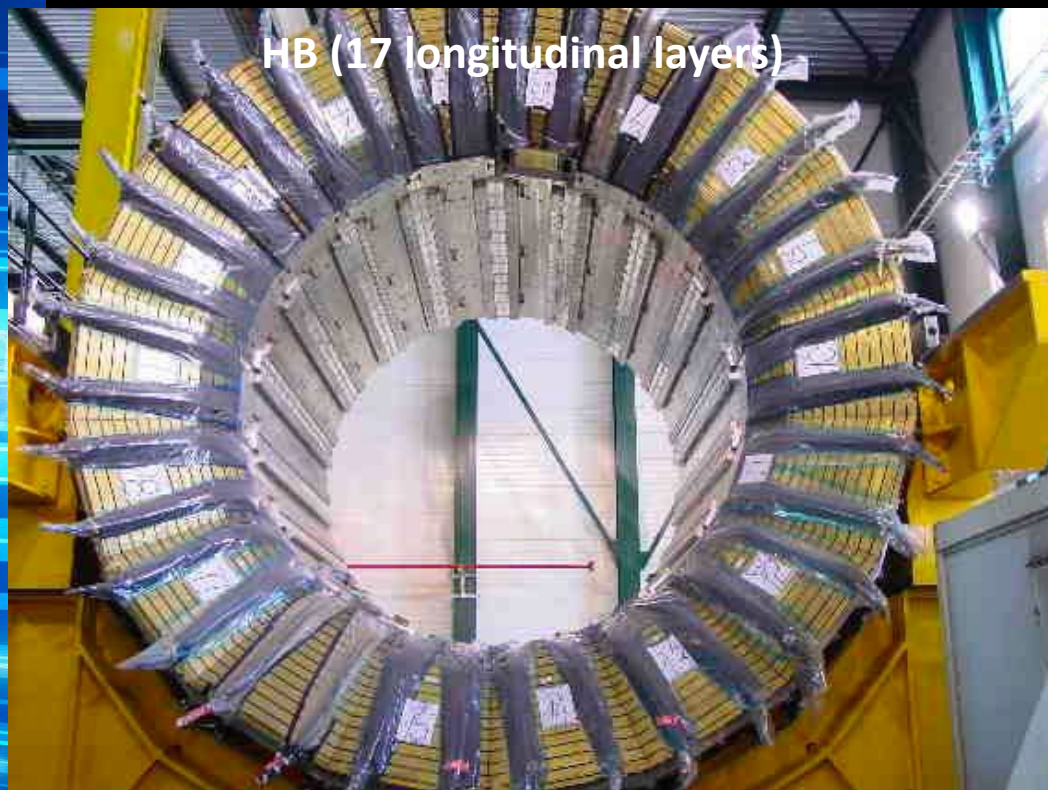


$$\frac{\sigma}{E} = \frac{2.8\%}{\sqrt{E(\text{GeV})}} \oplus \frac{125}{E(\text{MeV})} \oplus 0.3\%$$

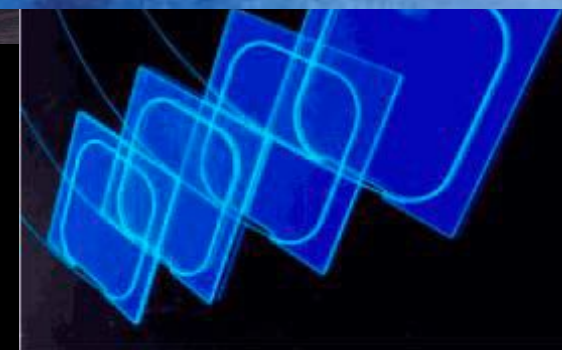
$$\frac{\sigma}{E} = \frac{10\%}{\sqrt{E}} \oplus \frac{0.3}{E} \oplus 0.7\%$$

# CMS HCAL

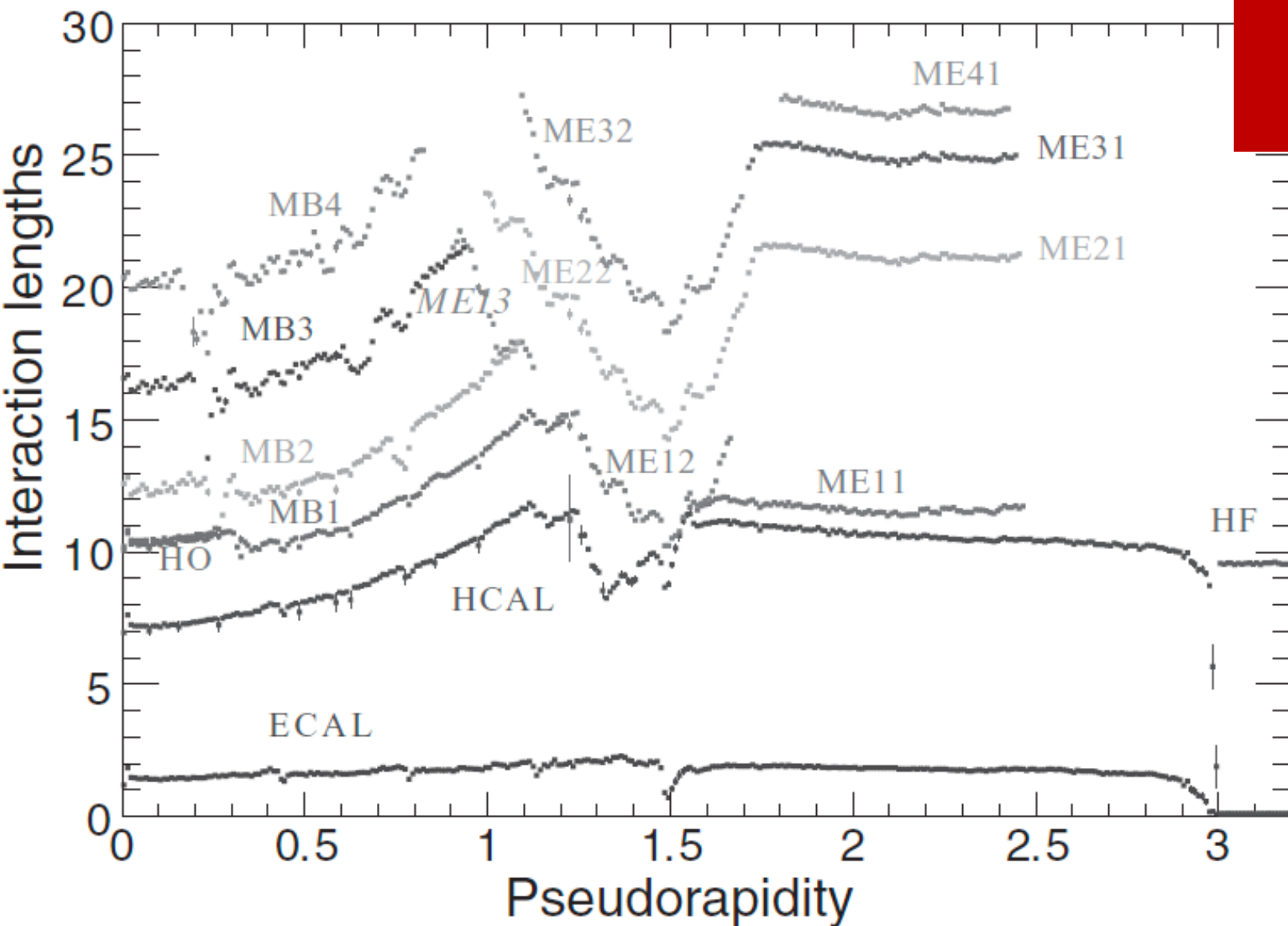
- HB/HE: Sampling Brass/plastic scintillator calorimeter



Segmentation:  $\Delta\eta \times \Delta\phi = 0.087 \times 0.087$  (larger at high  $\eta$ )  
8x20° “wedges” with alternate brass plates (5-8 cm) and “tiles” embedded with Wave Length Shifter (WLS).  
Light from scintillator: blue-violet → WLS: absorb light then fluorescence in green → Green light read by Hybrid Photo Diode (HPD)



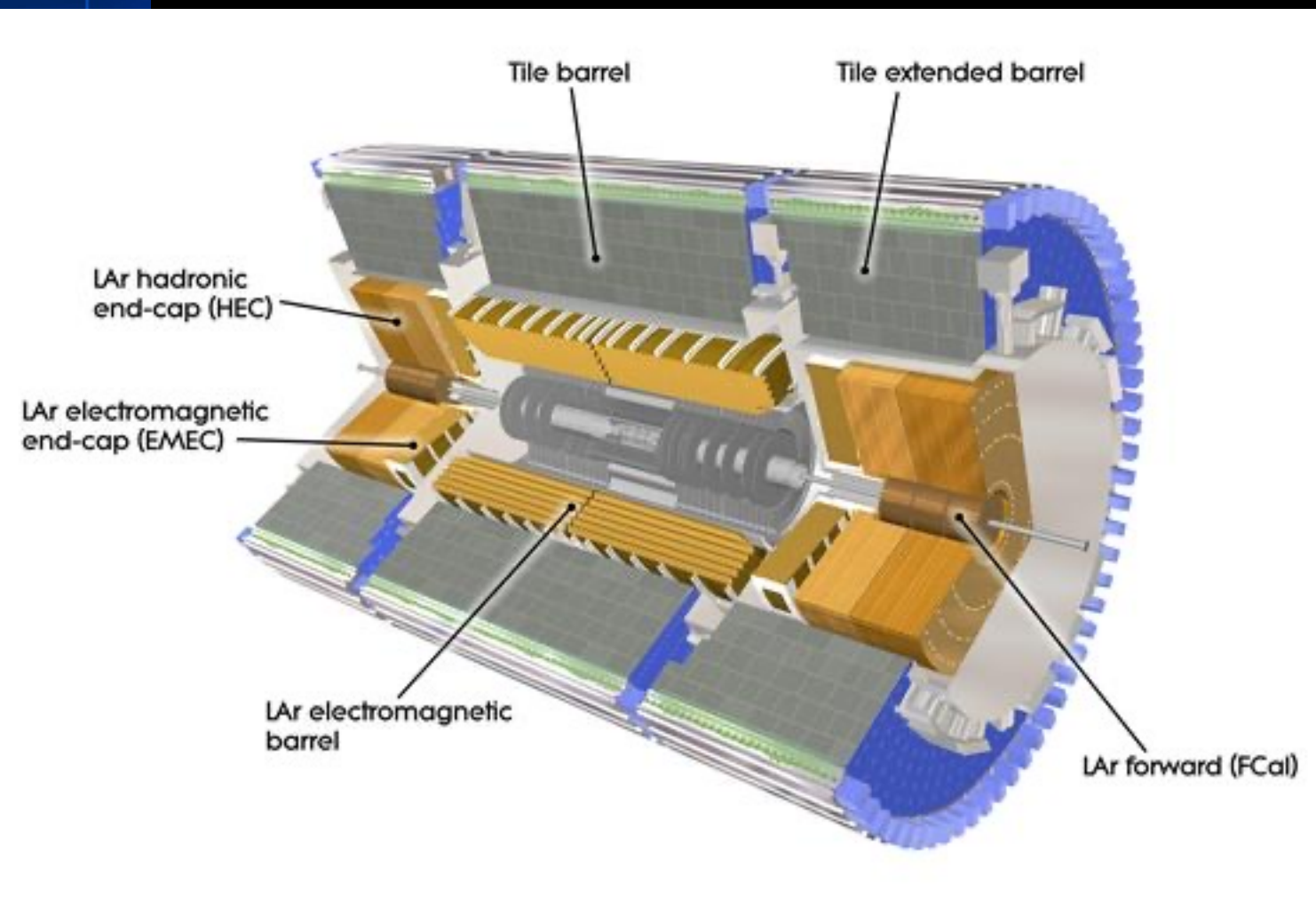
# CMS HCAL



- At  $|\eta|=0$ ,  $\lambda_{\text{int}}$  from HB = 5.8 (7.2 with ECAL) → Large leakage...
- CMS adds HCAL Outer (HO):
  - Scintillator + WLS outside coil acting as “tail catcher”
  - Standalone resolution 100%/sqrt(E)



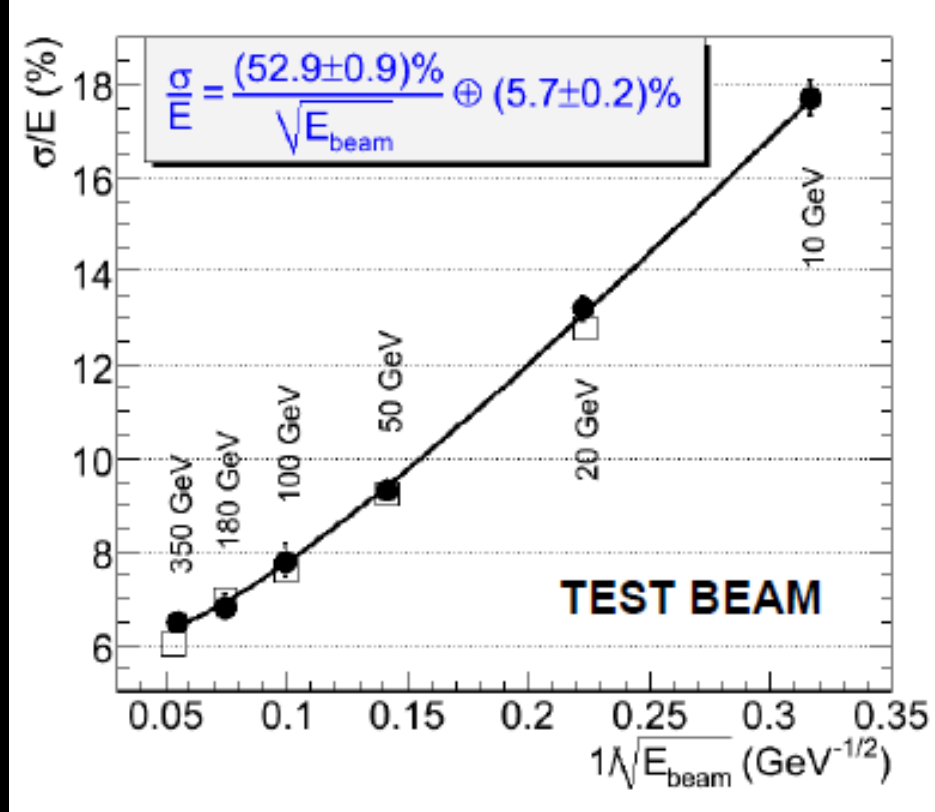
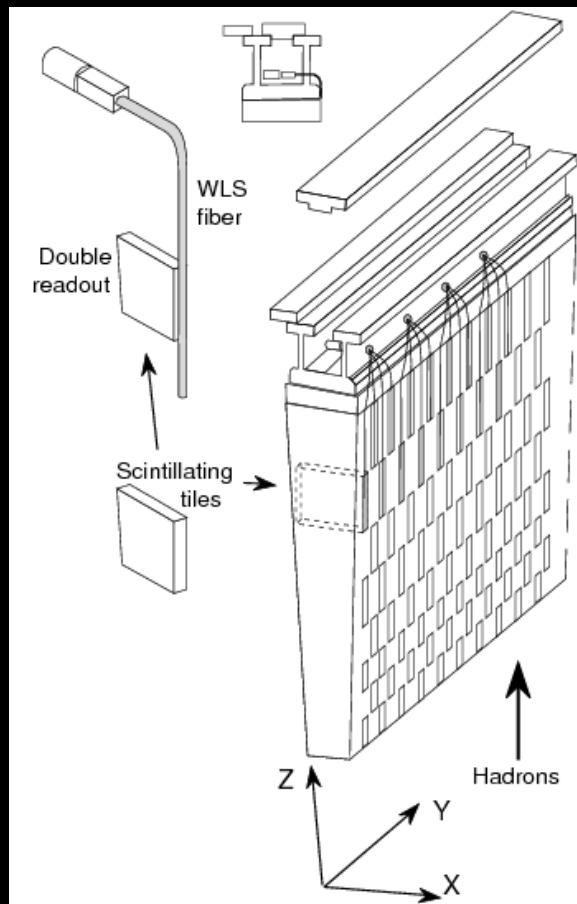
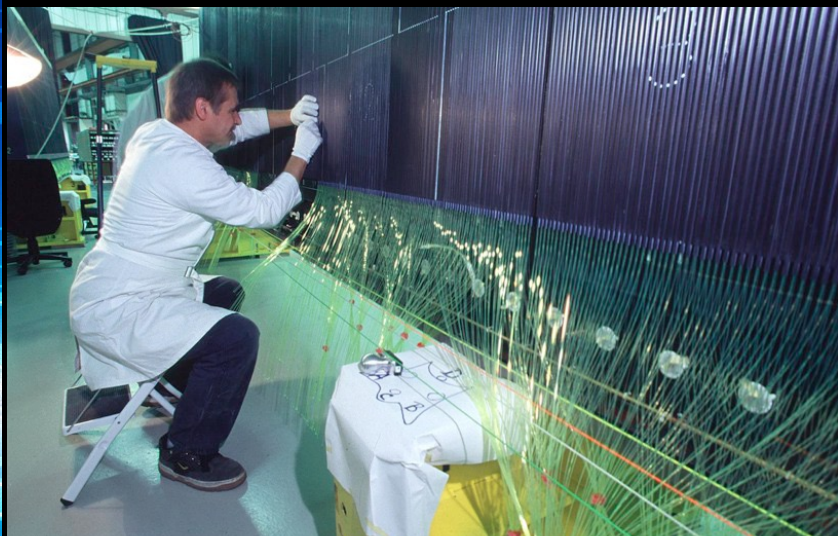
# ATLAS HCal



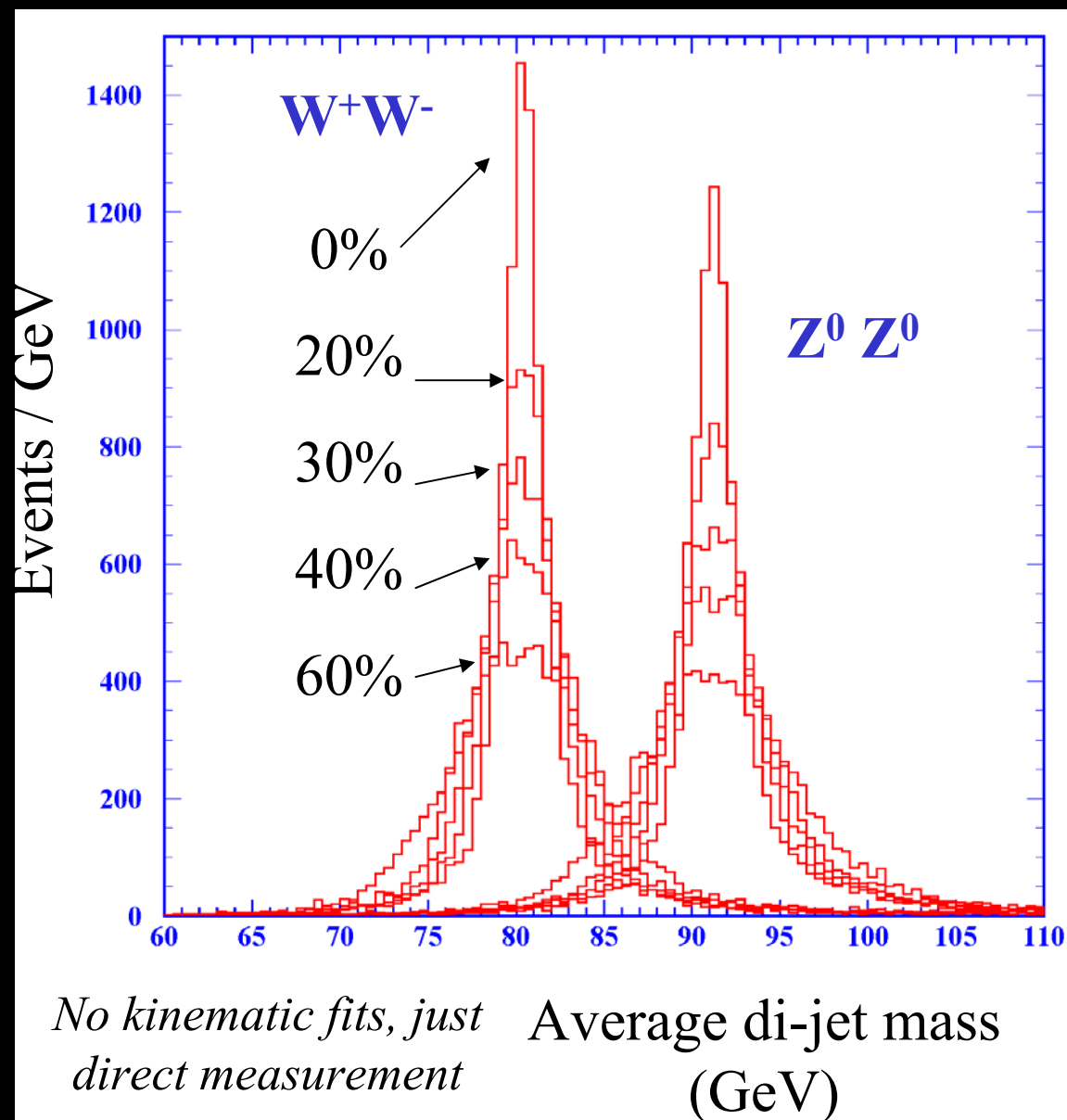
- Different technologies depending location due to different dose
- Total thickness about 8-10  $\lambda_{\text{int}}$
- $|\eta| < 1.7$  - Tile calorimeter Iron and scintillator
- $1.7 < |\eta| < 3.2$  LAr/Cu
- $3.2 < |\eta| < 4.9$  Forward calorimeter LAr/Cu or W

# ATLAS Tile calorimeter

- steel/scintillator, scintillating fibers, readout by photomultiplier



# Impact of calorimeter resolution

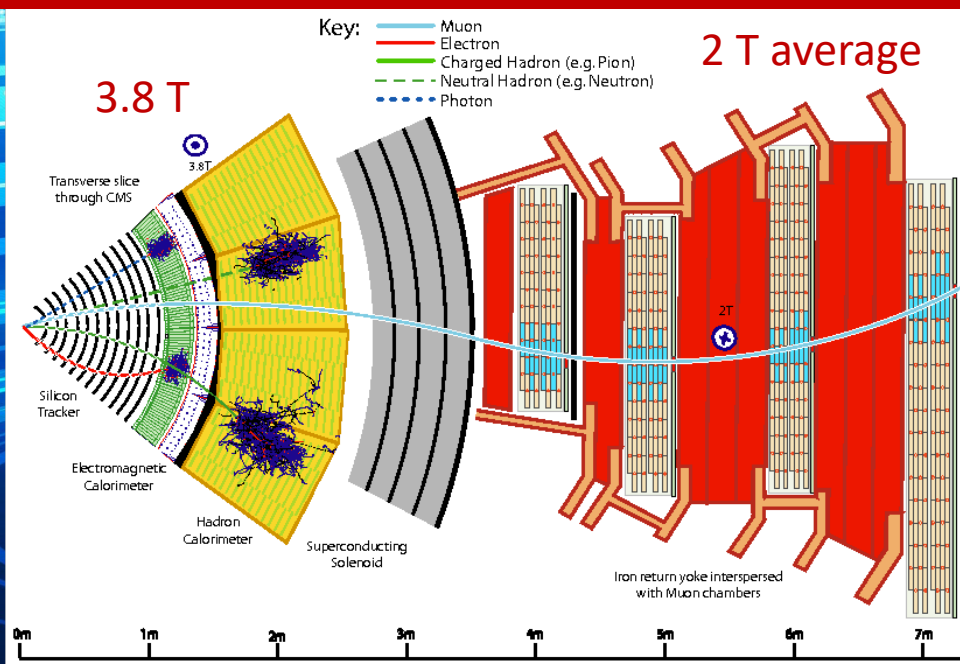


- Comparing  $e^+e^- \rightarrow WW$  and  $e^+e^- \rightarrow ZZ$  at  $\sqrt{s}=300$  GeV (hadronic decays only, assume  $WW:ZZ = 1:1$  for illustration)
- *Reality = 7:1 !*
- $30\% \sqrt{E_{\text{jet}}}$  is a good target. Physics may demand even more !

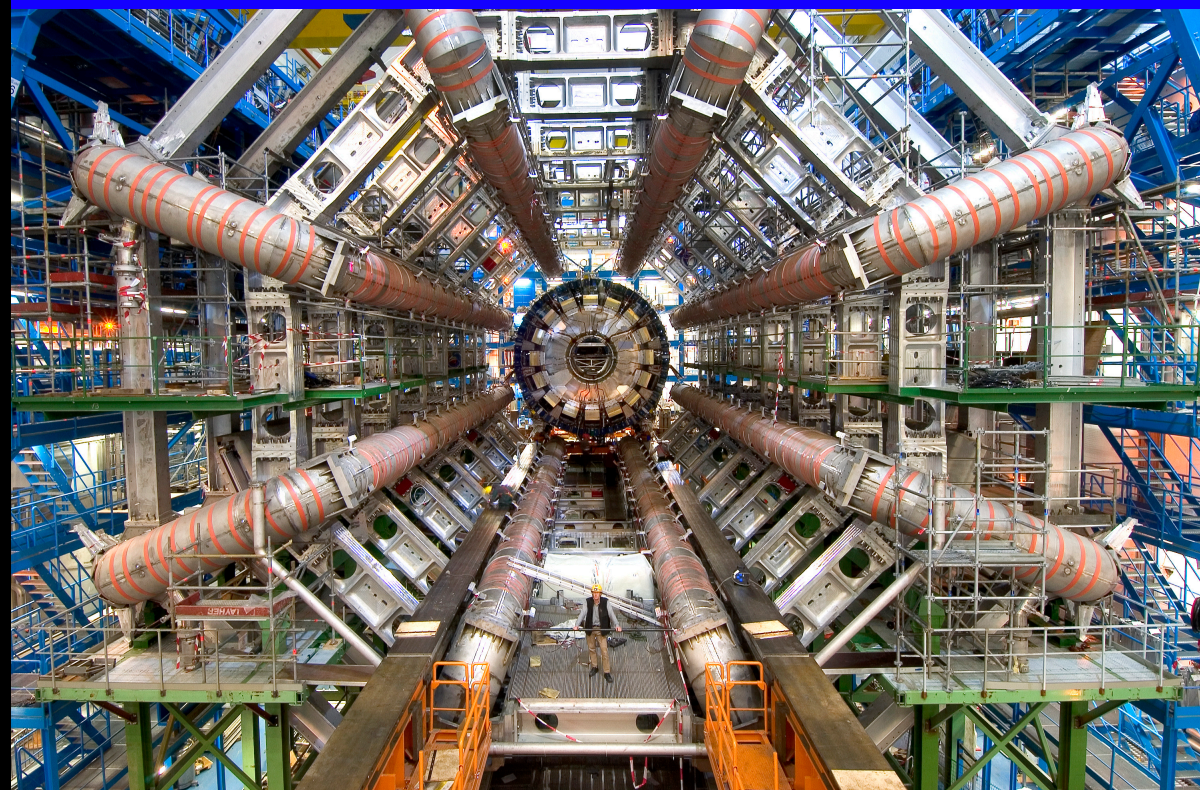
# Muon Detection

- Muon identification, momentum measurement, and triggering depends on inner tracking system and muon spectrometers located after the calorimeters
- Layout depends critically on the magnet configuration adopted for the experiment.
- Both ATLAS and CMS inner trackers are in a solenoidal B field along the beam direction

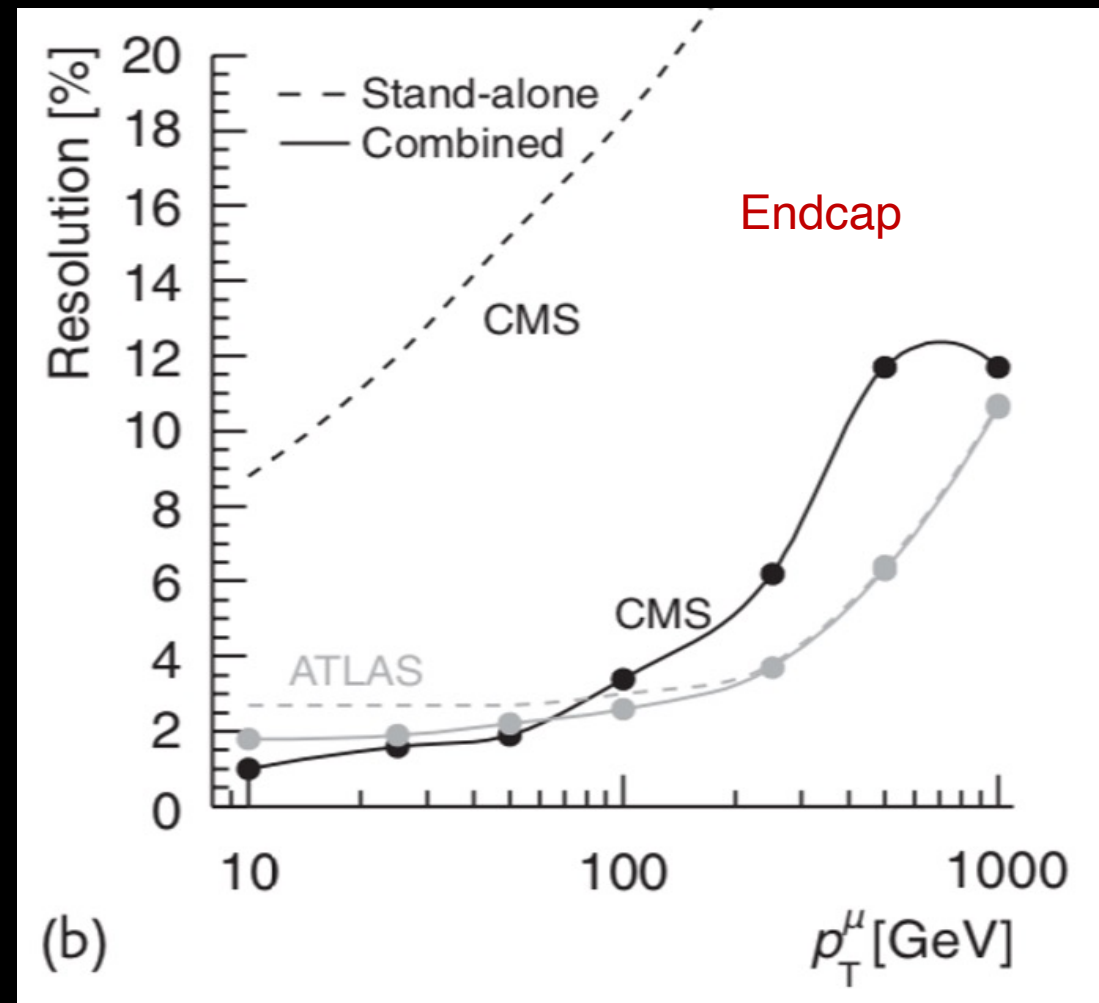
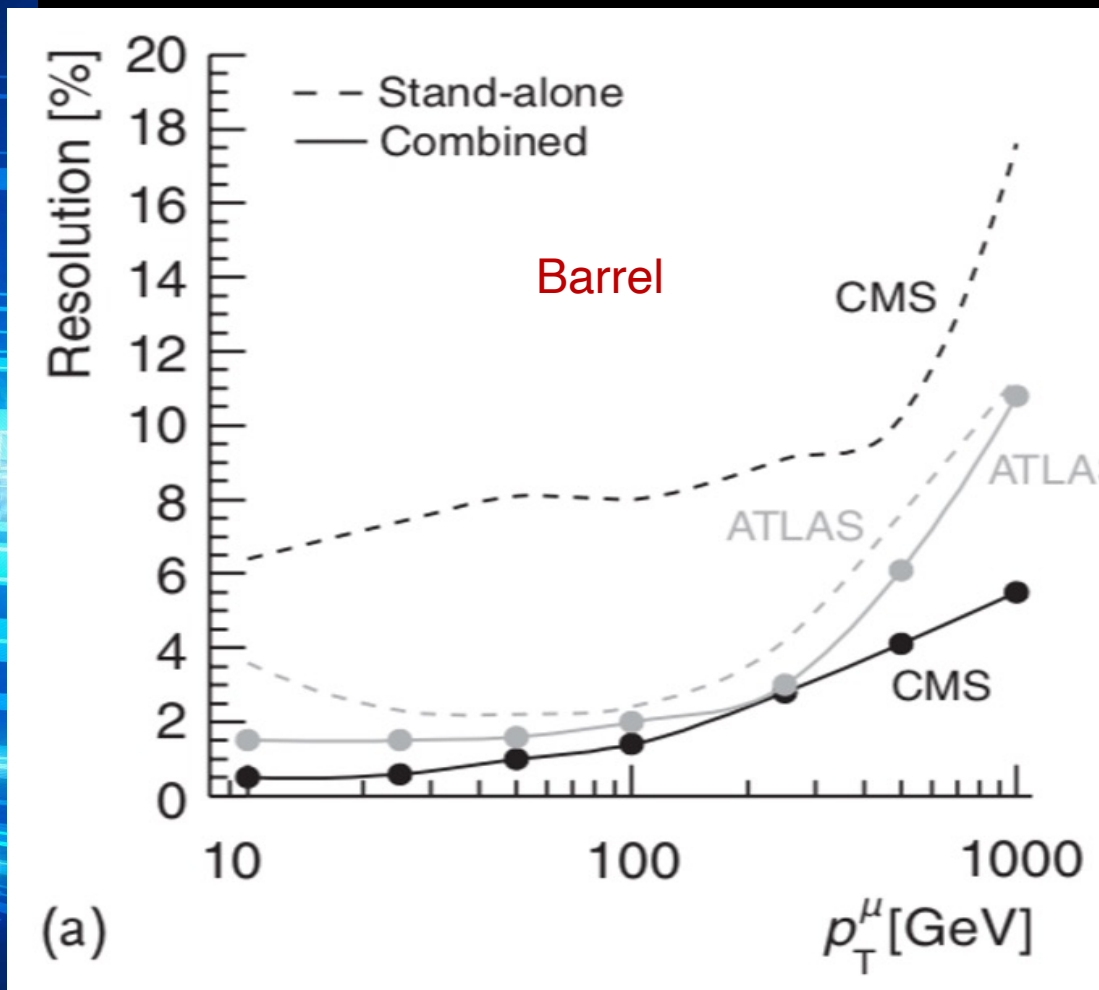
## CMS Muon spectrometer return field of solenoid for CMS



ATLAS muon spectrometer in air core Toroids (3.8 T peak) 0.8 T average in Barrel Toroid



# ATLAS vs CMS Muon resolution

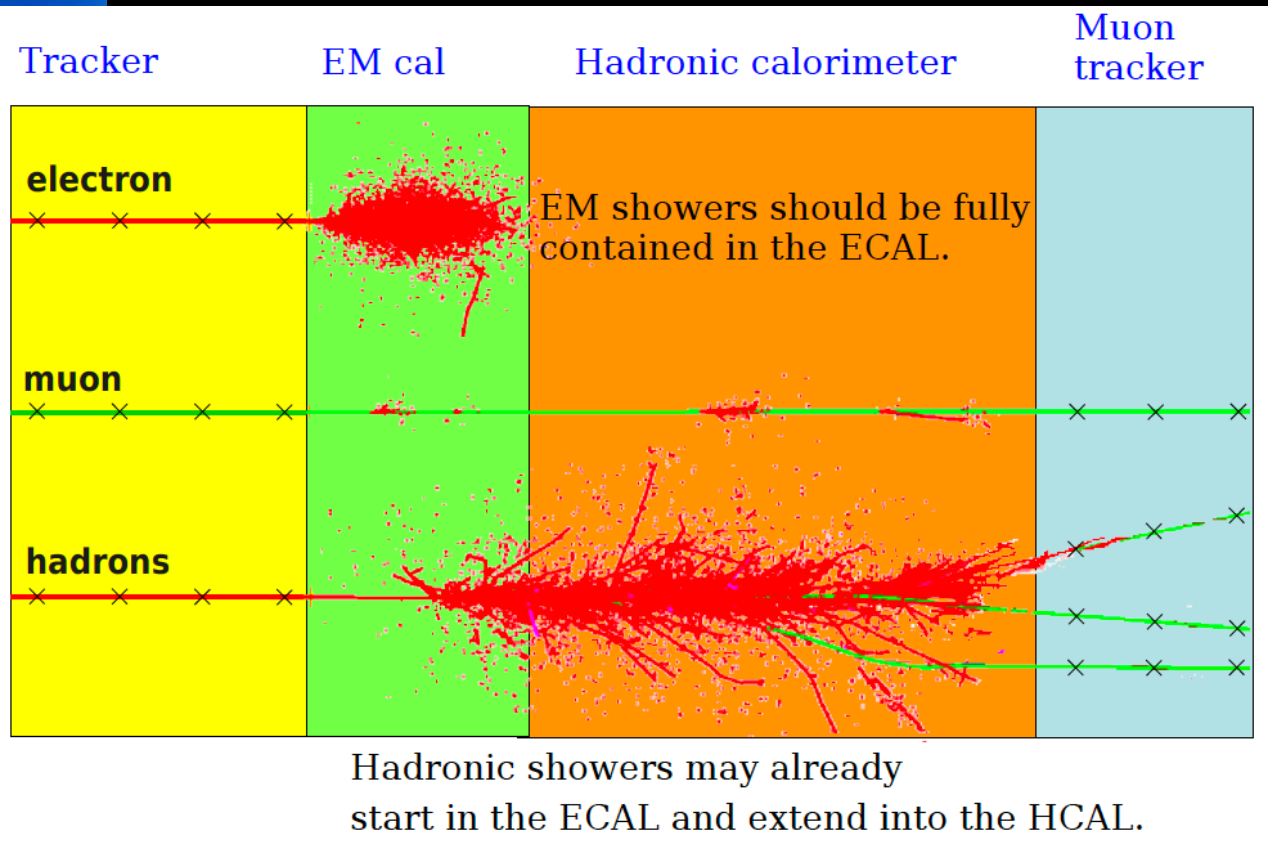




# Punchthrough

- When does a pion look like a muon?

- Total punchthrough probability of hadronic showers at a given depth  $x$  is  $P(x) = \frac{N_{hit}(x)}{N_{tot}}$



## Pion Punchthrough probability – from RD5

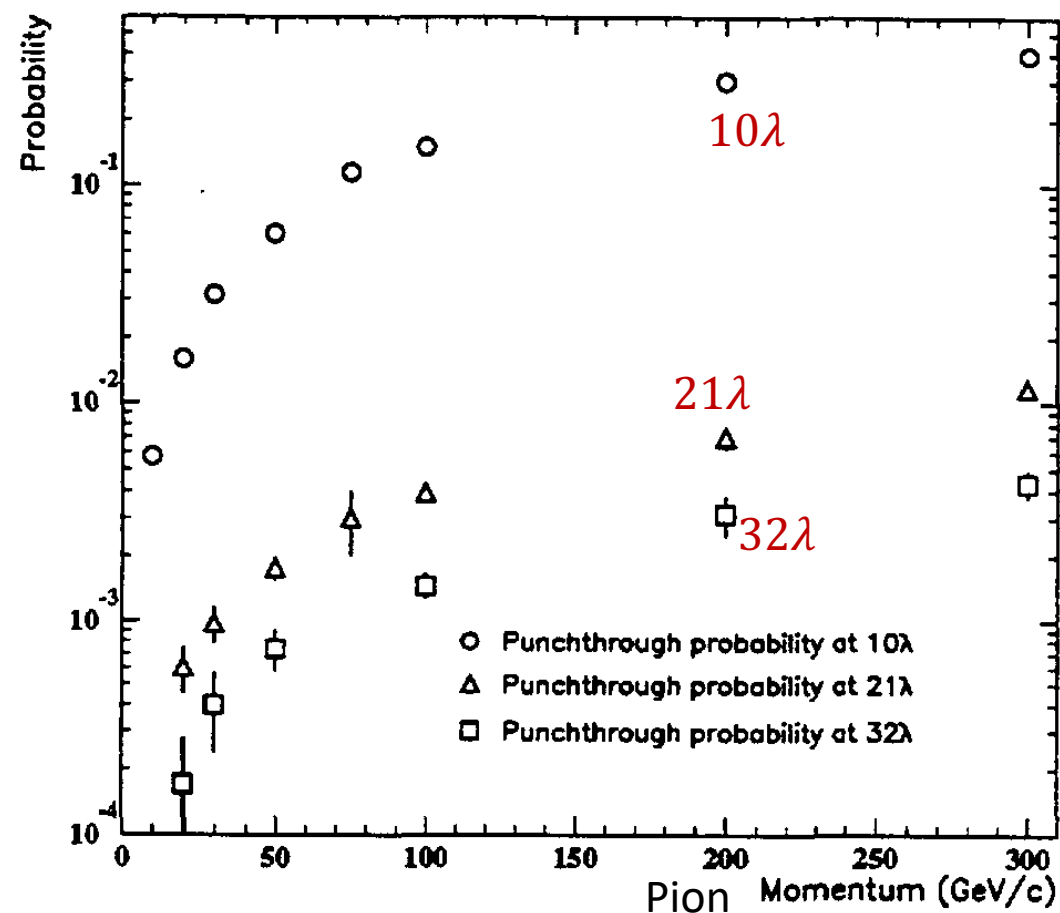
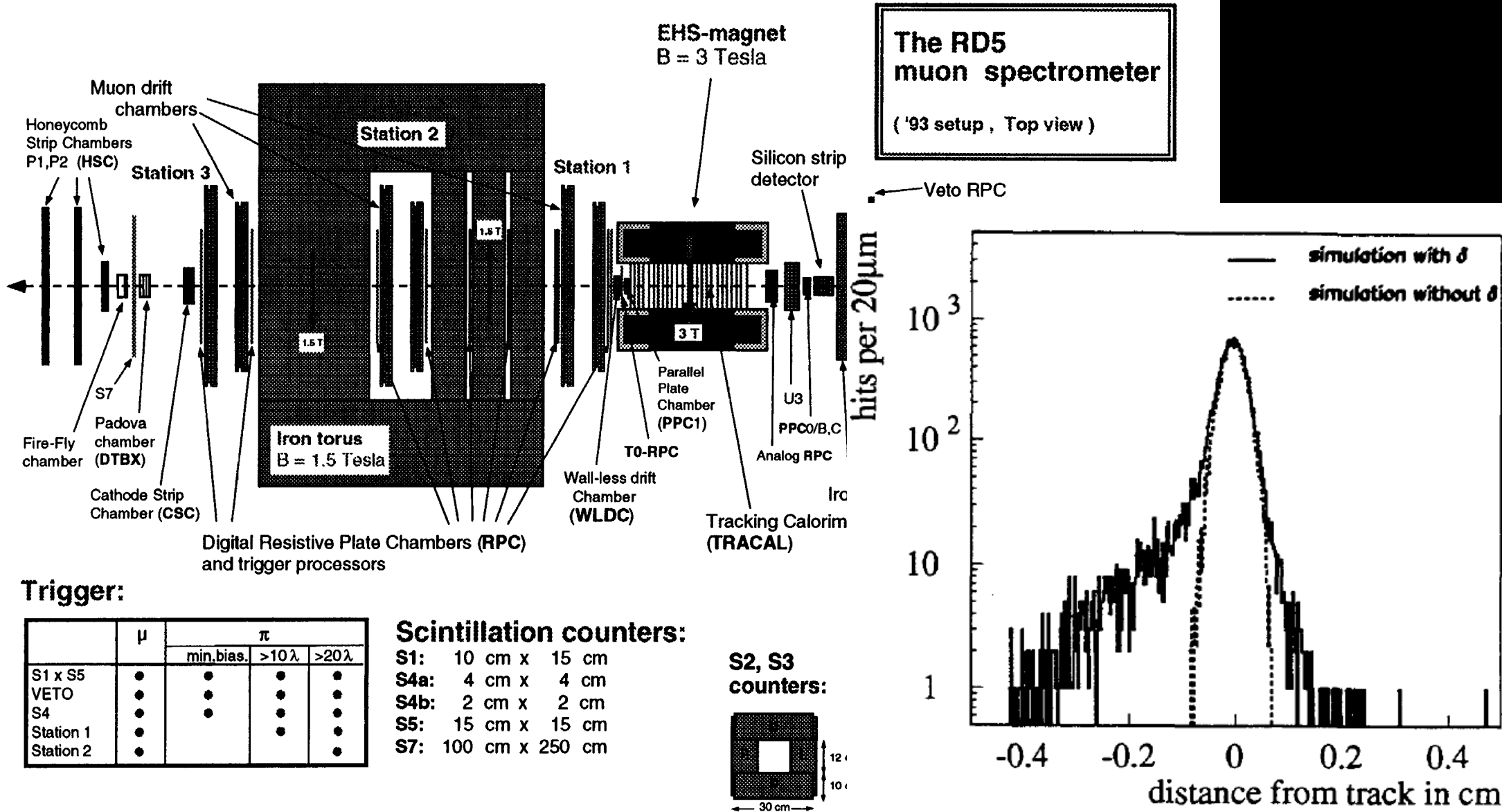
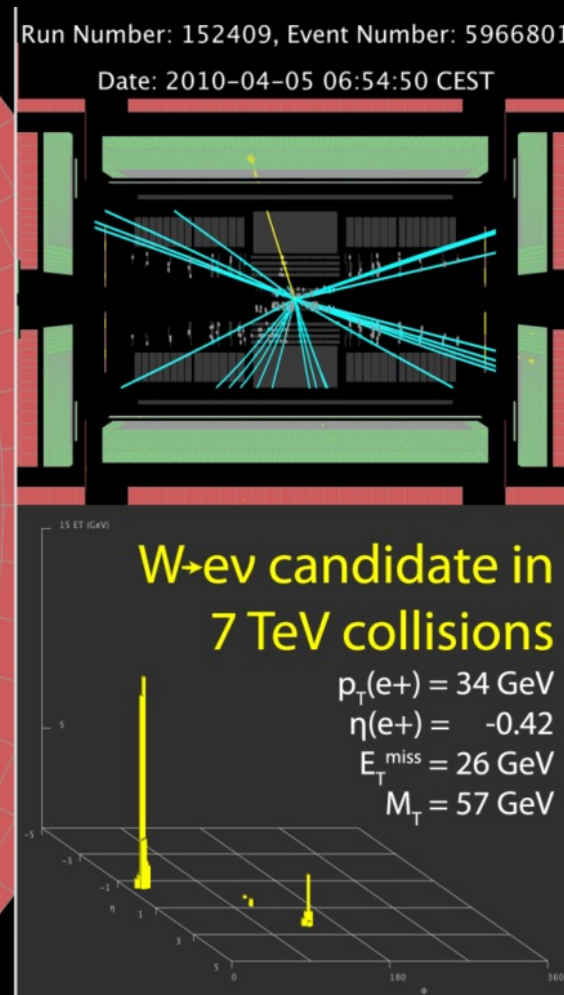
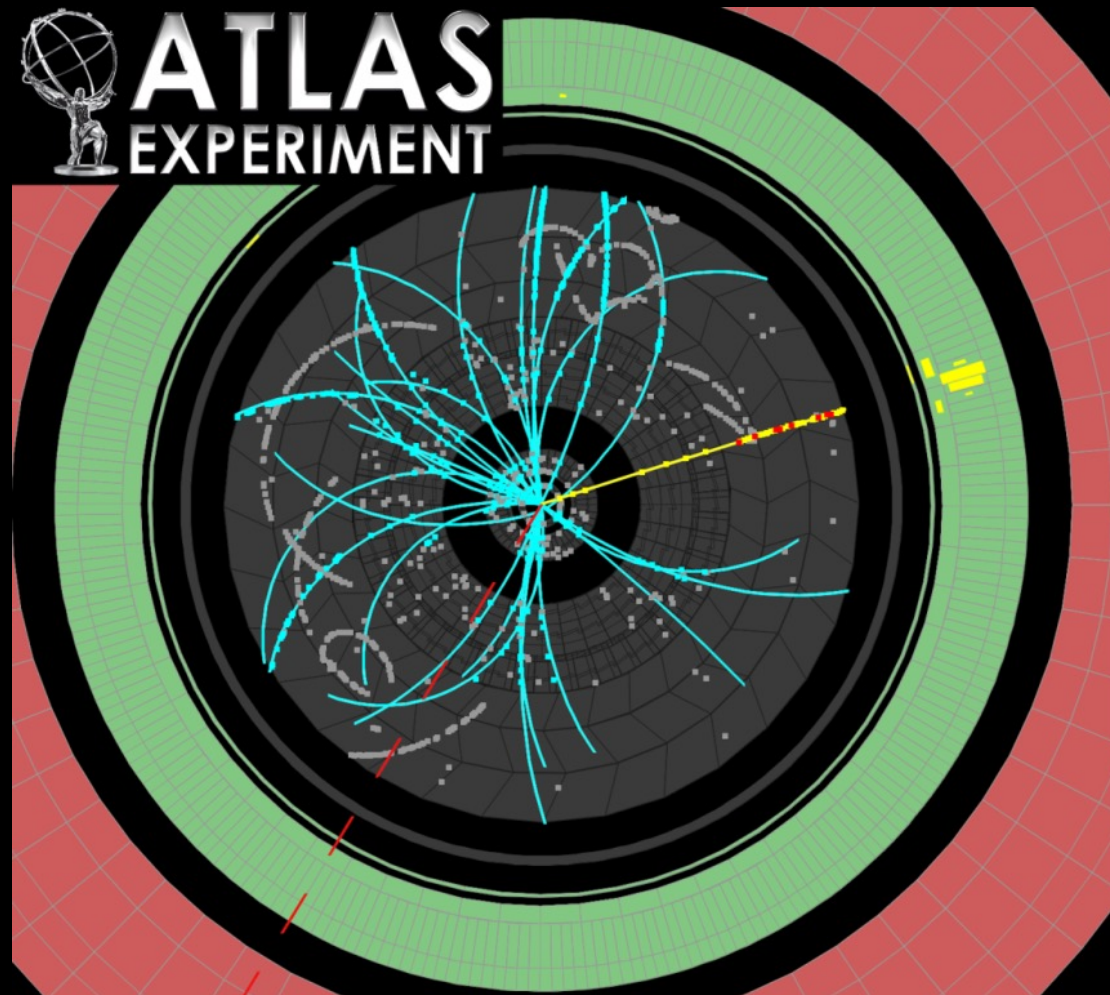


Figure 1: Schematic of the RD5 detector in its 1993 configuration.



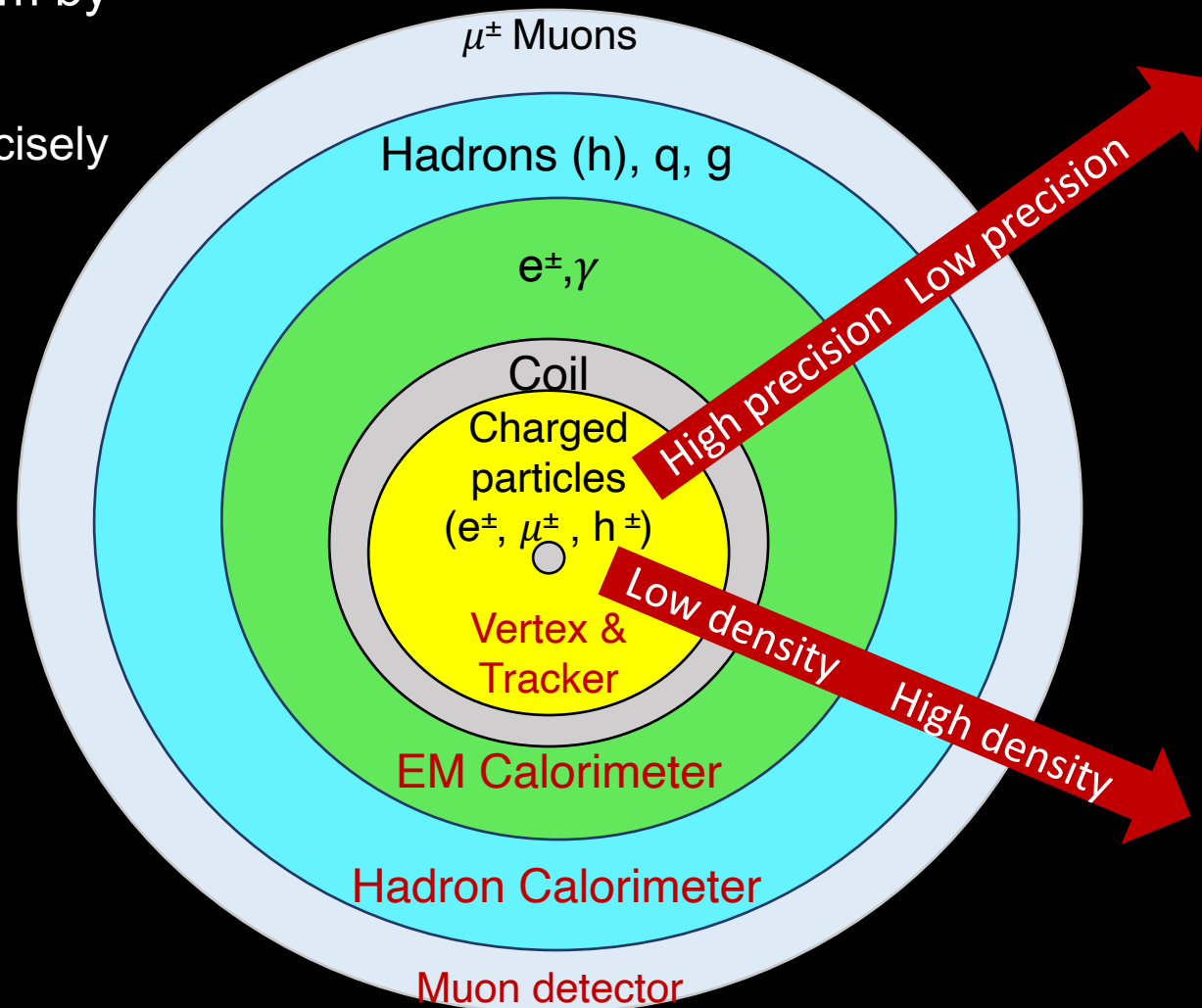
# Neutrinos

- “Detected” by missing momentum – Must make sure your detector is hermetic !



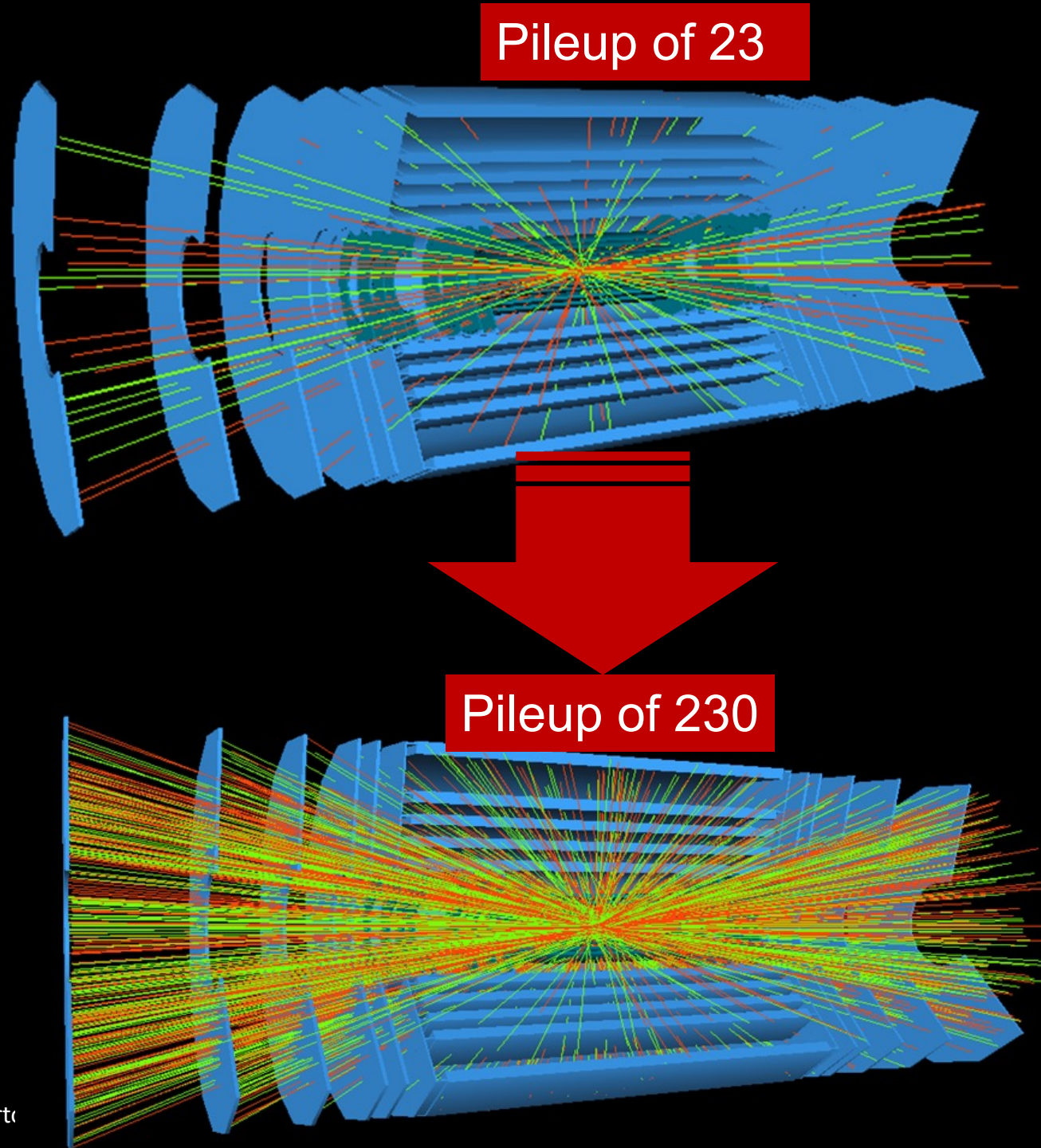
# Building a collider detector

- Vertex Detectors: measure origin
- Trackers: Measure “charge” and momentum by bending the particle in a magnetic field
  - Light weight, low Z materials to measure precisely the position of the particle
- Calorimeters: detection of particles through total absorption
  - Process is destructive for almost all particles except muons and neutrinos
  - EM calorimeters: high Z materials to catch electrons and photons
  - Hadron Calorimeters: hadron interact mainly via the strong interaction, high A materials (Iron, Copper)
- Muon detectors: tracking detectors



# Next lecture

- Silicon detectors
- New technologies for the HL-LHC
- The challenges of new colliders



# Experiments have to be clever

Facility	Original Purpose	Discovery with Precision Instruments
CERN PS (1973)	$\pi N$ (interactions)	Neutral Currents $\rightarrow Z, W$
BNL AGS (1962-1974)	$\pi N$ (interactions)	Two kinds of neutrinos, Time reversal non Symmetry, charm quark
FNAL (1977)	Neutrino Physics	Bottom quark, top quark
SLAC SPEAR (1968-1976)	$e p$ , (QED)	Partons, charm quark, tau lepton
CERN ISR (1971-1980)	$pp$	Increasing $pp$ cross-section
DESY PETRA (1979)	top(quark)	Gluon
Super-K (1996-)	Proton(Decay)	Neutrino Oscillations

# INSTRUMENTATION

“New directions in science are launched by new tools much more often than by new concepts.

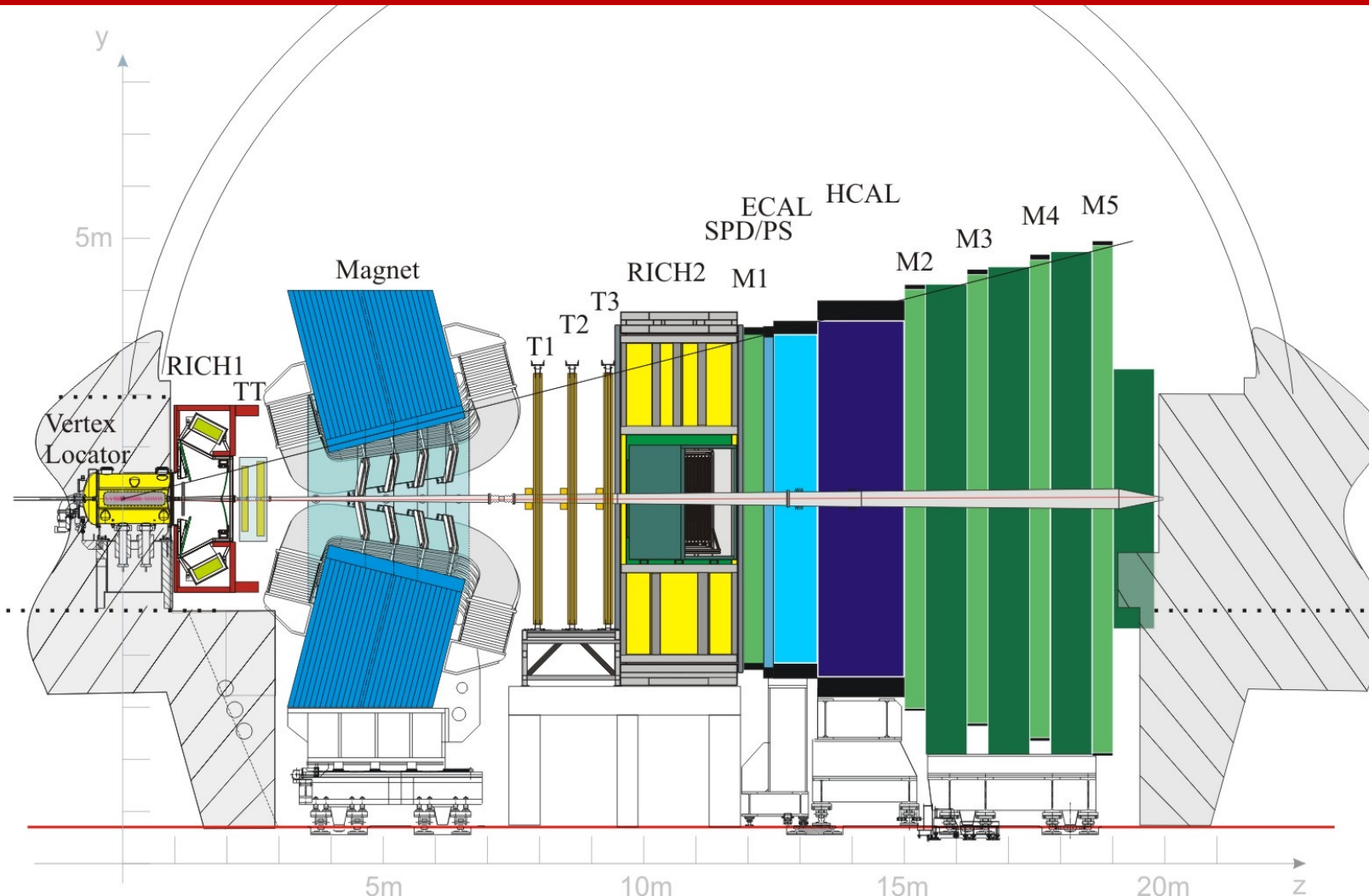
The effect of a concept-driven revolution is to explain old things in new ways.

The effect of a tool-driven revolution is to discover new things that have to be explained”



Freeman Dyson

## Dipole LCb integrated field 4Tm



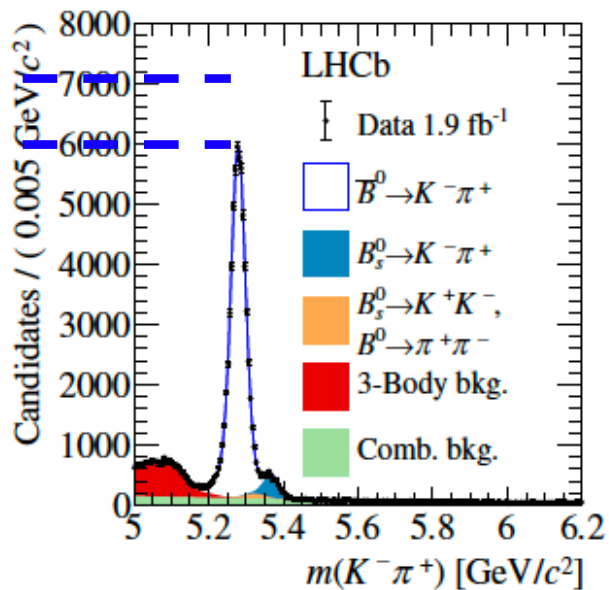
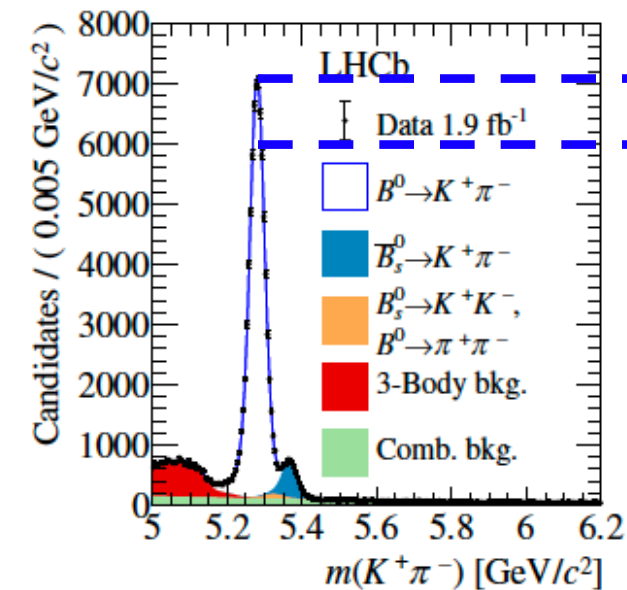
- Forward Spectrometer Configuration
  - At high energies b- and b- hadrons are produced mainly in the same forward or backward cone.
  - $\langle p_T(b) \rangle \sim 80 \text{ GeV}/c \rightarrow 7 \text{ mm}$  mean decay distance  $\rightarrow$  good separation between primary and decay vertices.
- Dipole magnet
  - Particle deflected in x - z plane
  - Detectors are arranged in parallel planes along z
  - Bending from difference of the slopes before and after magnet



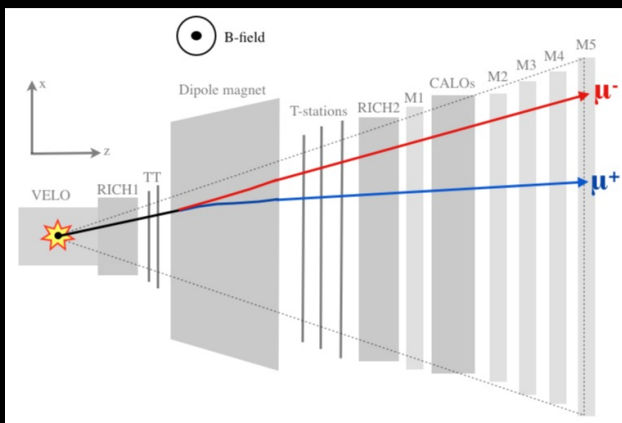
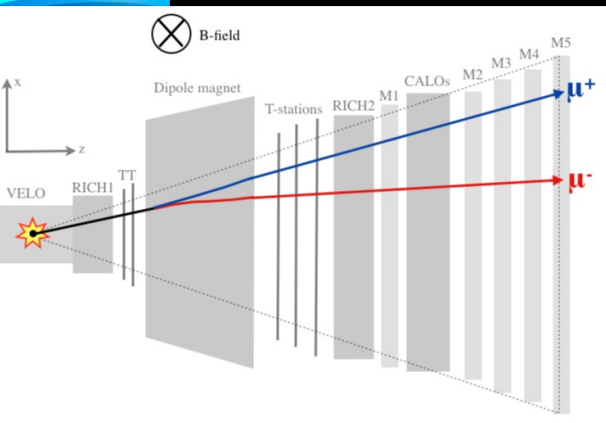
# LHCb

$B^0 \rightarrow K^+ \pi^-$

$\bar{B}^0 \rightarrow K^- \pi^+$



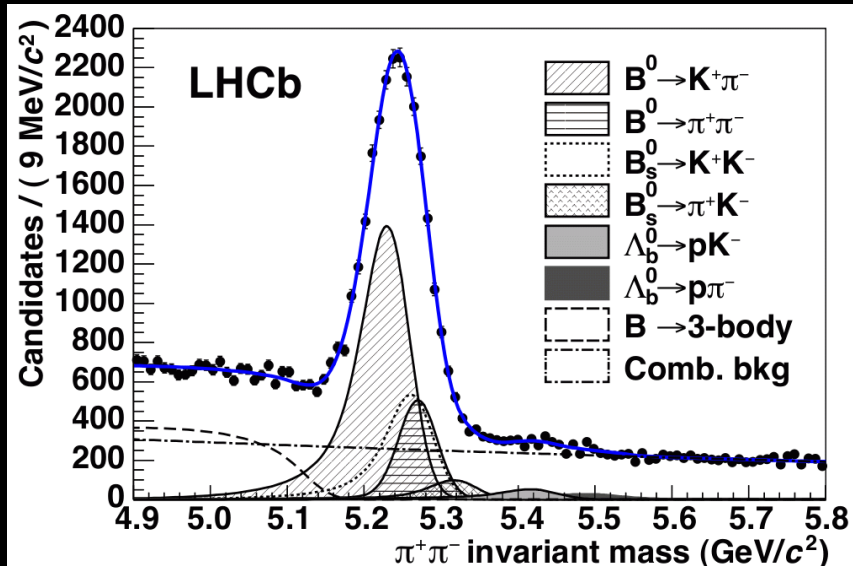
$$A^{CP} = (-8.2 \pm 0.03 \pm 0.03)\%$$



- Physics goals:
  - precision measurements of the CKM matrix to probe the validity of the SM and CP violation
  - Measurements of processes strongly suppressed in the SM which could be enhanced by NP
  - Measurements of rare decays  $B_s \rightarrow \mu^+ \mu^-$
  - Studies of lepton universalities
- Detector
  - Excellent vertex and proper time resolution (VELO)
  - Precise particle identification (ID): hadron  $\pi/K$  separation with Ring Imaging Cherenkov counters (RICH)
  - High momentum resolution for precise invariant mass reconstruction
  - A versatile trigger scheme

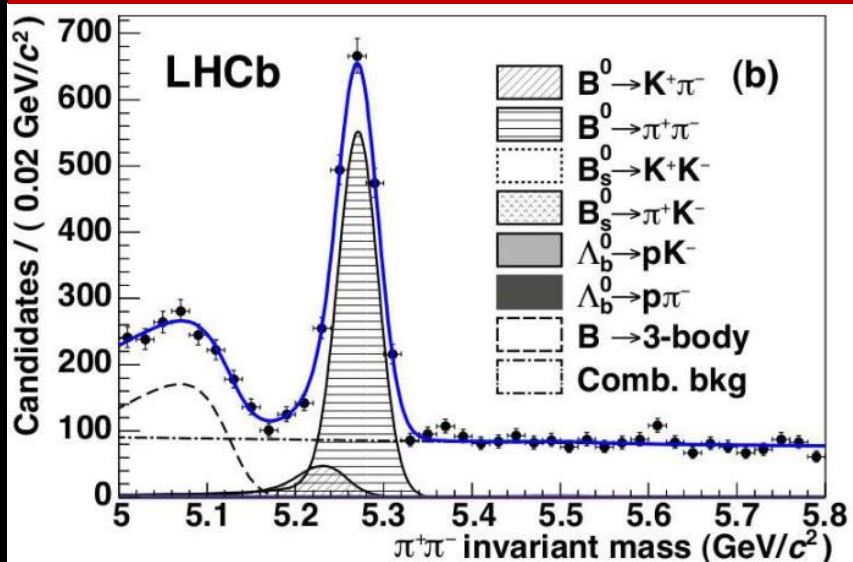
# LHCb

Before  
RICH PID



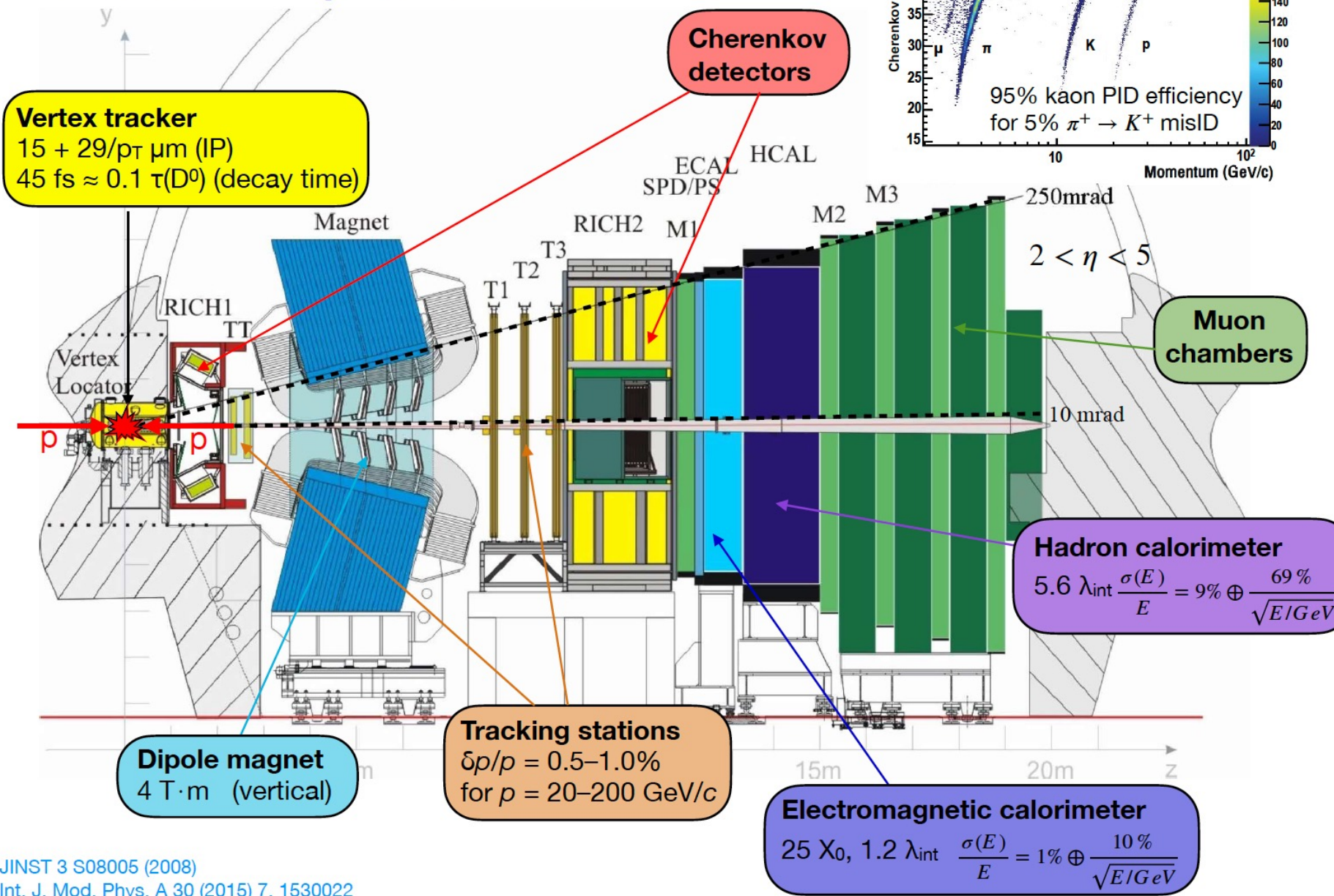
After  
RICH PID

Needed to distinguish  $B^0 \rightarrow \pi^+ \pi^-$   
from  $B^0 \rightarrow K^+ \pi^-$



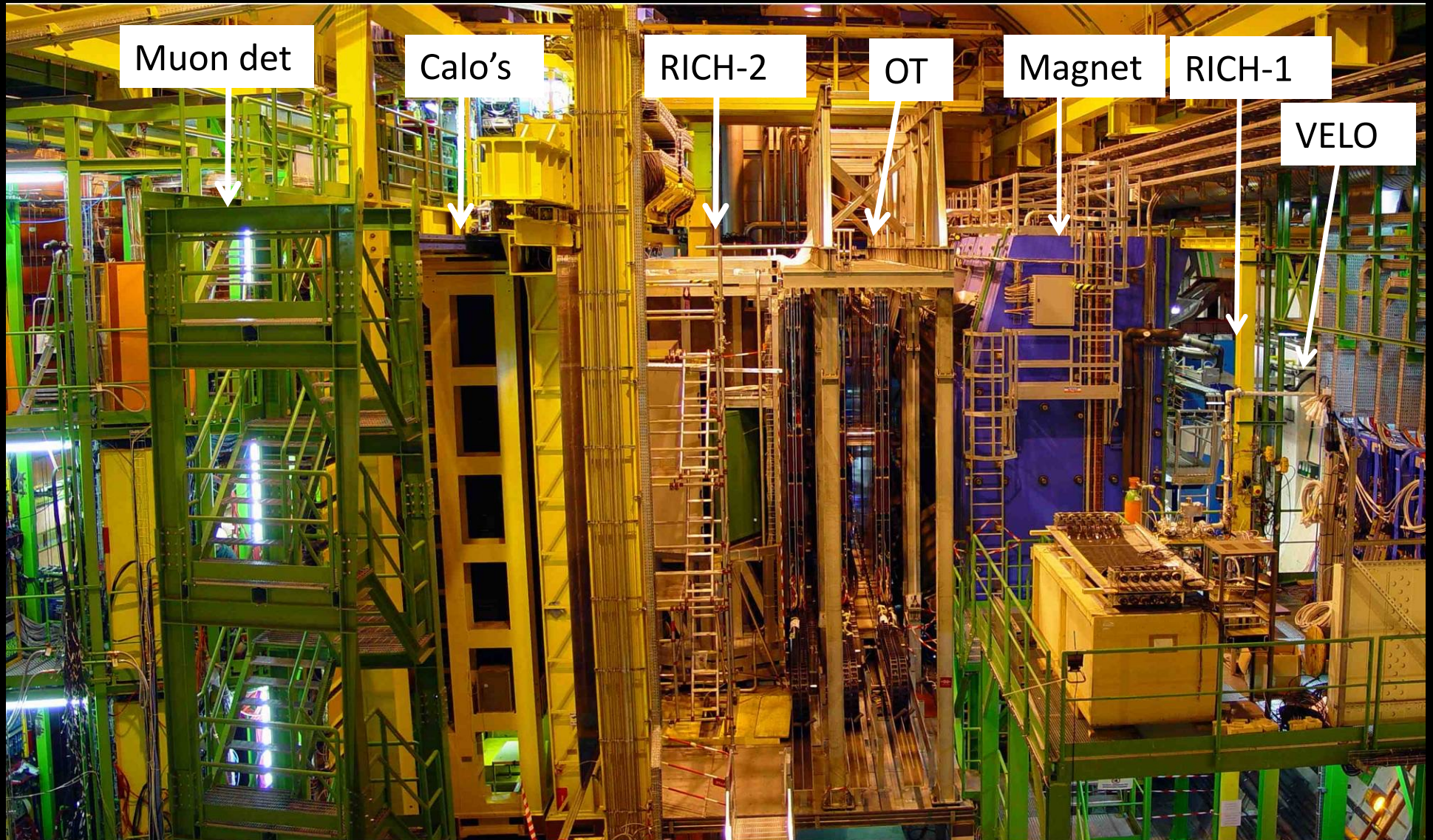
- Physics goals:
  - precision measurements of the CKM matrix to probe the validity of the SM and CP violation
  - Measurements of processes strongly suppressed in the SM which could be enhanced by NP
  - Measurements of rare decays  $B_s \rightarrow \mu^+ \mu^-$
  - Studies of lepton universalities
- Detector
  - Excellent vertex and proper time resolution (VELO)
  - Precise particle identification (ID): hadron  $\pi/K$  separation with Ring Imaging Cherenkov counters (RICH)
  - High momentum resolution for precise invariant mass reconstruction
  - A versatile trigger scheme

# LHCb experiment

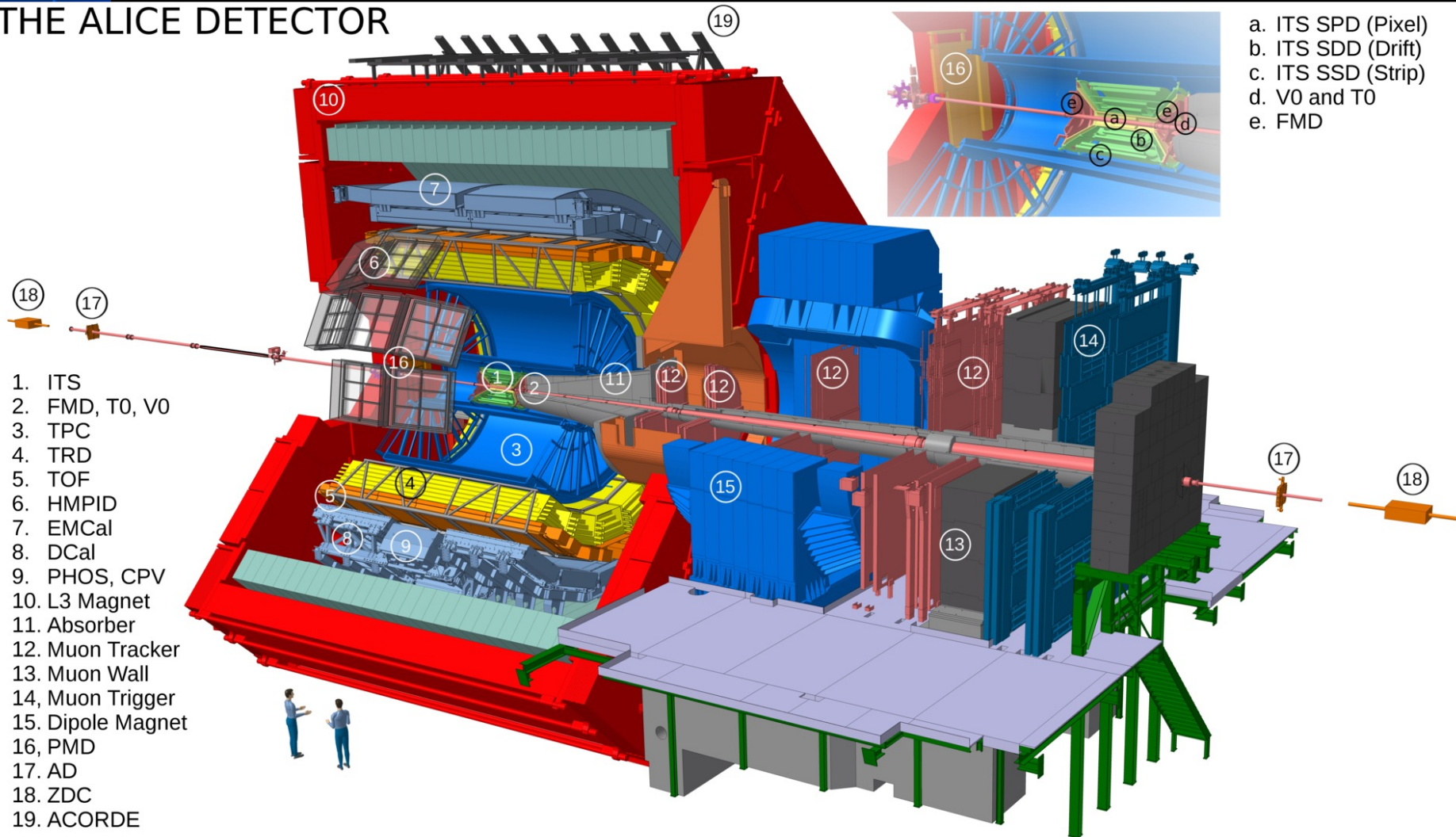


JINST 3 S08005 (2008)  
Int. J. Mod. Phys. A 30 (2015) 7, 1530022

# LHCb



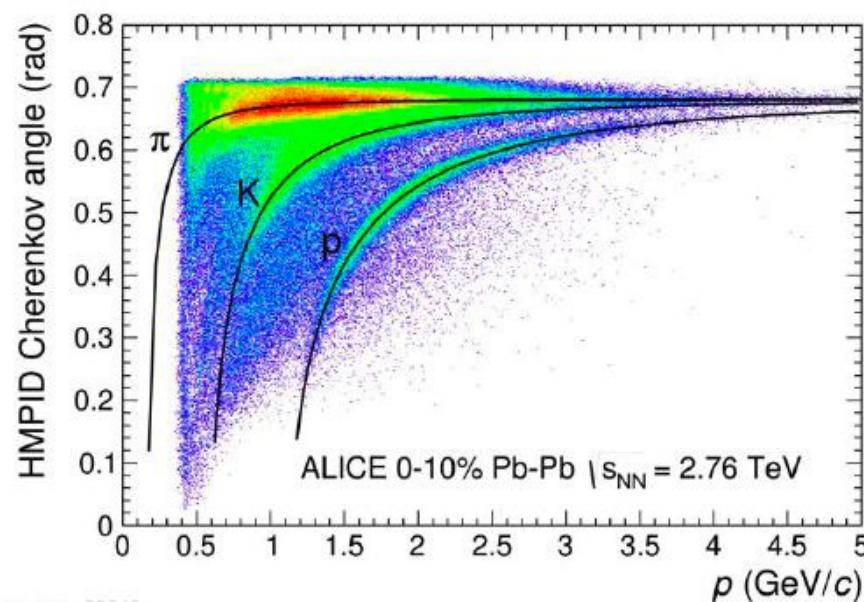
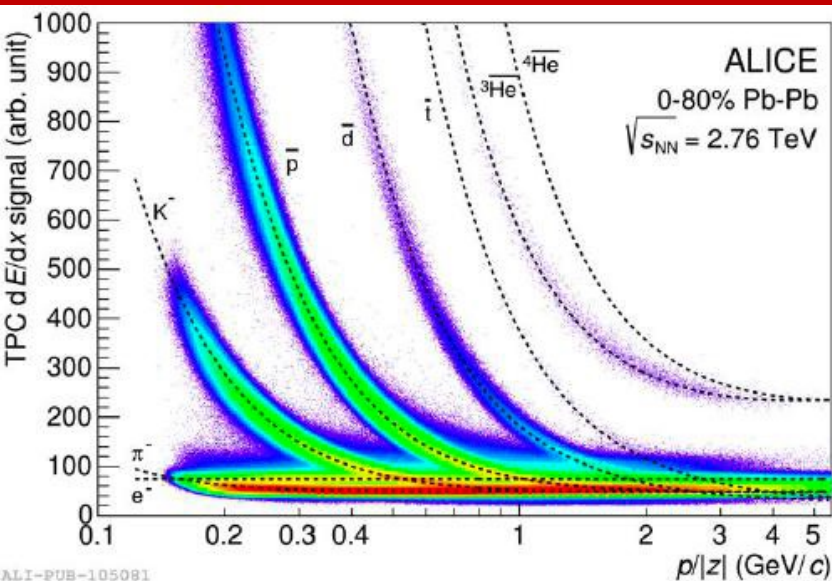
## THE ALICE DETECTOR



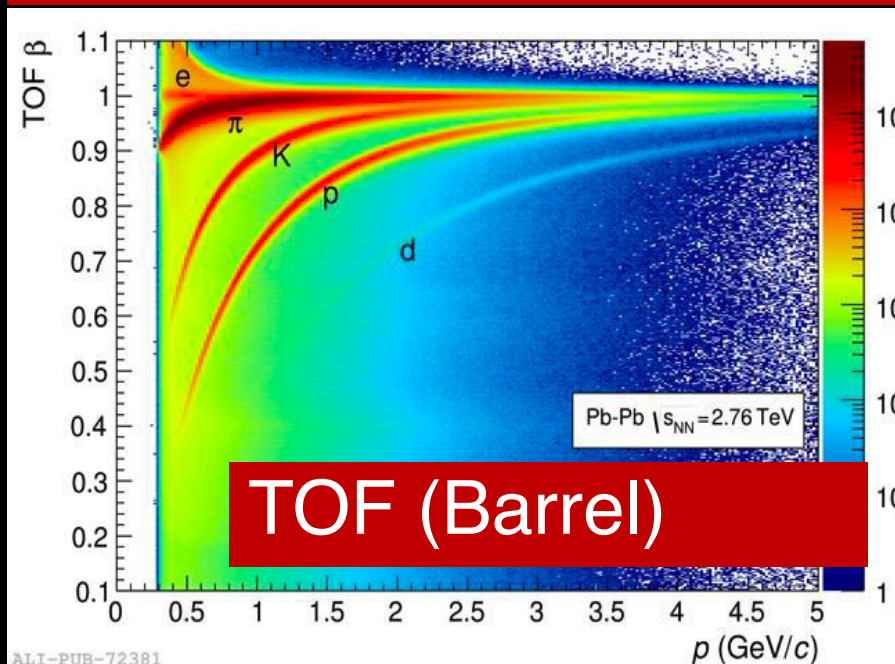
- Measurements down to very low  $p_T$
- Particle ID in the Time Projection Chamber and Time of Flight detectors
- Excellent vertex detectors to measure heavy flavour charmed and beauty baryons
- Forward muon spectrometer studies the complete spectrum of heavy quarkonia ( $J/\psi$  and  $\Upsilon$  resonances)

# ALICE PID

## TPC (+ITS) dE/dx



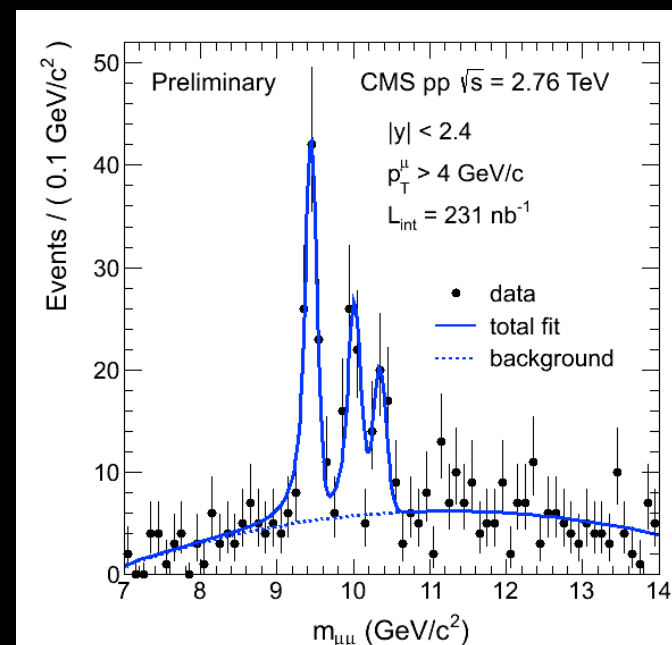
## HMPID – Cherenkov radiation



## TOF (Barrel)

Plus

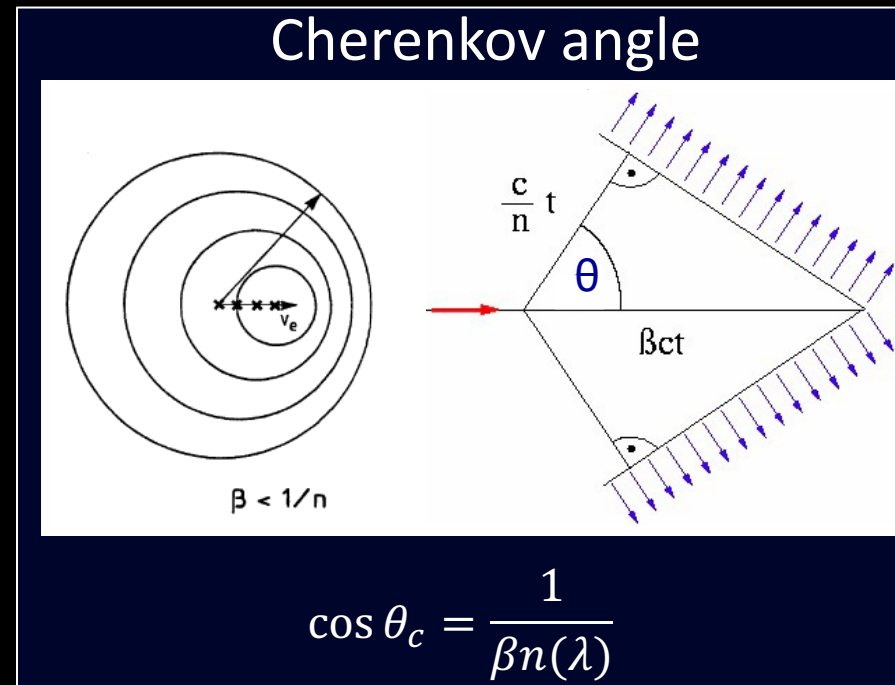
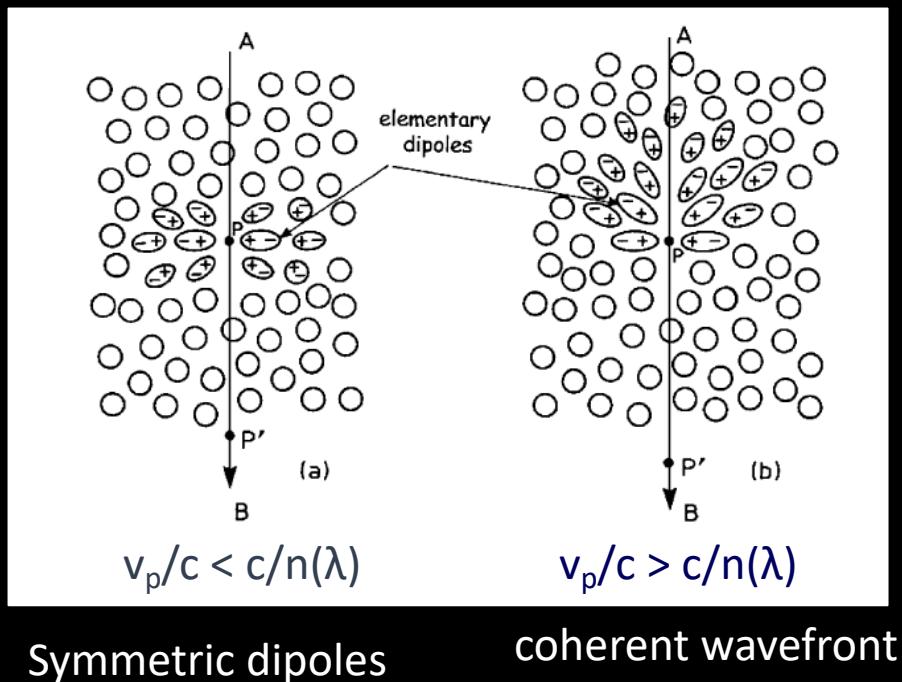
- Transition radiation detector (TRD)
- Photon spectrometer (PHOS)
- EM calorimeter (EMCAL)
- Muon spectrometer



# Cherenkov emission



- If the velocity of a particle is such that  $\beta = v_p/c > c/n(\lambda)$  where  $n(\lambda)$  is the index of refraction of the material, a pulse of light is emitted around the particle direction with an opening angle ( $\theta_c$ )



- The **threshold velocity**

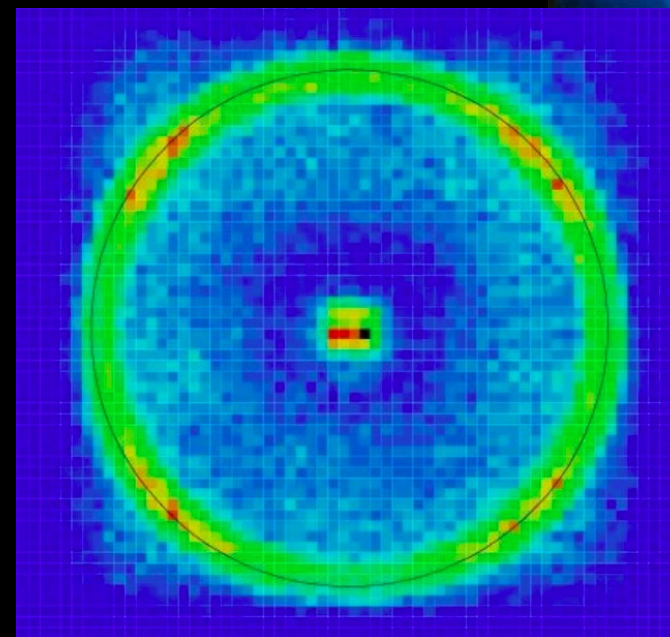
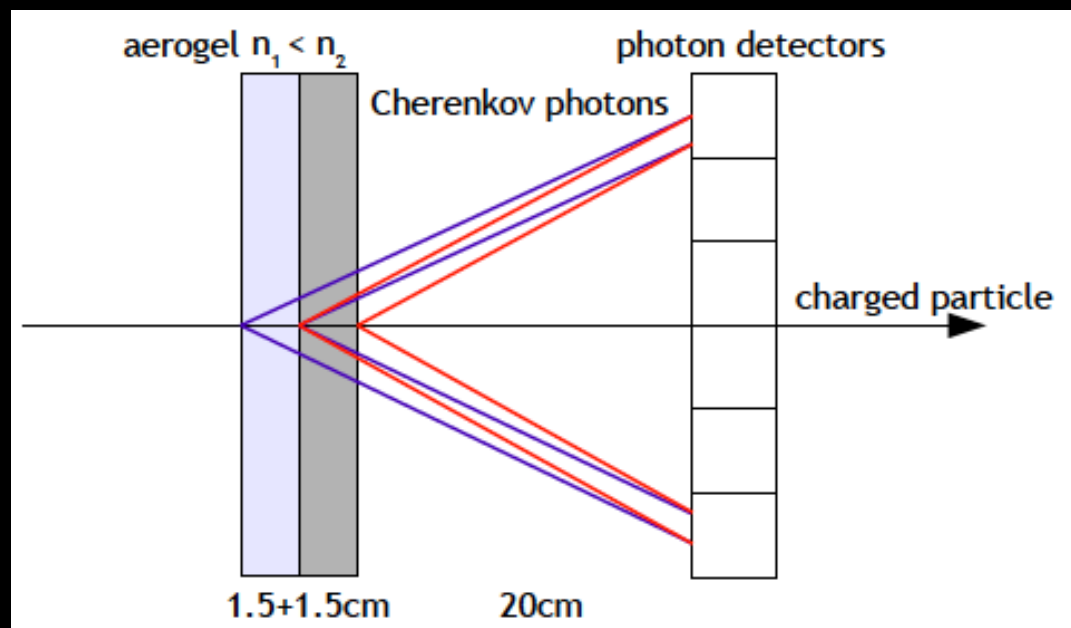
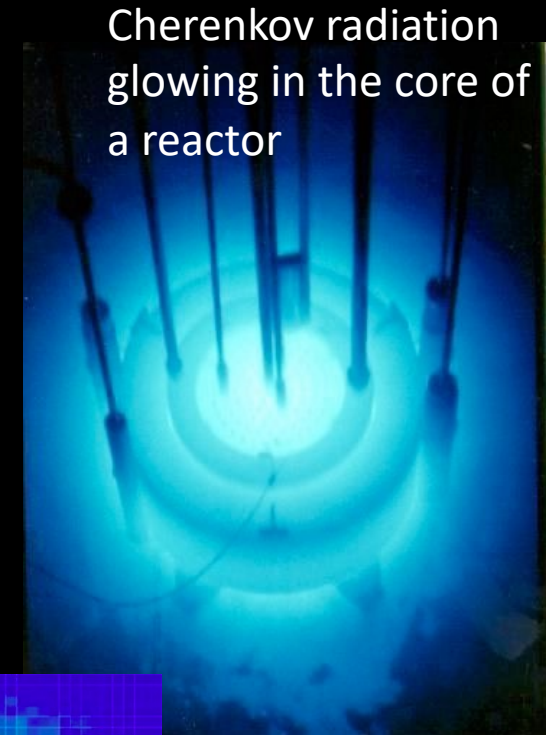
$$\beta_{th} = \frac{v_{th}}{c} = \frac{1}{n(\lambda)}$$

Number of produced photons:

$$N_{photons} = L \frac{\alpha}{\hbar c} Z^2 \int \sin^2 \theta_c(E) dE$$

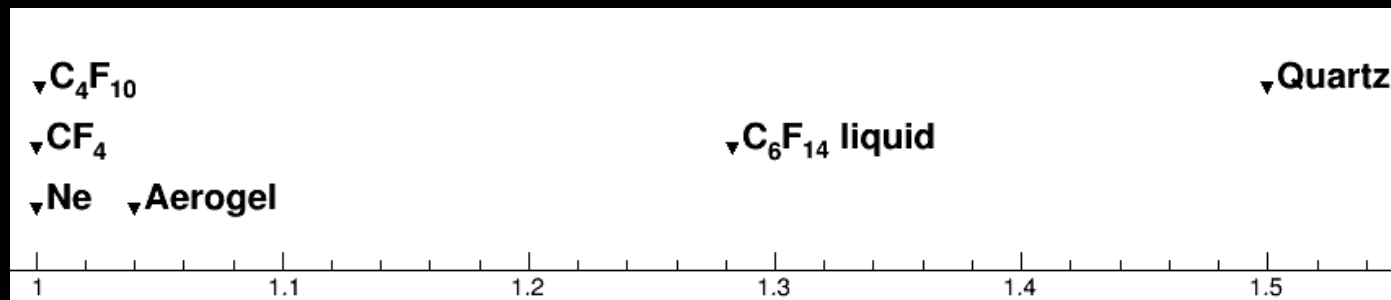
# Cherenkov photon emission

- Cherenkov emission is a weak effect and causes no significant energy loss (<1%)
- It takes place only if the track  $L$  of the particle in the radiating medium is longer than the wavelength  $\lambda$  of the radiated photons.
- Typically  $O(1-2 \text{ keV / cm})$  or  $O(100-200)$  visible photons /cm





# Refractive index range



~100 GeV/c



~1 GeV/c

Momentum



Silica Aerogel



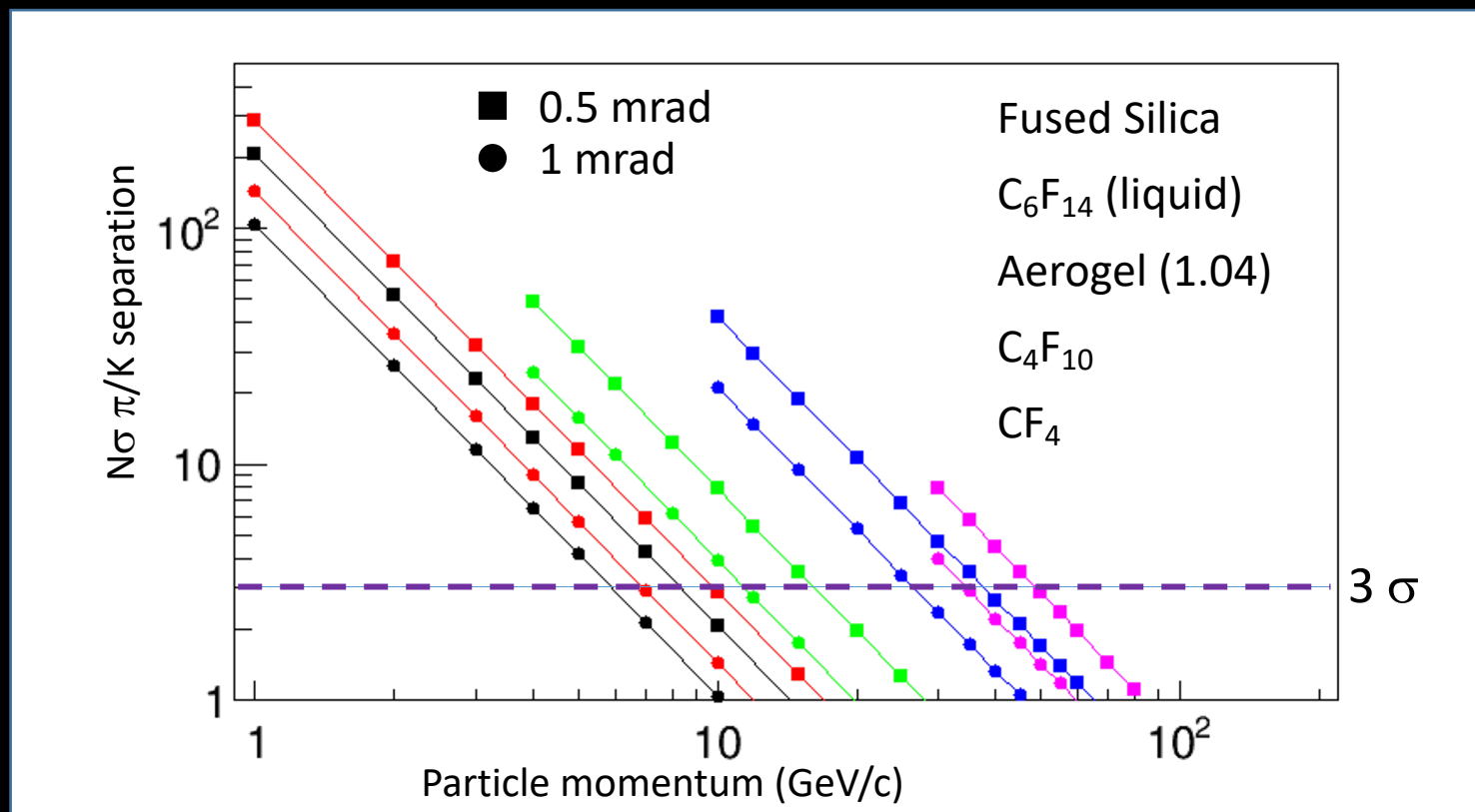
Quartz fibers

# RICH performance

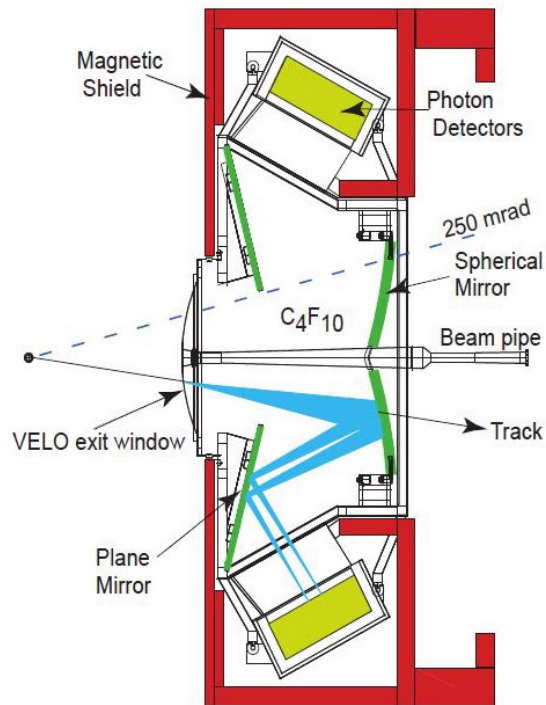
$$N_\sigma \approx \frac{|m_1^2 - m_2^2|}{2P^2 \sigma[\theta_c(\text{tot})] \sqrt{n^2 - 1}}$$

For particles well above threshold

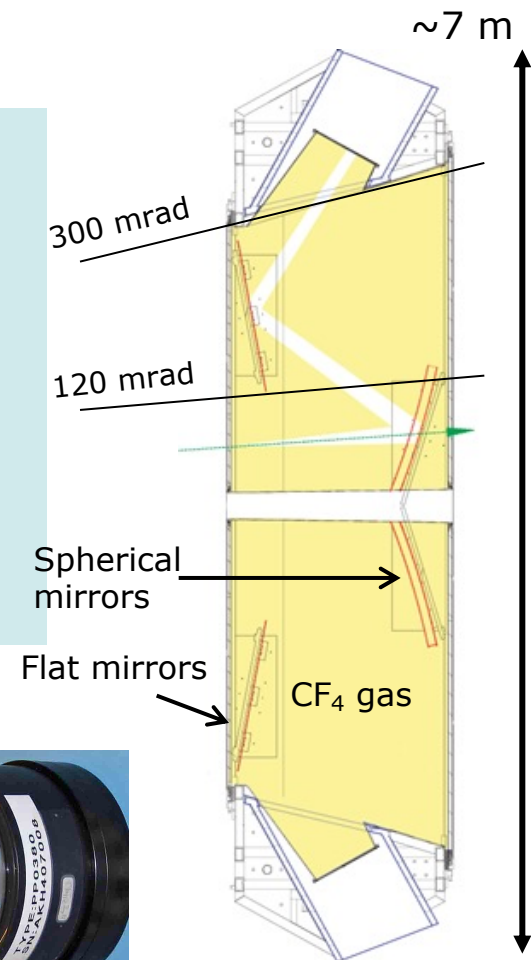
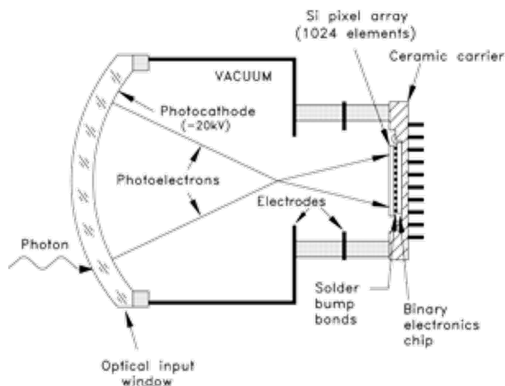
B. N. Ratcliff, NIMA 502 (2003) 211-221



# LHCb

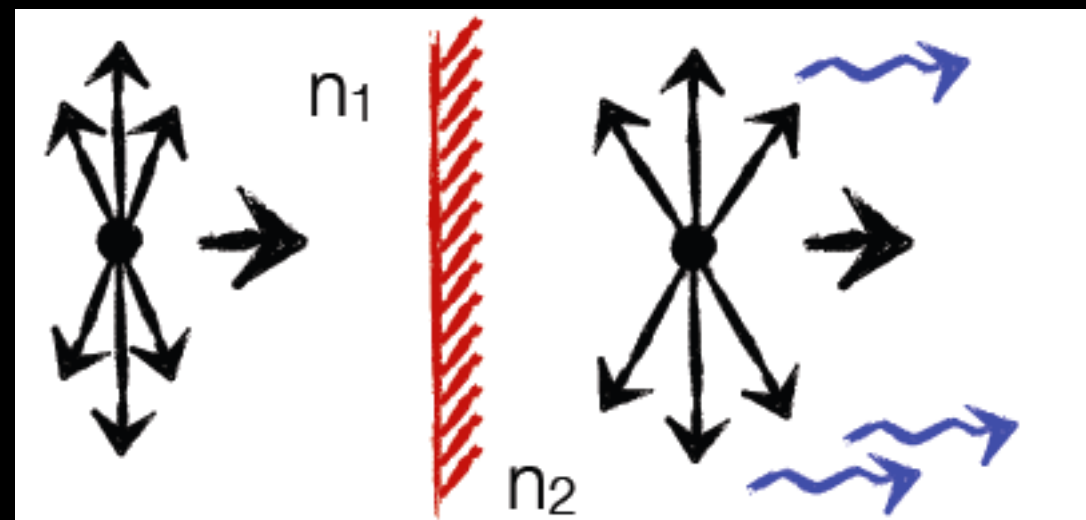
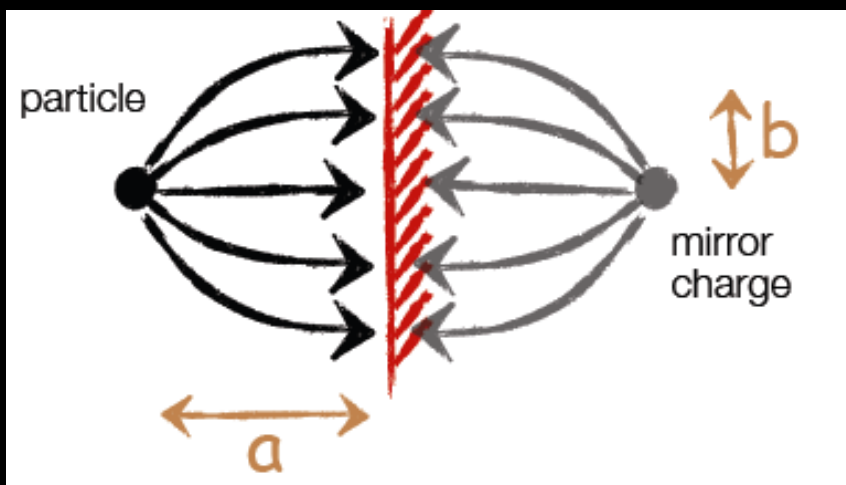


- ❑ Two detectors with gas radiators ( $C_4F_{10}$  and  $CF_4$ )
  - Originally with a 3<sup>rd</sup> radiator (aerogel)
- ❑ “Novel” photon detectors, pixel HPDs
  - Aging, issues with vacuum
- ❑ Two mirror systems
- ❑ Complex pattern recognition
  - 100s of tracks
  - Global likelihood method



# Transition radiation

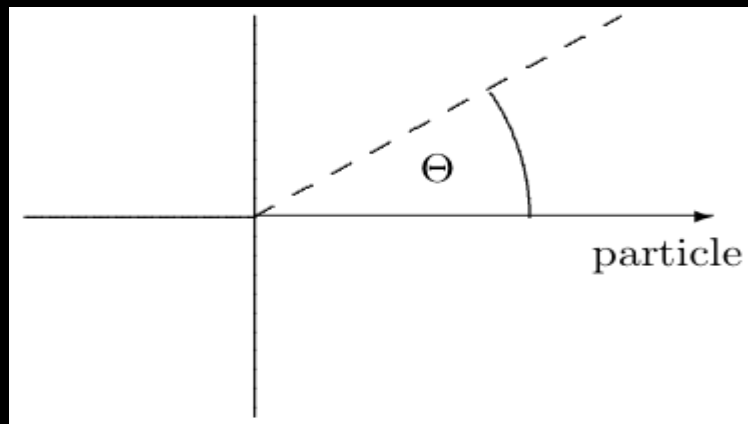
- Transition radiation occurs if a relativist particle (large  $\gamma$ ) passes the boundary between two media with different refraction indices ( $n_1 \neq n_2$ ) [predicted by Ginzburg and Frank 1946; experimental confirmation 70ies]
- Effect can be explained by re-arrangement of electric field
- A charged particle approaching a boundary creates a dipole with its mirror charge



The time-dependent dipole field causes the emission of electromagnetic radiation

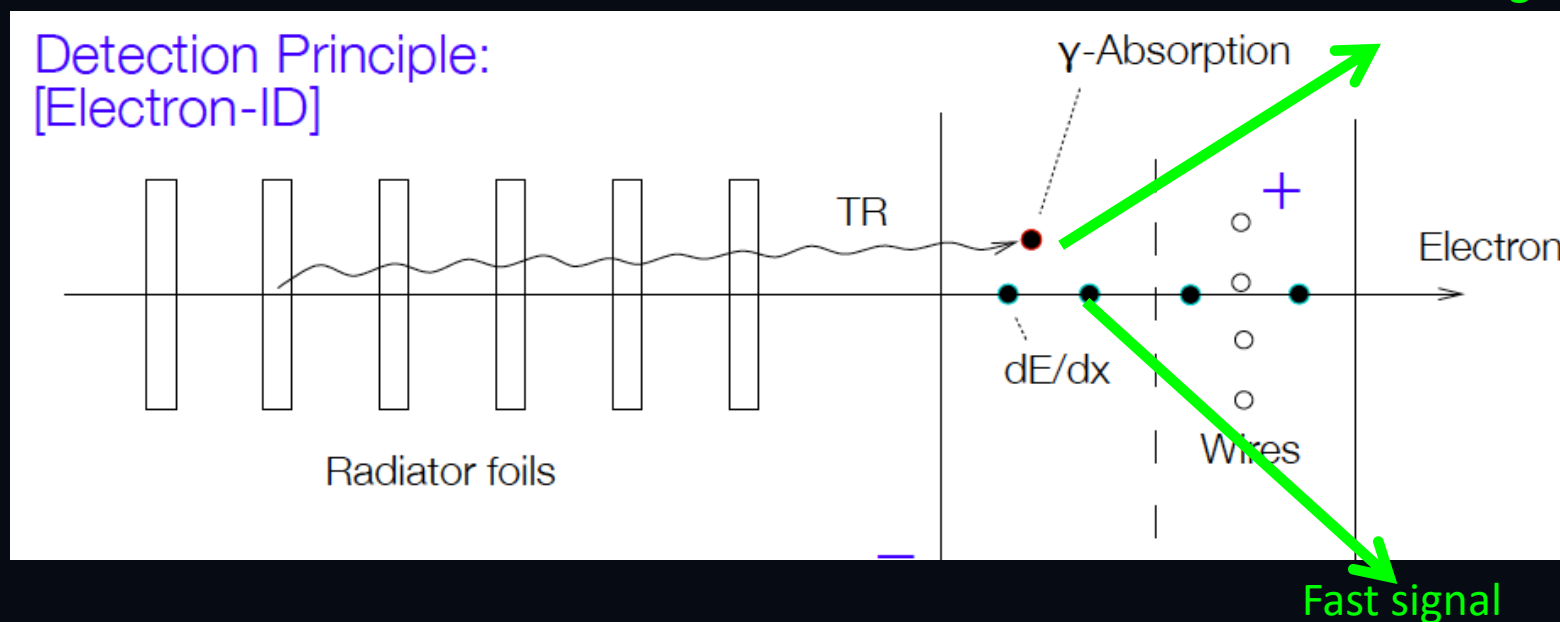
$$S = \frac{1}{3} \alpha z^2 \gamma \hbar \omega_p \quad (\hbar \omega_p \approx 28.8 \sqrt{\frac{Z\rho}{A}} eV)$$

# Transition Radiation



- Typical emission angle:  $\theta = 1/\gamma$
- Energy of radiated photons:  $\sim \gamma$
- Number of radiated photons:  $\alpha z^2$
- Effective threshold:  $\gamma > 1000$

- Use stacked assemblies of low Z material with many transitions and a detector with high Z



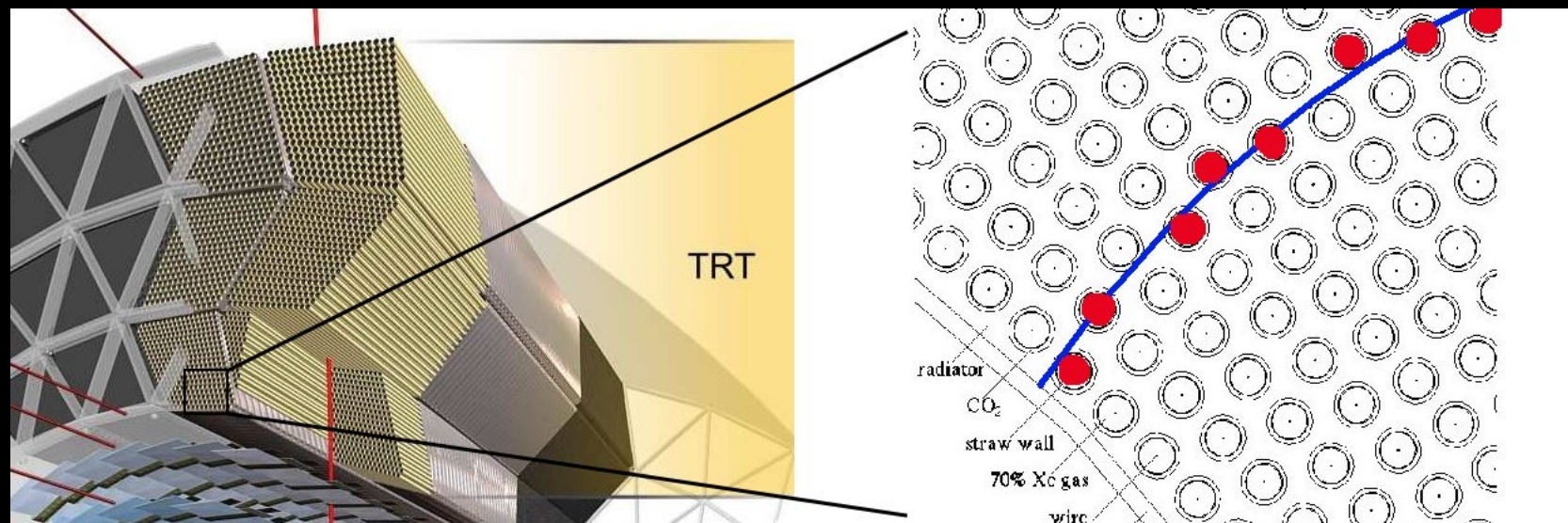
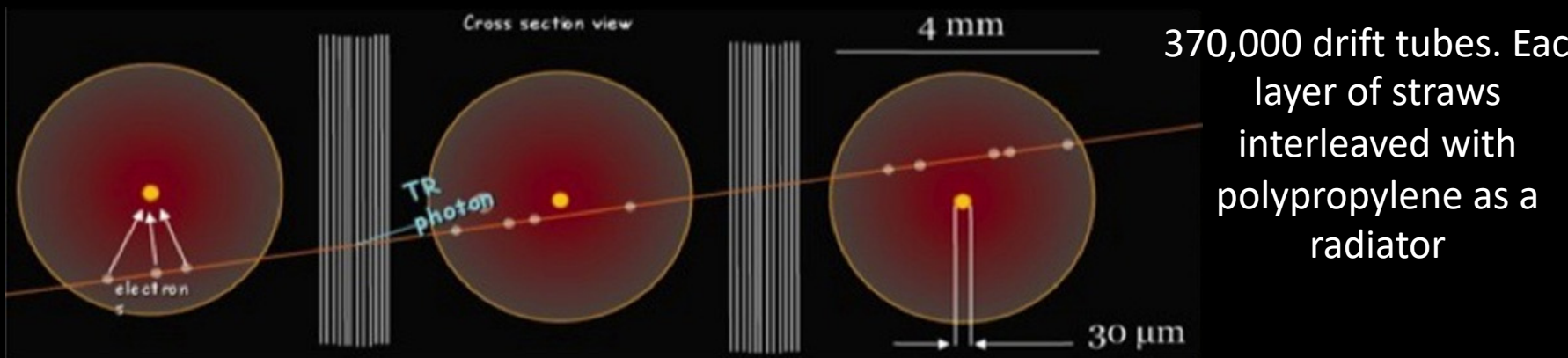
Note: Only X-ray ( $E > 20\text{keV}$ ) photons can traverse the many radiators without being absorbed

# The ATLAS Transition Radiation Tracker

- The TRT main element are gas filled tubes (d=4 mm, 40-150 cm long) to measure precisely the position



Polypropylene fibers fill the gap between straws to distinguish  $e^-$  from hadrons



# ATLAS Transition radiation tracker

